QUANTITATIVE INTERFERENCE AND CAPACITY ANALYSIS OF BROADBAND MULTI-HOP RELAYING NETWORKS

BY

HASSAN AAMER AHMED

A thesis submitted to the

Electrical and Computer Engineering Department

in conformity with the requirements for

the degree of Doctor of Philosophy

Queen's University

Kingston, Ontario, Canada

May 2011

To My Parents,

My Family,

My siblings,

And My Friends

Abstract

Broadband Wireless Access Networks (BWANs) such as Worldwide Interoperability for Microwave Access (WiMAX) and Long Term Evolution (LTE) provide significant opportunities for increased throughput and affordable service. Such BWANs are typically based on orthogonal frequency division multiple access (OFDMA). OFDMA is desirable as it divides the available OFDM subcarriers to a number of subchannels. One or more subchannels are assigned to one user. To achieve high data rates, it is necessary to increase the number of subcarriers per OFDM symbol. However, as the number of subcarriers increases, the frequency spacing between subcarriers in the OFDM symbol is reduced. This makes the OFDM system more sensitive to phase noise, which destroys the orthogonality of the subcarriers causing inter-carrier interference (ICI). Also, as the number of users increases in the system, more users will share the same OFDM symbol. This increases the subcarriers collision and makes OFDMA systems more sensitive to the resulting interference. BWANs are, however, challenged by limited capacity in busy cells and also suffer from coverage holes.

Mobile multi-hop relaying (MMR) system has been adopted in several BWANs as a cost-effective means of extending the coverage and improving the capacity of these wireless networks. In a MMR system, the communication between the source node and destination node is achieved through an intermediate node (i.,e., Relay Station). It is widely accepted

that multi-hop relaying communication can provide higher capacity and can reduce the interference in BWANs. Such claims though have not been quantified. Quantification of such claims is an essential step to justify a better opportunity for wide deployment of relay stations.

In this thesis, we address the interference issues in multi-hop BWANs and propose a solution using directional antennas in order to deal with some interference effects, and hence improve the bit error rate (BER) performance in the system. Specifically, we develop an analytical model to study the effects of the nonlinearity of high power amplifier (HPA) and the Doppler Shift on the transmitted OFDM symbols over multi-hop relying channels. Our research also includes a development of an analytical model to capture the effect of subcarriers collision in OFDMA systems. Finally, the capacity of multi-hop relaying OFDMA systems employing the amplify-and-forward (AF) scheme at relay stations as well as taking into consideration the ICI effect, is quantified. The results show that the BER performance is degraded as the HPA nonlinearity and the mobile station's speed increase. Also, the symbol error rate (SER) performance is degraded as the number of subcarriers collisions increases. It is reported that these effects cause some loss of the capacity of the MMR system.

Co-Authorship

Chapter 2

- Hassan A. Ahmed, Ahmed Iyanda Sulyman, Hossam S. Hassanein, "BER Performance of OFDM System with Channel Impairments", *Proceedings of the IEEE Conference on Local Computer Networks*, pp. 1027-1032, October, 2009.

Chapter 3

- Hassan A. Ahmed, Ahmed Iyanda Sulyman, Hossam S. Hassanein, "BER Performance of OFDM System with Channel Impairments", *Proceedings of the IEEE Conference on Local Computer Networks*, pp. 1027-1032, October, 2009.

- Hassan A. Ahmed, Ahmed Iyanda Sulyman, Hossam S. Hassanein, "BER Performance of OFDM Systems in Mobile Multi-Hop Relaying Channels", *Proceedings of the International Wireless Communications and Mobile Computing Conference*, pp. 905 - 910 , June, 2010.

- Hassan A. Ahmed, Ahmed Iyanda Sulyman, Hossam S. Hassanein, "BER Performance of OFDM Relaying Systems with High power Amplifiers and Doppler Effects", *To appear, Wireless Communications and Mobile Computing, accepted Feburary 2011*.

Chapter 4

- Hassan A. Ahmed, Ahmed Iyanda Sulyman, Hossam S. Hassanein, "BER Performance Improvement Using Directional Antennas in Multi-Hop Relaying Channels", *Conference Paper to be submitted.*

- Hassan A. Ahmed, Ahmed Iyanda Sulyman, Hossam S. Hassanein, "Directional Antennas for BER Performance Improvement of OFDM Systems in Multi-Hop Relaying Channels", *Journal paper submitted to IEEE Transactions on Vehicular Technology*.

Chapter 5

- Hassan A. Ahmed, Ahmed Iyanda Sulyman, Hossam S. Hassanein, "Symbol Loss Probability of OFDMA Technique in Mobile Multi-Hop Relaying Systems", *Proceedings of the IEEE Wireless Communications and Networking Conference*, pp. 1 - 6 , April, 2010.

- Hassan A. Ahmed, Ahmed Iyanda Sulyman, Hossam S. Hassanein, "Collision Probability of OFDMA Technique in Mobile Multi-Hop Relaying Systems", *Journal Paper to be submitted*.

Chapter 6

- Hassan A. Ahmed, Ahmed Iyanda Sulyman, Hossam S. Hassanein, "Capacity of OFDM Systems over Relaying Channels with ICI Effect", *Journal Paper to be submitted*.

Acknowledgments

I thank Allah Almigty, the Holy, the Creator, the most Gracious, the most Merciful, and the Wise, whose help and support are unbounded and gave me patience and ability to reach this stage of knowledge.

I would like to thank Prof. Hossam S. Hassanein and Dr. Sulyman Iyanda Ahmed for their supervision of my Ph.D studies.

Prof. Hassanein, I am grateful to you for giving me the opportunity to be a member of the Telecommunications Research Lab and to pursue my Ph.D. degree under your supervision. I would like to express my thankfulness and gratitude for a wonderful time and experience. Your encouragement, experience, and unlimited support are all much appreciated.

Dr. Sulyman, I thank you for your patience, guidance, experience, and encouragement which helped me throughout the course of my research.

I would like to thank the examination committee members for their insightful comments and valuable recommendations.

I would like to thank Basia Palmer for proofreading my thesis. Your comments and suggestions make my thesis much better.

I would especially like to express my deepest gratitude to my parents, family, siblings and my friends. Mother and Father thank you very much for your sincere love. Without

your continuous support and prayers this work would not have been accomplished.

For my wife and children thank you for your patience in the long journey. To wife, your support, understanding, and patience, which mean much more than I can express, all are appreciated. To children, your smiles, and love were a great source of happiness during the course of my research.

Also, I would like to thank my brother Khaled Ali for his support and encourgenment. Khaled I am grateful to you for your unbelievable support, invaluable advice and standing by me at all times.

Brothers and sisters, you cannot imagine how I am grateful to you for your unlimited support and encourgenment. I owe you respect and thankfullness forever.

I would like to thank all of the TRL Lab members for the joyful and worthwhile experience that made the course of my studies and stay at Queen's Unversity wonderful.

A special thanks to the Libyan Education Ministry for their financial support.

Contents

List of Figures

List of Tables

List of Acronyms

1G	First Generation
2G	Second Generation
3G	Third Generation
3GPP	3rd Generation Partnership Project
AF	amplify-and-forward
AMC	Adaptive Modulation and Coding
AoA	Angle-of-Arrival
AWGN	Additive White Gaussian Noise
BER	Bit Error Rate
Bs	Base Station
BWANs	Broadband Wireless Access Networks
CDF	Cumulative Distribution Function
CF	Compress-and-Forward

CP	Cyclic Prefix
DF	Decode-and-Forward
DL	Downlink
DSL	Digital Subscriber Lines
FFT	Fast Fourier Transform function
FR	Frequency Reuse
HARQ	Hybrid Automatic Repeat Request
HPA	High Power Amplifier
ICI	Inter-carrier Interference
IFFT	Inverse Fast Fourier Transform Function
ISI	Inter Symbol Interference
LOS	Line-of-Site
LTE	Log Term Evolution
MIMO	Multiple-Input-Multiple-Output
MMR	Mobile Multi-hop Relaying
MR-BS	Mobile Multi-Hop Relay Base Station
MS	Mobile Station
NLOS	Non Line-of-Sight

NTRS	Non-Transparent Relay Station
OFDM	Orthogonal frequency division multiplexing
OFDMA	Orthogonal frequency division multiple Access
PAPR	Peak-to-Average Power Ratio
PDF	Probability Density Function
QAM	Quadrate Amplitude Modulation
QoS	Quality of Service
RF	Radio Frequency
RS	Relay Station
SER	Symbol Error Rate
SINR	Signal-to-Interference and Noise Ratio
SIR	Signal-to-Interference Ratio
SNR	Signal-to-Noise Ratio
TRS	Transparent Relay Station
TWTA	Traveling Wave Tube Amplifier
UL	Uplink
UMTS	Universal Mobile Telecommunications System
WiMAX	Interoperability for Microwave Access

WLANs	Wireless Local Area Networks

List of Important Symbols

Φ_{Dop}	Doppler Shift
Φ_{Amp}	Amplifier Distortion
μ	Service Time
R	Number of Hops
N	Number of Relays
N_c	Number of Subcarriers
$X[.]$	Transmitted signal
K	Subcarrier index
$Y[.]$	Received signal
W[.]	Additive White Gaussian Noise
f_d	Frequency offset
f_c	Transmitted frequency
c	Speed of the wave
T_s	OFDM symbol period
$\beta[.]$	Inter-carrier Interference
$\gamma[.]$	Signal-to-Interference and Noise Ratio

P	Transmit Power
$\sigma^2_{\Phi_{Amp}}$	Power of the Amplifier distortion
$\sigma^2_{\Phi_{Dop}}$	Power of the Doppler Shift
$\alpha[.]$	Amplification Factor
$P_e[.]$	Probability of Error
$f[.]$	Probability density function
M	Size of constellation
$erfc$	Complementary error function
θ	Angle of Arrival
ψ_a	Antenna's Beamwidth
λ	Wave Length
$P(\theta)$	Probability Density Function of the Angle of Arrival
C	Specific area
L	Radios of the coverage area
D	Distance between a transmitter and receiver
Q	Normalizing Constant
$\sigma^2_{W[.]}$	Variance of the Complex Gaussian Noise
$\gamma_{eq}[.]$	Signal-to-Interference-plus-Noise Ratio equivalent
G	Number of Subchannels
S	Occupied Subcarriers
$\overline{E}_s[.]$	Expected Value of the Number of collisions
$\widehat{P}_s(.)$	Probability of Collision
i	Number of Collisions

ξ_n	Shadowing Effect
ρ	Signal-to-Noise Ratio Threshold
E_s	Transmitted Signal Power
U	Number of Users
V	Number of Calls Belonging to Class C
$\overline{\omega}$	Antenna Orientation is parallel to the direction of the motion
$-\overline{\omega}$	Antenna Orientation is Perpendicular to the direction of the motion
$F(\theta)$	Cumulative Distribution Function of the Angle of Arrival
H[.]	Channel fading Coefficient between a Transmitter and receiver
g	Random Variable denoting the Subchannel where a collision could occur
$V_{S,D}$	Velocity of the transmitter relative to the receiver
$C(.)$	correlation function
$\overline{\gamma}[.]$	Average of Signal-to-Interference and Noise Ratio
$C_{AF-R-Relay}$	Capacity of the System
γ_{upp}	Signal-to-Interference-plus-Noise Ratio upper bound

Chapter 1

Introduction

The era of wireless communications started when the first generation (1G) of wireless cellular systems was launched in the early 1980s. These systems utilized analog air interface and supported voice applications only. With the higher user demand for cellular services and the increased need for better quality of service (QoS), the second generation (2G) of wireless cellular systems was introduced. 2G utilized digital air interface, providing higher bandwidth and better voice quality. In addition to supporting voice applications, 2G had the capability to support limited data applications. The capabilities of supporting higher bandwidths and better voice quality have led to the tremendous popularity of 2G wireless cellular systems, which were successfully deployed and attracted a large number of users around the world.

The remarkable success of 2G wireless cellular systems, however, together with the continuous growth of the Internet have resulted in an increased demand for wireless data services "any time and anywhere" using any wireless device. This has motivated the development of the third generation (3G) wireless cellular systems for better QoS and a higher

capacity support. One of the 3G systems is Universal Mobile Telecommunications System (UMTS) that was developed by the 3rd Generation Partnership Project (3GPP) [81]. UMTS has the capability to support a transmission rate of up to 2 Mbps, consequently to offer new data services.

The increased demand for supporting new applications with a higher data rate, led to the need for data rates beyond what is supported by current 3G wireless systems. To fulfill the support for such high data rate, Broadband Wireless Access Systems (BWASs) have been developed. For example, 3GPP is developing a new standardized system called Long Term Evolution (LTE) [45]. The LTE has been introduced as an evolutionary step for UMTS in terms of capacity and architecture improvements, therefore it provides higher data rates, and improved coverage and spectrum efficiency [45]. The LTE system supports data rates greater than 100 Mbps, and efficiently utilize the spectrum using an OFDM system. Another BWANs is the Worldwide Interoperability for Microwave Access (WiMAX), which has been standardized by the IEEE 802.16 group [25]. WiMAX is a BWANs that has the capability to support data rate up to 70 Mbps.

BWANs such as LTE and WiMAX have gained tremendous attention lately for leveraging the support of a wide range of applications with different QoS requirements. Despite the support for such range of applications, satisfying the different QoS requirements while maximizing the network capacity and extending the network coverage are still major issues in these networks. Mobile Multi-hop relaying (MMR) system has been adopted in several BWANs such as LTE-advanced (Release10) [41], [3], and WiMAX (IEEE802.16j) as a cost-effective means of extending the reach and/or capacity of these wireless networks. The emerging MMR extension enhances the conventional BWANs to enable support of multi-hop communication between a mobile station (MS) and a base station (BS) through

intermediate relay stations (RSs) [26].

OFDM is the defacto transmission mechanism for BWANs. OFDM provides efficient broadband data transmission by sending parallel data streams over a number of closely-spaced subcarriers as illustrated in Figure 1.1. However, for high data rates, it is necessary to increase the number of subcarriers per OFDM symbol, and as the number of subcarriers increases the frequency spacing between the subcarriers in the OFDM symbol is reduced. This makes the OFDM system more sensitive to phase noise which destroys the orthogonality of the subcarriers, causing inter-carrier interference (ICI).

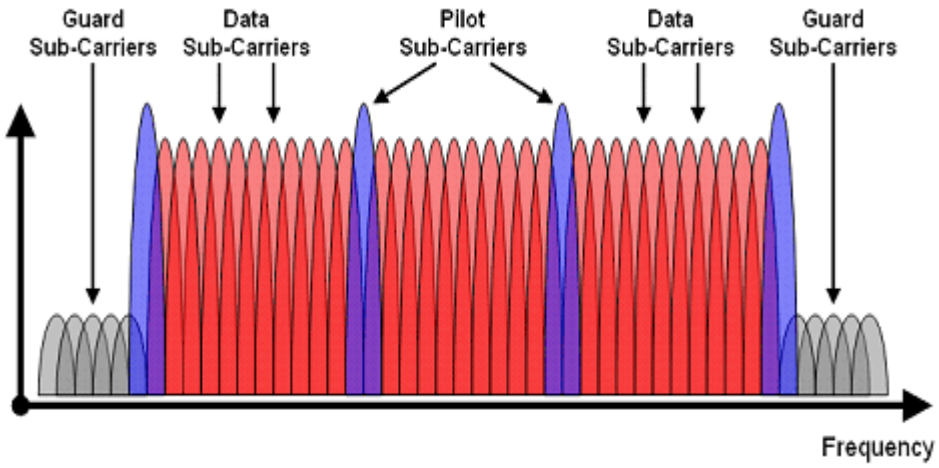

Figure 1.1: OFDM Symbol

The main issues causing phase noise, consequently ICI in BWANs based on OFDM systems, can be enumerated as follows: (i) Imperfect synchronization in local oscillators (LO): mismatch between the LO at the transmitter and the receiver introduces frequency off-sets which contributes to ICI. (ii) High peak-to-average power ratio (PAPR) with non-linear amplifiers: in OFDM systems, because of the high fluctuations in the level of the instantaneous signals transmitted, the PAPR is typically large, making operation over the

linear region of the high power amplifier (HPA) difficult. When some parts of the transmitted OFDM signals operate in the nonlinear region of the HPA, nonlinear distortions are introduced in the OFDM signals, resulting in phase noise which also contributes to ICI [63], [11]. (iii) Doppler Effect: the relative speed between the transmitter and receiver in a wireless channel, introduces Doppler Shift in the received frequencies, also contributing to ICI.

Another issue facing BWANs is frequency reuse (FR) because the channel can only be reused if the interference in the network is reduced. FR increases interference by allowing more MSs to access the same channel. As the number of MSs increases in the system, more MSs will share the same OFDM symbol. This increases the chance for subcarriers to be collided which increases the interference level.

In most practical systems, several high performance classical frequency offset estimators for oscillator synchronization problems in OFDM systems are available [39], [42], [43] and [58]. However, the HPA nonlinearity and Doppler Shift effects still pose significant problems in most practical systems and should be given due considerations in the design of MMR broadband communication systems. In addition, the subcarriers collision resulting from FR should be quantified because it increases the interference level in these systems. Moreover, the cascade effect of the multi-hop relaying channel dramatically amplifies the phase noise problem, consequently the ICI resulting from HPA nonlinearity and Doppler Shift effects as well as the interference resulting from subcarriers collisions [81], [82].

In this thesis, we quantify the effects of ICI on the transmitted OFDM symbol over multi-hop relaying channels. Specifically, the effects of HPA nonlinearity and Doppler Shift are analyzed. Also, we propose a solution using directional antennas to overcome the

effects of the ICI on the transmitted OFDM symbol. Our research also include a development of an analytical model to capture the effect of the subcarriers collision in OFDMA systems. The capacity of the MMR systems employing amplify-and-forward (AF) scheme at RSs considering the ICI effect is quantified.

1.1 Motivations and Objectives

The MMR system is a promising approach for extending the coverage and improving the capacity of the conventional cell[1]. These expectations are widely accepted since the early discussions of the MMR system's objectives. Investigating some issues related to the MMR system is an essential step for further research in this area.

One of the major issues affecting the transmitted OFDM symbol, consequently the supportable data rate is HPA nonlinearity. In OFDM systems, because of the high fluctuations in the level of the instantaneous signals transmitted, PAPR is typically large, making the operation over linear region of HPA difficult. When some portions of the OFDM signals transmitted operate in the nonlinear region of the HPA, nonlinear distortions are introduced in the OFDM signals, resulting in phase noise which contributes to ICI.

Another important issue that must be taken into consideration is Doppler Shift. Relative speed between the transmitter and receiver in a wireless channel, introduces Doppler Shifts in the received frequencies, also contributing to ICI.

Furthermore, the performance of BWANs is affected by subcarriers collision. When the same subcarrier is used simultaneously by more then one user in different RSs, collision will occur and the symbol will be lost. A quantification of the total number of collisions is needed to capture theses effects, and develop effective techniques to improve the network

[1]The term "cell" means the coverage area of a base station

performance.

Existing interference analysis efforts were designed for single-hop and they do not consider the accumulative effect of the ICI and subcarriers collisions over the multi-hop relaying channels. We, therefore, aim at considering all of the aforementioned issues and effects over relaying channels. Also, we proposed a solution using directional antennas to overcome the Doppler Shift effect. Finally, we analyzed the system capacity with the consideration of the effect of ICI.

1.2 Thesis Contributions

BWANs such as LTE and WiMAX are proposed to provide high data rates and better QoS to the end user. The MMR system is adopted in both LTE-advanced and WiMAX systems for extending the cell coverage and increasing the system capacity. In this thesis our objectives are to:

- Quantify issues that destroy the orthogonality between subcarriers in OFDM symbols and introduce ICI as well as study their accumulative effect over multi-hop relaying channels.
- Mitigate the ICI effect resulting from Doppler Shift by deploying directional antennas at both RS and MS side.
- Quantify the subcarriers collision effects in the MMR system, and study the accumulative effect over multi-hop relaying channels.
- Analyze the system capacity of multi-hop relaying channels taking into consideration the effect of ICI, and the accumulative effect over relaying channels.

Simulation and analytical results are reported for the aforementioned contributions, and recommendations are given for a better design of BWANs. The work in this thesis focuses on the uplink (i.e., from mobile station through the relay station to the base station), and interference issues and system capacity are analyzed. The main contributions of this thesis include the following:

1) Inter-Carrier Interference

In Chapter 3, we quantify issues that introduce some distortions into the transmitted OFDM signal and destroy the orthogonality between subcarriers in OFDM symbol, consequently introduce ICI in the MMR system. The effects of HPA nonlinearity and Doppler Shift on the transmitted OFDM signal are analyzed. We develop an analytical method to study those effects, and present the statistical characteristics of these impairments over two-hop relaying channels. Specifically, we derive a formula for SINR expression as a function of HPA nonlinearity and Doppler Shift effects. The SINR expression is used to study the performance of SER and BER in the MMR system.

2) Directional Antennas for BER Performance Improvement

In Chapter 4, we present the first documented work in the literature, on the effect of deploying directional antenna on the error rate performance of the MMR system. We derive a formula to study the BER performance of the MMR system employing directional antennas and evaluate analytically and by simulation, the effectiveness of this solution in multi-hop relaying channels.

3) Subcarriers Collision

In Chapter 5, we derive the probability of the expected number of collisions between two or more non-transparent relay stations (NTRSs)[2]. Using the derived expression, we calculate the probability of symbol loss for OFDMA techniques in the MMR systems. It is note worthy to clarify that not all symbols involved in a collision are lost, but collisions can increase the level of interference, making the symbol loss probability high. The IEEE 802.16 standard [25] defines a threshold for the SNR, below which the BER is unacceptable ($> 10^{-6}$). Using this threshold, we also estimate the proportion of symbols with degraded SNR as well as the collision rate in the MMR systems with two or more NTRSs.

4) Multi-Hop Relaying System Capacity

In Chapter 6, we evaluate the capacity of OFDM systems over multi-hop relaying channels employing amplify-and-forward (AF) relaying scheme and consider the effect of the ICI on the system capacity. We derive a closed-form expression for the MMR system capacity and also compare the results for different number of hops as well as different MS's speeds. Simulation results are provided to validate the analysis.

1.3 Thesis Organization

This thesis is organized as follows. Chapter 2, presents background materials and related work. Chapter 3, presents the analytical analysis of HPA nonlinearity and Doppler Shift effects on the MMR system; also performance evaluation of the obtained analysis are illustrated. Chapter 4, introduces our solution using directional antennas to mitigate the effect of Doppler Shift on OFDM symbol; also a performance evaluation of the effectiveness

[2]NTRS is a relay station that generates the control information to its associated mobile stations.

of the proposed solution is presented. Chapter 5, presents the quantification of the possible number of subcarriers collision in the MMR system, and also performance results to evaluate the quantification are presented. Chapter 6, presents the MMR system capacity analysis, as well as results are presented to validate the obtained analysis. Chapter 7 presents the conclusions drawn from the thesis and discusses possible directions for future research works.

Chapter 2

Background and Related Work

This chapter provides a background material which is related to broadband wireless access networks (BWANs). Section 2.1 presents an overview of two of the most prominent BWANs, Long-Term-Evolution (LTE) and Worldwide Interoperability for Microwave Access (WiMAX). Common aspects between LTE and WiMAX are discussed in this section. In section 2.2, the concept of a mobile multi-hop relaying (MMR) system is described. Section 2.3 provides a detailed description of the OFDM system and different steps the transmitted signals traverse through from source to destination as well as the channel impairments which affect the transmitted OFDM symbol. This chapter also highlights some issues that still pose significant problems in the MMR systems. Sections 2.4, 2.5 and 2.6 provide a comprehensive literature review of inter-carrier interference, subcarriers collision and system capacity, respectively.utilize

2.1 Broadband Wireless Access Networks

Long Term Evolution (LTE), considered as BWAN, has been introduced as an evolutionary step for Universal Mobile Telecommunications System (UMTS) in terms of capacity and architecture improvements. LTE systems provide higher data rates, and improved coverage and spectrum efficiency [45]. The LTE system supports data rates greater than 100 Mbps, and efficiently utilize the spectrum using an OFDM system. The Worldwide Interoperability for Microwave Access (WiMAX) is another BWAN that has been standardized by the IEEE 802.16 group [25]. WiMAX can support up to 70 Mbps, hence, enabling high-speed wireless access over large metropolitan areas. WiMAX promises compelling economics and a simplified IP-based architecture that reduces complexity and cost. LTE and WiMAX are two different BWANs technologies that differ in a number of characteristics including air interface, coverage, and system architecture. These two technologies, however, rely on many similar aspects that allow them to achieve high data rates. The two most important common aspects are utilizing adaptive modulation and Hybrid Automatic Repeat Request (HARQ), which are coupled and rely on rapid adaptation of the transmission parameters to the instantaneous channel conditions. Adaptive modulation techniques enable the use of spectrally efficient higher order modulation when channel conditions permit, and switch to more robust lower order modulation for bad channel conditions. This implies that MSs with good channel conditions will potentially experience higher supportable data rates by using higher order modulation, whereas MSs with bad channel conditions will experience lower data rates. HARQ only requests the retransmission of missing data bits and combines the soft information from the original transmission and any subsequent retransmissions before any attempts are made to decode a message. The main advantage of HARQ is reducing the number of data retransmissions in BWANs, hence improving the delay latency of these

systems.

Another common aspect between LTE and WiMAX is the use of OFDM system for data transmission. OFDM basically based on squeezes multiple modulated carriers together reducing the required bandwidth and at the same time keeping the modulated signals orthogonal to each other so they do not interfere with each other, and hence it enables these systems to accommodate more users.

Furthermore, another common feature between LTE and WiMAX is the use of a shared channel for data transmissions. The use of shared channel has some advantage over a dedicated one. First, it improves the utilization of the BWANs resources, enabling these systems to accommodate more users. Second, it reduces the cost of bit transmission, and hence lowers the cost of providing wireless services. Using shared channel for data transmission, however introduces some issues such as interference, subcarriers collision, and there by reduces the system capacity.

2.2 Mobile Multi-Hop Relaying Systems

BWANs are needed for capacity and coverage extension because of the increased number of users and their growing demand for new applications and cheaper services, therefore some groups are working to develop standards to support multi-hop communications. For instance, the IEEE 802.16j task group [26] is developing a standard to support multi-hop relaying communication mode for IEEE 802.16 systems. This standard extends the coverage area of a BS using multi-hop technique and overcomes the coverage holes (i.e., building shadow), as well as increases system capacity using multiple access links. Also, the Third Generation Partnership Programs-Long-Term Evolution (3GPP-LTE) group is developing a new standard for mobile broadband access that will improve the throughput and extend

the coverage to meet the requirements of the fourth generation cellular technology.

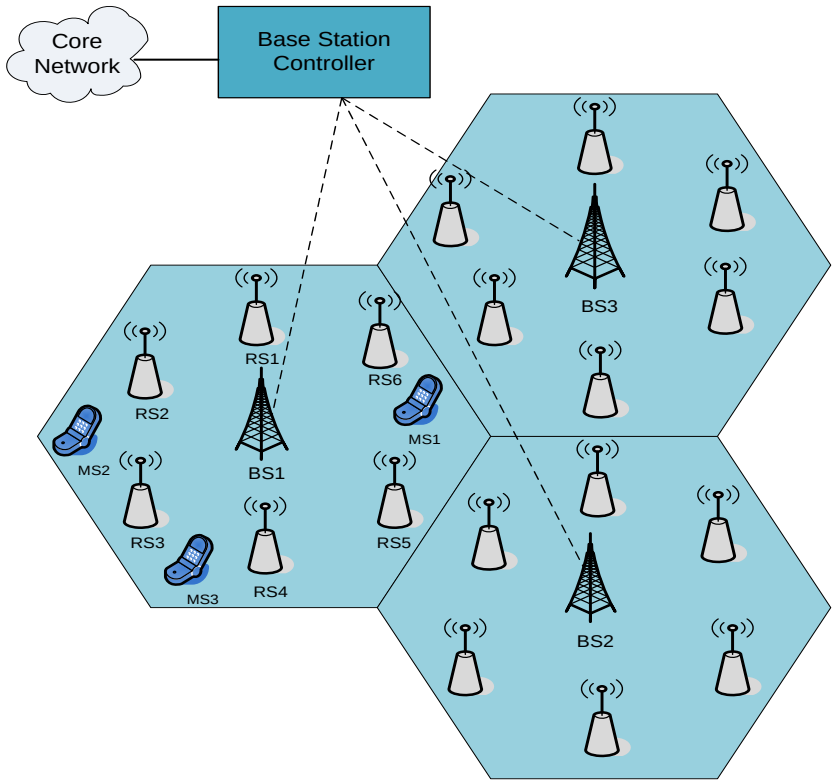

Figure 2.1: Mobile Multi-hop Relaying System Architecture

The MMR systems consist of a multi-hop relay base station (MR-BS)[3], one or more relay stations (RSs) and a number of mobile stations (MSs)[4]. Figure 2.1 illustrates a typical example of the MMR system architecture, where the MR-BS receives the signal from an MS through RS. The channel between RS and MS is called access link, while the link between the BS and RS is called relay link. There are two options that can be employed at the RS, depending on how the RS processes the received signal: Amplify-and-Forward

[3]"multi-hop relay base station" is the name used by the IEEE 802.16j Task Group for a "base station". This term is interchangeably used with "base station" in this thesis.

[4]The terms "user" and "mobile station" are used interchangeably throughout this thesis

(AF) and Decode-and-Forward (DF). When the AF relay option is employed, the RS simply amplifies and forwards the symbol at the radio frequency (RF) stage, without decoding its content. The received signal is effected by the channel fading and Additive White Gaussian Noise (AWGN) at the receiver. Both the degraded signal and the noise are amplified and forwarded, hence increasing the network noise. In contrast, when the DF option is employed, the RS demodulates and decodes the received signal before retransmission, therefore increasing the delay latency. There are three possible deployment scenarios for RSs in BWANs, each scenario has it's own characteristics which can be explained as follows

- **Fixed Relay Stations (FRSs)**

Fixed RSs are similar to BSs. The service provider chooses Line-of-Site (LOS) locations with the MR-BS for the deployment of such RSs. They are intended to extend the coverage and increase overall throughput. Hence, this type of RSs will be similar in deployment, but will have a lower cost and functionality compared to an MR-BS.

- **Mobile Relay Stations (MRSs)**

Unlike fixed RSs, mobile RSs are deployed in mobile locations such as a train or bus to route mobile stations traffic in specific locations. In this scenario, RSs are more complex since they are responsible for providing reliable coverage, as well as supporting a highly mobile environment.

- **Nomadic Relay Stations (NRSs)**

Nomadic relay station type is suitable for applications where a group of MSs gather in one small area. Nomadic RSs can be temporarily located near such dense areas to route the generated traffic to MR-BS. Another application for nomadic RSs is in emergency events,

when a temporary coverage is needed to forward generated traffic to a nearby MR-BS. The RS manages all communication steps within an MR-BS coverage area through a centralized or decentralized manner.

Two modes are proposed for relay operations in BWANs, transparent and non-transparent. In the former mode, the RS operates in the same frequency band as the MR-BS, while in the latter mode the RS operates in a different frequency band then the MR-BS. Furthermore, transparent RSs serve MSs that can decode MR-BS's information, and hence it will not generate any control information, while non-transparent RSs serve MSs that can not decode MR-BS's information, thus these RSs need to generate control information by which MSs consider this RS as the BS. Due to the aforementioned functionalities, non-transparent RS operation is more involved than transparent RS. In the following, we consider the functionalities and advantages of both transparent and non-transparent modes.

1) Transparent Relay Station Mode

A transparent RS (TRS) mode does not generate control information but simply forwards data for the MR-BS and MSs. In this mode the maximum number of hops between the MR-BS and an MS is two hops. That is, at most one TRS can participate in relaying data packets between the MR-BS and an MS. The main objective of deploying TRSs in the network is to increase network capacity within the MR-BS coverage rather than increasing the coverage of the MR-BS. The frame is divided into uplink (UL) and downlink (DL). Both the DL subframe and the UL sub-frame are divided into two zones, the access zone and the relay zone. The DL access zone is defined for the MR-BS to communicate with MSs or TRSs. The DL relay zone, which is called the transparent zone in the standard (IEEE802.16j), is defined for TRSs to communicate with MSs. When MSs communicate with the MR-BS

through TRSs in the upstream direction, they transmit data in the UL access zone and then the TRSs relay their data to the MR-BS in the UL relay zone.

2) Non-Transparent Relay Station Mode

The main difference between a TRS and a non-transparent RS (NTRS) is that a NTRS generates the control information to its associated MSs, while a TRS does not. In this mode when an MS is out of range of the MR-BS and thus cannot receive the DL information from the MR-BS, a NTRS should forward the DL information sent from the MR-BS to the MS. The main objective of using NTRSs is to extend the coverage of the MR-BS rather than increasing network capacity. When scheduling subcarriers, a NTRS can either operate in the centralized scheduling mode or in the distributed scheduling mode.

In the former mode, the subcarriers assignment for all MSs in the network are scheduled at the mobile multi-hop relay base station (MR-BS). In the latter mode, NTRSs can make their own scheduling decisions for the MSs associated with them. Both the MR-BS and the NTRS generate control information to their associated MSs; by this design, an MS can view a NTRS as the MR-BS and synchronize to it. The DL relay zone is defined for the MR-BS to communicate with NTRSs, and hence the MS should be idle in the DL relay zone.

2.3 Orthogonal Frequency Division Multiplexing System

The OFDM system has been widely accepted in wireless communication to overcome multipath problems, for instance wireless local area networks (WLAN), WiMAX and LTE , [7] [24], [25], [26] and [45]. In OFDM system, the OFDM symbol is divided into a number of subcarriers, therefore OFDM provides an efficient broadband data transmission by sending

parallel data over a closely-spaced subcarriers, however it is sensitive to carrier frequency offset and phase noise.

A block diagram of a transceiver (MS and BS) in OFDM system with Inverse Fast Fourier Transform (IFFT) and Fast Fourier Transform (FFT) functions is shown in Figure 2.2.

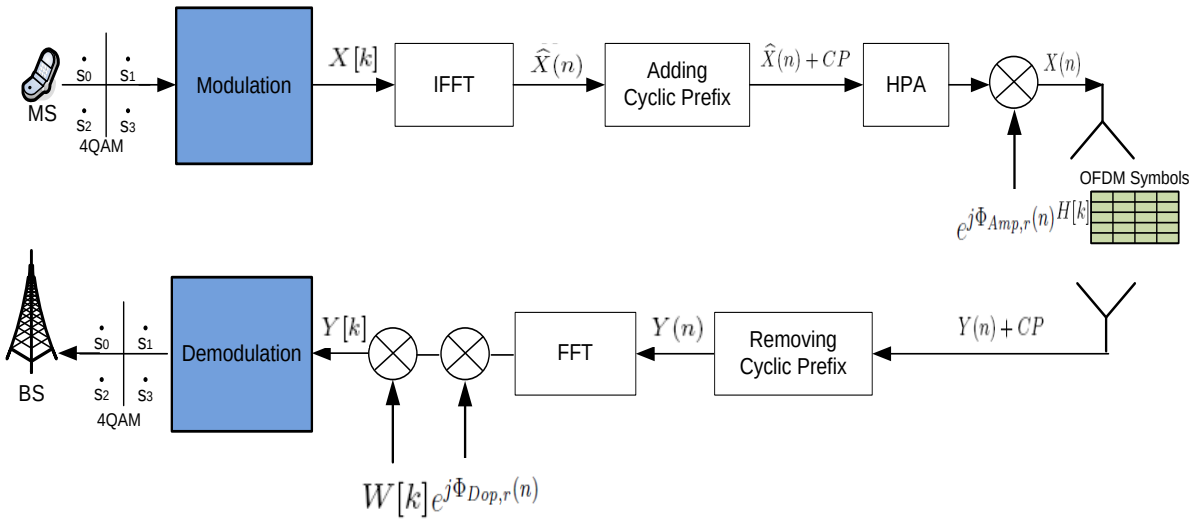

Figure 2.2: Block diagram of an OFDM transceiver

This diagram illustrates the different stages each transmitted signal traverses through. Each MS's data which in our case generated by quadrate amplitude modulation (QAM) is modulated with a number of N_c subcarreirs to produce N_c data points in frequency-domain. These data points are fed to an IFFT function whose output is a time-domain signal to transmit over a fading channel after adding cyclic prefix (CP) as illustrated in Figure 2.3, to remove inter symbol interference (ISI), which is introduced by the multipath channel. It worth to mention that no coding scheme is used.

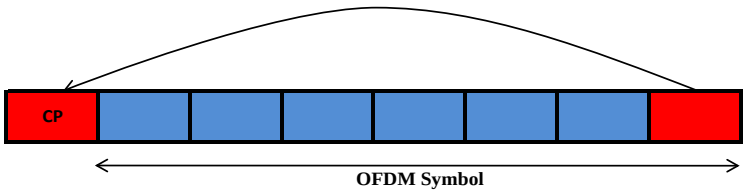

Figure 2.3: OFDM Symbol with Cyclic Prefix

Therefore, at the receiver side after the cyclic prefix is removed, the time-domain received signal is fed to FFT function whose output is the frequency-domain signal. Then the demodulation is performed to recover N_c data points. Accordingly, consider an OFDM symbol $\widehat{X}(n)$ generated by performing IFFT operation on QAM data points $X[k]$ modulated onto N_c subcarriers.

$$\begin{aligned} \widehat{X}(n) &= IFFT\{X[k]\} \\ &= \frac{1}{\sqrt{N_c}} \sum_{k=0}^{N_c-1} X[k] e^{j(\frac{2\pi}{N_c})kn} \end{aligned} \tag{2.1}$$

$X[k]$ denotes the QAM modulated signal onto the k^{th} subcarrier. The generated OFDM symbol $\widehat{X}(n)$ is extended by a CP to overcome ISI. The CP extension can be achieved by copying the last part of OFDM symbol, than added to the first part of the OFDM symbol. The extended signal transmitted through a fading channel $h(n)$ whose FFT is denoted $H[k]$ on subcarrier k. The time-domain received signal $Y(n)$ can be written as

$$Y(n) = \widehat{X}(n)h(n) + w(n) \tag{2.2}$$

where $w(n)$ is the AWGN. The transmitted signal $\widehat{X}(n)$ is affected by two deterministic impairments, namely amplifier distortion and Doppler Shift [4]. The first impairment can

be considered as generated before the fading channel. Therefore, when the transmitted signal is amplified by HPA experiences a phase distortion $\Phi_{Amp}(n)$. The well known non-linear memoryless amplifier [55], is adopted in this chapter, the expressions for amplitude AM/AM (amplitude modulation/amplitude modulation) $A_{Amp}(.)$ and the phase AM/PM (amplitude modulation/phase modulation) $\Phi_{Amp}(.)$ characteristics for a traveling wave tube amplifier (TWTA) are given by

$$A_{Amp}(X(n)) = \frac{\nu X(n)}{(1+\eta_a X^2(n))} \tag{2.3}$$

$$\Phi_{Amp}(X(n)) = \frac{\alpha_\phi X^2(n)}{(1+\eta_\phi X^2(n))} \tag{2.4}$$

where $X(n) = |\widehat{X}(n)|$ and $|.|$ is the magnitude of its argument, ν denotes the small-signal gain, $A_s = 1/\sqrt{\eta_a}$ is the amplifier input saturation voltage, and the HPA maximum output amplitude is $A_0 = max_{X(n)} = \{A[X(n)]\} = \frac{\nu A_s}{2}$. A typical choice for the above parameters is $\nu = 1, \quad \eta_a = 0.25, \quad \alpha_\phi = \frac{\pi}{12} \quad and \quad \eta_\phi = 0.25$, therefore the received signal can be given by

$$Y(n) = X(n)h(n)e^{j\Phi_{Amp}(n)} + w(n) \tag{2.5}$$

However, in the OFDM system, the desired signal is frequently impaired by interfering signals that are generated after the fading channel, because they do not pass through the same channel as the desired signal. Therefore, the transmitted signal is shifted by Doppler effect $\Phi_{Dop}(n)$ which given by $2\pi f_d T_s$. Where f_d denotes the frequency offset between the

transmitter and the receiver, which can be expressed as

$$f_d = \frac{f_c * V_{S,D}}{c} = \frac{V_{S,D}}{\lambda} \tag{2.6}$$

Where f_c is the transmitted frequency, $V_{S,D}$ is the velocity of the transmitter relative to the receiver (m/s), c is the speed of the wave $(3 \times 10^8(m/s))$, $\lambda = \frac{c}{f_c}$ is the wavelength, and T_s is the OFDM symbol period. Hence, we rewrite the time-domain received signal in Eq.(2.5) as

$$Y(n) = X(n)h(n)e^{j\Phi_{Amp}(n)}e^{j\Phi_{Dop}(n)} + w(n) \tag{2.7}$$

After CP removal, and the FFT operation, the frequency-domain received signal per sub-carrier k, $Y[k]$ can be expressed as

$$Y[k] = \frac{1}{\sqrt{N_c}} \sum_{n=0}^{N_c-1} Y(n)e^{-j(\frac{2\pi}{N_c})kn} + W[k] \tag{2.8}$$

Substituting the time-domain received signal $Y(n)$ from Eq.(2.5) yields:

$$Y[k] = \frac{1}{\sqrt{N_c}} \sum_{n=0}^{N_c-1} X(n)h(n)e^{-j(\frac{2\pi}{N_c})kn}e^{j\Phi_{Amp}(n)}e^{j\Phi_{Dop}(n)} + W[k] \tag{2.9}$$

Substituting the time-domain transmitted signal $X(n)$ yields to rewrite Eq.(2.9) as

$$\begin{aligned} Y[k] &= \frac{1}{\sqrt{N_c}}\frac{1}{\sqrt{N_c}}\sum_{n=0}^{N_c-1} h(n)\sum_{m=0}^{N_c-1} X[m]e^{j(\frac{2\pi}{N_c})mn}e^{-j(\frac{2\pi}{N_c})kn}e^{j\Phi_{Amp}(n)}e^{j\Phi_{Dop}(n)} + W[k] \\ & m = 0, 1, \ldots, N_c - 1 \end{aligned} \tag{2.10}$$

After some rearrangements, Eq.(2.10) can be simplified as follow

$$Y[k] = \frac{1}{N_c}\sum_{n=0}^{N_c-1} h(n)\sum_{m=0}^{N_c-1} X[m]e^{j(\frac{2\pi}{N_c})(m-k)n}e^{j\Phi_{Amp}(n)}e^{j\Phi_{Dop}(n)} + W[k] \tag{2.11}$$

At this point, we can consider two cases, one is $m = k$, and another is $m \neq k$, therefore Eq.(2.11) can be rewritten as

$$\begin{aligned} Y[k] &= \frac{X[k]}{N_c}\sum_{n=0}^{N_c-1} h(n)e^{j\Phi_{Amp}(n)}e^{j\Phi_{Dop}(n)} + \frac{1}{N_c}\sum_{m=0,m\neq k}^{N_c-1} X[m]\sum_{n=0}^{N_c-1} h(n)e^{j(\frac{2\pi}{N_c})(m-k)n} \\ & e^{j\Phi_{Amp}(n)}e^{j\Phi_{Dop}(n)} + W[k] \end{aligned} \tag{2.12}$$

Eq.(2.12) can be simplified as

$$\begin{aligned} Y[k] &= \underbrace{X[k]H[k]\Phi_{Amp}[0]\Phi_{Dop}[0]}_{desired \quad signal \quad \times \quad \Phi[0]} + \underbrace{\frac{1}{N_c}\sum_{m=0,m\neq k}^{N_c-1} X[m]\sum_{n=0}^{N_c-1} h(n)e^{j(\frac{2\pi}{N_c})(m-k)n}e^{j\Phi_{Amp}(n)}e^{j\Phi_{Dop}(n)}}_{\beta[k]} \\ &+ W[k] \end{aligned} \tag{2.13}$$

From Eq.(2.13) it is clear to state that the common phase error components $\Phi_{Amp}[0]$ and

$\Phi_{Dop}[0]$ are multiplied to every subcarrier and cause a constant rotation to the whole OFDM symbol [42]. All subcarriers contribute to the ICI term $\beta[k]$ and is added to the desired signal of each subcarrier. Hence, the frequency-domain received signal in subcarrier k can be expressed as

$$Y[k] = H[k]X[k]\Phi_{Amp}[0]\Phi_{Dop}[0] + \beta[k] + W[k] \tag{2.14}$$

where $X[k]$ is the frequency-domain transmitted signal, $H[k]$ is the frequency-domain channel coefficient, $\Phi_{Amp}[0]$ and $\Phi_{Dop}[0]$ are the common phase error components, $W[k]$ is the AWGN can be considered as a Gaussian random variable with zero mean and variance σ_W^2, and $\beta[k]$ is the ICI signal given by

$$\beta[k] = \sum_{m=0,m\neq k}^{N_c-1} X[m]H[m]\Phi_{Amp}[m-k]\Phi_{Dop}[m-k] \tag{2.15}$$

As aforementioned, the multiplexing mechanism for BWANs is achieved using OFDM technology, therefore sharing the same OFDM symbol between MSs, increases the ICI level and the probability of subcarriers collision, thus decreasing the system's capacity. These issues become more complicated in the MMR system, hence degrade the overall system performance. Quantification of the ICI and subcarriers collision is needed to improve the user's experience, thus increasing the system capacity. In the following, related works to ICI and subcarriers collision as well as the OFDM system capacity over multi-hop relaying channels are discussed in detail.

2.3.1 Inter-carrier Interference

OFDM is one of the key component broadband technology deployed in both fixed and mobile BWANs, therefore networks based on OFDM have gained considerable attention lately. OFDM provides an efficient broadband data transmission by sending parallel data over a number of subcarriers. To increase the data rate for a given OFDM system, the number of subcarriers per OFDM symbol should be increased. As the number of subcarriers increases however, the frequency spacing between the subcarriers in the OFDM symbol reduces. This makes the OFDM system more sensitive to phase noise which destroys the orthogonality of the subcarriers, causing ICI.

Several issues cause ICI in OFDM system, hence degrade the bit error rate (BER) performance. To name two of these issues: first, high PAPR (peak-to-average power ratio) with nonlinear amplifier. In OFDM systems, because of the high fluctuations in the level of the instantaneous signals transmitted, PAPR in OFDM systems is typically large, making the operation solely over the linear region of high power amplifier (HPA) difficult. When some portions of the OFDM signals transmitted operate in the nonlinear region of the HPA, nonlinear distortions are introduced in the OFDM signals, resulting in phase noise which contributes to the ICI [5], [11], [12], [51], [19], [29], [39], [42], [48], [53] and [63], and second, Doppler Shift effect, relative speed between the transmitter and receiver in a wireless channel, introduces Doppler Shift in the received frequencies, contributing also to the ICI [54], [59], [77] and [68].

To study the performance of an OFDM relaying system, effects such as HPA nonlinearity and Doppler Shift should be taken into consideration. However, HPA effects on the OFDM symbol have received little research attention. The work in [11], investigates the effect of HPA on the transmitted OFDM signal. The outcome of this investigation is a

development of an accurate statistical analysis, which identifies the HPA effect that affects the transmitted OFDM signal, these statistical findings are verified by simulation.

An algorithm for estimating the ICI caused by HPA is proposed in [42]. This algorithm estimates the ICI effect using a repeated data symbol. It has been shown that for small error in the estimation, the estimation is still consistent. Furthermore, the transmitted signal and the ICI caused by HPA contribute to the estimation, therefore it is possible to obtain very accurate results even when the ICI effect is unacceptable. The performance is computed analytically and compared with simulation results. In [5], the pilot-based channel estimation scheme is suggested. This scheme is used to combat the channel impairment as well as correct the ICI effect. The results show that the channel impairment is completely eliminated and the ICI effect is mitigated.

In [19], the effect of the HPA is avoided by considering a sufficient back-off period, therefore the power amplifier is considered to be linear. However, this is considered as a suboptimal solution for power efficiency. The receiver cancelation of power amplifier nonlinearity as well as a detection technique for clipped OFDM symbols in a cooperative relay network is proposed in [51]. The objective of this proposal is to consider the nonlinear amplifier effect at the receiver to improve the power efficiency of the system.

Several theoretical characteristics of the nonlinear effects on the transmitted OFDM signal is presented in [12]. An analytical method to evaluate error probability is obtained and simulation results are carried out for a comparison to verify the accuracy of the obtained method.

The BER of OFDM relay links with a nonlinear power amplifier is analyzed in [53]. An exact closed-form expressions for the BEPs are determined. The expressions help to analyze the effect of HPA on the transmitted signal. The analysis proves that the consequences

of the amplifier nonlinearity effects can be mitigated by adjusting the power amplifier back-off.

Doppler Shift arising from MS's mobility, destroys the subcarriers' orthogonality, causing ICI, however a number of efforts have been reported in the literature [59], [77], [68] and [54] for OFDM system performance analysis considering Doppler Shift. In [59], an algorithm was proposed for Doppler Shift estimation, but this algorithm can only be applied to signals on the pilot subcarriers. Therefore, to obtain an accurate estimation of the Doppler Shift, a large number of OFDM symbols is required, and this results in a longer estimation delay. Another algorithm for Doppler Shift estimation is proposed in [77]. The algorithm is based on the autocorrelation of time-domain channel. However, the receiver still has to know the fading channel coefficient in order to perform the Doppler Shift estimation. This process results in higher complexity at the receiver.

The performance of an OFDM system was analyzed in [68] with the consideration of Doppler Shift. A statistical analysis for the ICI is provided, where a closed-form formula of the ICI is obtained that was used to determine the probability density function (pdf) of the ICI. The obtained formula is used to evaluate the performance of the OFDM system. In [54], authors examine the effects of ICI through an analytical analysis and the results were verified by simulation in the context of single-hop. It is shown that ICI can be modeled as additive Gaussian random process that causes an error floor which can be identified analytically as a function of the Doppler Shift.

Furthermore, the analysis of ICI in terms of signal-to-interference ratio (SIR) and signal-to-interference-plus-noise ratio (SINR) is available in [48], [5] and [44]. The performance of OFDM system was analyzed considering the assumption that the ICI follows

the Gaussian distribution [62], [54], [71], [10], [28], [78] and [57]. In [28], the Gaussian approximation of the ICI is applied to obtain expressions for BER analysis in AWGN channel. It is shown by simulation that such an approximation is pessimistic when the BER is small. A more accurate BER expression that uses the moments of the ICI distribution is proposed in [78]. Moreover, in [57], the exact SER in AWGN channel is derived. In [28], [78] and [57] however, the authors only consider the frequency shift effects in AWGN channel, while OFDM system is designed to overcome problems arising due to multipath fading channels. BER analysis using Gaussian approximation of the ICI in Rayleigh fading channel is reported in [21].

However, most of these works have been done only in the context of single-hop communications. Therefore, the extent to which OFDM subcarriers loose orthogonality and consequently the resulting ICI, when transmitting OFDM symbols over multi-hop relaying channel with HPA nonlinearity and Doppler Shift effects is to date not known for various OFDM configurations. Accurate characterization of the ICI problem due to Doppler Shift and HPA distortion over multi-hop relaying channel would allow the development of novel algorithms for alleviating the problem.

2.3.2 Subcarriers Collision

The worldwide intropera bility for microwave access (WiMAX) based on IEEE 802.16 and IEEE 802.16e standards technologies provides last mile broadband wireless access. IEEE 802.16e deploys OFDM as modulation scheme and OFDMA as an access mechanism to serve fixed and mobile users. WiMAX technology is considered as an alternative to existing technologies such as digital subscriber lines (DSL) and cable. OFDM provides an efficient

broadband data transmission by sending parallel data over a number of closely-spaced subcarriers. For multi-user support, OFDMA is used. In OFDMA, the OFDM subchannels are assigned to users for their radio access, where each subchannel consists of a number of subcarriers. One or more subchannels can be assigned to a MS depending on the application (i.e., voice or data, etc.).

One of the limitations of the OFDM-based systems is frequency reuse, as a channel can only be reused if the interference in the network is minimized. Frequency reuse allows one or more MSs to share the same OFDM symbol, therefore interference level in the network increases as the number of MSs sharing OFDM subchannels increases. This also makes the OFDMA system more sensitive to subcarriers collision, which further increases the level of interference.

In the literature, a number of solutions are available for reducing the interference caused by subcarriers reuse in a single-hop BWAN [22], [56], [23], [8], [65], [35], and [33]. In [22], cell sectorization and special channel allocation for reducing the interference are proposed. The cell area is divided into a number of sectors then different channels are assigned to different sectors. This scheme helps to reduce interference, but the number of supported MSs is reduced as well. Fractional frequency reuse (FFR) scheme is proposed in [56]. This scheme is used to minimize interference, where each cell sector is assigned a fraction (e.g. $1/3^{rd}$) of the available subcarriers. In this case, fewer subcarriers are used, therefore interference can be reduced. The disadvantage of using this scheme is the limited capacity in terms of the possible number of users that can be supported. For IEEE 802.16 networks, interference calculations for *single-hop* based on simulations are available in [23].

An analytical model for calculating the BER in OFDMA system using multiple antennas at each BS is developed in [8], where the system performance is estimated using a

collision-based approach. In [65], authors analyzed the capacity of the downlink OFDMA system focusing on the effect of adaptive modulation and coding (AMC) scheme as well as reuse partitioning in the case of more than one cell. In [35], BER performance is evaluated in frequency-hopping OFDMA system considering the effect of subcarriers collision. The available number of subcarriers is divided into a number of clusters, then two cases were studied, random and cluster subcarrier hopping. It was observed that the collision rate is the same for both cases, therefore it is better to consider cluster hopping for system design simplicity. A space-frequency coding is used to reduce the subcarriers collision in a single-hop system. It is shown that the number of subcarriers collision is reduced resulting in a better BER performance using the space-frequency coding [35], [33].

Frequency reuse becomes more complicated in the MMR system, because more RSs, consequently more MSs use the same frequencies, therefore the interference level becomes high, which degrades the system performance. A quantification of the expected number of collisions between the occupied subcarriers is still needed for devising a technique to improve the performance of the MMR system.

2.3.3 OFDM System Capacity

The multi-hop relaying concept in which the communication between a source node and a destination node can be achieved through a number of relays, is considered to be a promising solution to extend the coverage area and improve the capacity of wireless communication systems. The concept of a relaying channel was introduced in [69] and [70] while standardized in [26]. The capacity of Gaussian relaying channel was investigated for single relay in [14], [15], [20] and [72], while for multiple relays was studied in [38], [52] and [32].

Relaying concept is more tractable in fading channels to improve the communication link between the source node and destination node. Although the capacity of relaying system considering Nakagami-*m* fading was evaluated in [27], and also considering independent frequency-flat slow fading channels was studied in [76]. K. Hamdi in his work [18], derived the capacity of OFDM system with frequency offset in Rician Fading channel. It is shown that the capacity drops as the frequency offset increases.

For single relay, the upper and lower bounds on the capacity were derived considering a relay channel in Rayleigh fading with optimal power allocation in [20]. A practical constraint on the transmission and reception duplexing at the relay station and on the synchronization between the source station and the relay station as well as the power allocation are considered. The obtained results show that optimum relay channel signaling can significantly outperform the direct transmission and traditional multi-hop protocols. Also, the power allocation has significant impact on the system performance.

In [6], the capacity of multi-hop wireless transmission systems in Rayleigh fading, considering both AF and DF relaying schemes is studied. Two upper bounds for the capacity of AF multi-hop transmission systems are obtained. Also, the capacity of a DF multi-hop transmission system is derived. It is concluded that multi-hop transmission systems employing DF relaying schemes performed better than multi-hop transmission systems with AF schemes. Numerical results are provided to test the tightness of the two upper bounds. Authors in [15], provide a detailed discussion and several extensions of the bounds on capacity and minimum energy-per-bit for AWGN relay channels presented in [80] and [7].

The capacity of a class of relay channels is studied in [14]. In this work, the main focus was on finding the optimal broadcasting strategy from source to destination. The optimal strategy discussed in this study however, is to split the transmitted signal into two parts,

one to be coded by the relay and send simultaneously with the other part from the sender directly to the receiver. It is shown that other strategies such as linear relaying and side information coding can achieve better results.

For multiple relays, a coding scheme to achieve better data rate in a multi-level relay channel is proposed in [38]. An expression for the achievable rate is presented. The results show that, the achievable rate is higher than what have been achieved using pervious proposals. The work presented in [38] for single-relay is extended in [52], a power allocation scheme that maximizes the system capacity is derived. The obtained results demonstrate that there are some advantages which can be achieved using relays approach.

In [32], coding strategies are developed to exploit node cooperation for relay networks. Two schemes are studied: first, the decode-and-forward (DF), by which the relays DF the source message to the destination, second, the compress-and-forward (CF), by which the relays CF the channel outputs to the destination. In order to achieve better performance, the DF scheme is used in multi-hop communications, but the transmitters should also cooperate and each receiver uses the past channel output to decode the messages. For the CF scheme, the relays consider the statistical dependence between the channel outputs and the destinations channel output. These strategies are applied to relaying channels, and it is shown that DF scheme achieves better performance than CF scheme.

In [72], the capacity of the multiple-input-multiple-output (MIMO) relay channel is studied. The MIMO relay channel with fixed channel conditions is considered, then a Rayleigh fading is considered. For both cases, the upper bounds and lower bounds of the capacity are derived. The capacity is obtained when all nodes have the same number of antennas, and it is shown that the capacity can be achieved under certain SNR conditions.

The limitation of those efforts is that they do not consider the common issue that affects

the performance of the OFDM system, which is the ICI effect. As aforementioned, in OFDM systems, as the number of subcarriers per OFDM symbol increases, the data rate increases, however, the frequency spacing between the subcarriers in the OFDM symbol reduces. This makes the OFDM system more sensitive to phase noise which destroys the orthogonality of the subcarriers, causing ICI. The resulting ICI has an unacceptable impact on the data rate which causes degradation of the system capacity.

The cascade effect of the multiple relaying channel dramatically amplifies the ICI effect for the underlying OFDM system [63]. However, neither the available analysis is done for OFDM systems with the consideration of ICI effect nor takes into consideration the accumulative effect of ICI over multi-hop relaying channels. The evaluation of the OFDM system capacity over multi-hop relaying channels in the presence of the ICI is still an open issue, and should be considered to improve the overall system capacity.

2.4 Summary

This chapter presented an overview of broadband wireless networks, specifically we explained in detail the MMR system. The system architecture, relay stations types and possible deployment scenarios as well as their features were discussed. In this chapter we also, discussed the OFDM system and explained the different steps the OFDM symbol traverse through from source node to destination node as well as the channel impairments that affect the transmitted signal. Furthermore, this chapter provided existing research efforts that have been done for issues related to OFDM system. The available works for inter-carrier interference, subcarriers collision and capacity analysis in OFDM system were discussed.

In this thesis, we aim at quantifying the effects of the aforementioned issues in the

transmitted OFDM signal as well as the resulting accumulative effects over multi-hop relaying channels. This is achieved by performing a mathematical analysis for capturing the ICI effect on the transmitted OFDM symbol, and by defining the expected number of collisions in the deployed OFDMA system. The MMR system capacity is studied considering the effect of ICI on the transmitted signal; also simulation results are provided to validate the analysis.

Chapter 3

Analysis of Inter-Carrier Interference Effects

3.1 Introduction

Inter-carrier interference have a great impact on the performance of BWANs based on OFDM technology, since it results in orthogonality distortions between subcarriers of the OFDM symbol. The main issues causing phase noise, consequently ICI in OFDM systems are High power amplifier and Doppler Shift. The high PAPR in OFDM is typically large, because of the high fluctuations in the level of the instantaneous signals transmitted, making operation solely over the linear region of HPA difficult. Therefore, when some portions of the OFDM signals transmitted operate in the nonlinear region of the HPA, nonlinear distortions are introduced in the OFDM signals, resulting in phase noise which contributes to the ICI [63],[11]. Also, relative speed between the transmitter and receiver in a wireless channel, however introduces Doppler Shifts in the received frequencies, contributing to the ICI. With a digital implementation of the modulation circuits in most practical systems,

several high performance classical frequency offset estimators for synchronization problems in OFDM systems are available [39], [42], [58], [43], and [82]. However, Doppler Shift and HPA issues still pose significant problems in most practical systems and should be given due consideration in the design of broadband multi-hop relaying communication systems, where the OFDM symbols typically traverse several hops from source nodes to the destination nodes.

In this chapter, we develop an analytical method to study the effects of HPA nonlinearity and Doppler Shift on the transmitted OFDM signals and present the statistical characteristics of these impairments over two-hop relaying channels. The main contribution of this chapter is the derivation of the SINR expression as a function of HPA nonlinearity and Doppler Shift Effect. The obtained SINR expression is used to derive a closed-form formula for the probability of error which is used to calculate the average SER as well as measure the BER performance in the two-hop relaying OFDM system.

The remainder of this chapter is organized as follows. Section 3.2 describes the system model. Section 3.3, demonstrates the BER performance analysis. Section 3.4, illustrates the validation of the theoretical analysis by simulation results through a comprehensive performance evaluation, and finally, section 3.5 summarizes the chapter.

3.2 System Model

We consider a two-hop amplify-and-forward OFDM relaying system, with each OFDM symbol consisting of N_c subcarriers. We consider the uplink scenario, where the transmitted signal from a mobile station (MS) originating the data (or source node, $\mathcal{S}$), passes through R relay station (RS) to the multi-hop base station (MR-BS) (or the destination

node, $\mathcal{D}$). The direct channel between the source and destination is considered to be very attenuated and unable to provide a communication with acceptable quality. There are U users in the system, each user occupy one OFDM symbol, uniformly distributed in the coverage area of the BS, and that each user can be associated with the BS or a RS whichever provides stronger signal-to-noise ratio (SNR). An example of this model for the case $R = 2$ (*two-hops* relay network), $r = 1, \ldots, R$ is illustrated in Figure 3.1 for a cellular deployment, in which each cell is serviced by a BS, located at the center of the cell, and six fixed RSs $(N = 6)$, each equidistant from the BS and located at the center of each side of the hexagon as shown.

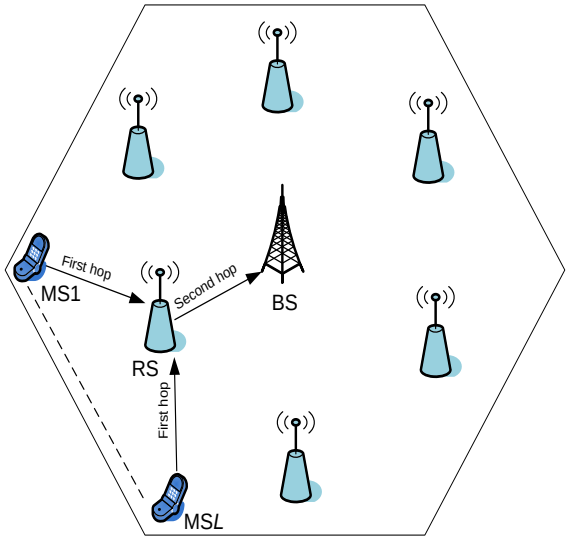

Figure 3.1: Mobile Multi-hop Relaying System

We model a MMR system where the transmitted OFDM symbol from an MS passes through two-hop relaying channels $H_r, r = 1, \ldots, R$ to the BS. As mentioned in chapter 2, each transmitted OFDM symbol is affected by the channel impairments of each hop traversed. Here we focus on two impairments namely amplifier distortion (Φ_{Amp}), and

Doppler Shift (Φ_{Dop}). We consider that the Amplify-and-Forward (AF) relay option is employed at the relay nodes, where RSs simply amplify and froward the OFDM symbol at the radio frequency (RF) stage, without decoding its content. The RS demodulates the OFDM symbol, then amplifies all subcarriers separately. All relay nodes employ amplifiers with gain (or amplification factor) α. The mobile channel for the first-hop transmission (MS-RS) is modelled as a Rayleigh fading channel, where $H_{r-1}[k]$ is the fading on the k^{th} OFDM subcarrier, $k = 0, 1, \ldots, N_c - 1$, therefore the SINR of the first-hop can be considered as an exponential random variable (RV). The average SINR $\overline{\gamma}_{r-1}[k] = E[\gamma_{r-1}[k]]$ can be different for all k. In the second-hop, the source and destination are fixed infrastructure (relay station and base station), therefore the (RS-BS) channel $H_r[k]$ can be considered as a slow fading [5]. Thus, $\gamma_r[k] = \overline{\gamma}_r[k]$ for all k. Figure 3.2 depicts the cascade effect of the two-hop relaying channel on the OFDM system.

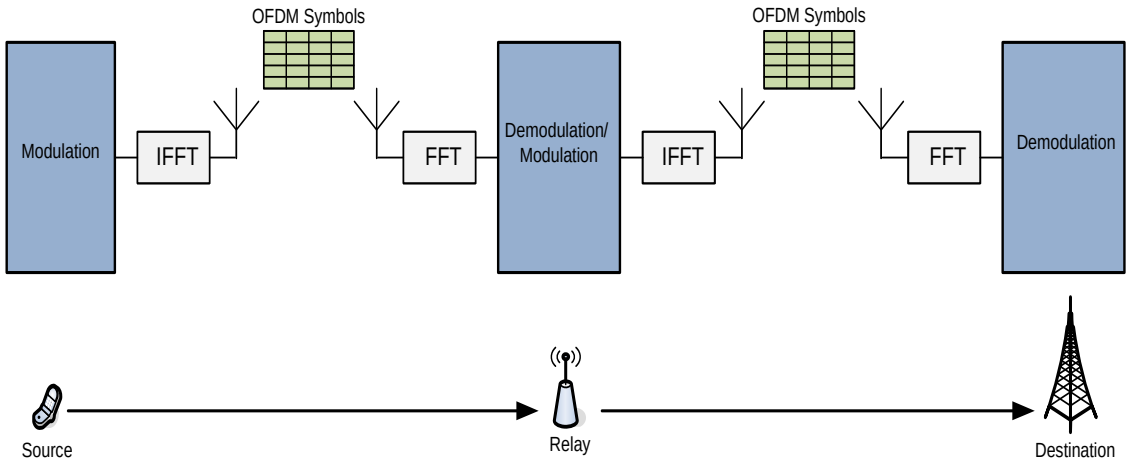

Figure 3.2: Amplify and Forward two-hop relaying channel model for OFDM systems

[5]Some channel fluctuations will be present due to mobile terminals in the propagation path between a source and destination, but the slow fading components will have stronger effects, therefore the channel variation during one OFDM symbol considered to be slow

Each MS's data which is considered in this system to be quadrature amplitude modulation (QAM) signal, is modulated with N_c subcarriers to produce N_c data points in frequency-domain $X[k]$, where the transmit power is $P = E[|X[k]|^2]$ for all k. These data points are fed to an Inverse Fast Fourier Transform (IFFT) function whose output is a time-domain signal $x(\tau)$. The cyclic prefix (*CP*)[6] is added to the OFDM symbol to combat inter symbol interference (ISI) introduced by the channel in each hop. It is worth to mention that no coding scheme is used. The time-domain signal $x(\tau)$ is fed to HPA which modeled by a static memoryless nonlinearity, $f(.)$ to produce an amplified time-domain signal $\widehat{x}(\tau)$ expressed as

$$\widehat{x}(\tau) \quad = \quad x(\tau) + \Phi_{Amp}(\tau) \tag{3.1}$$

where $\Phi_{Amp}(\tau)$ is the signal distortion caused by HPA nonlinearity. The time-domain signal $\widehat{x}(\tau)$ can be written in frequency-domain as

$$\widehat{X}[k] \quad = \quad X[k] + \Phi_{Amp}[k] \tag{3.2}$$

when the HPA operates close to the saturation point, the distortion term $\Phi_{Amp}[k]$, becomes Gaussian [29], with power $\sigma^2_{\Phi_{Amp}} = E[|\Phi_{Amp}[k]|^2]$. Figure 3.3 illustrates the amplifier response at each RS. For the second impairment, the transmitted signal is shifted by Doppler effect $\Phi_{Dop}[k]$ after passing through the channel $H[k]$, with f_d denoting the frequency offset between the transmitter and the receiver and is given by $f_d = \frac{f_c * V_{SD}}{c} = \frac{V_{SD}}{\lambda}$. Where f_c

[6]To simplify our analysis, the cyclic prefix is not directly reflected in our equations, but its use is implied.

is the transmitted frequency, V_{SD} is the velocity of the transmitter relative to the receiver (m/s), c is the speed of the wave $(3 \times 10^8 (m/s))$, and $\lambda = \frac{c}{f_c}$ is the wavelength. The distortion term $\Phi_{Dop}[k]$ has power $\sigma^2_{\Phi_{Dop}} = E[|\Phi_{Dop}[k]|^2]$.

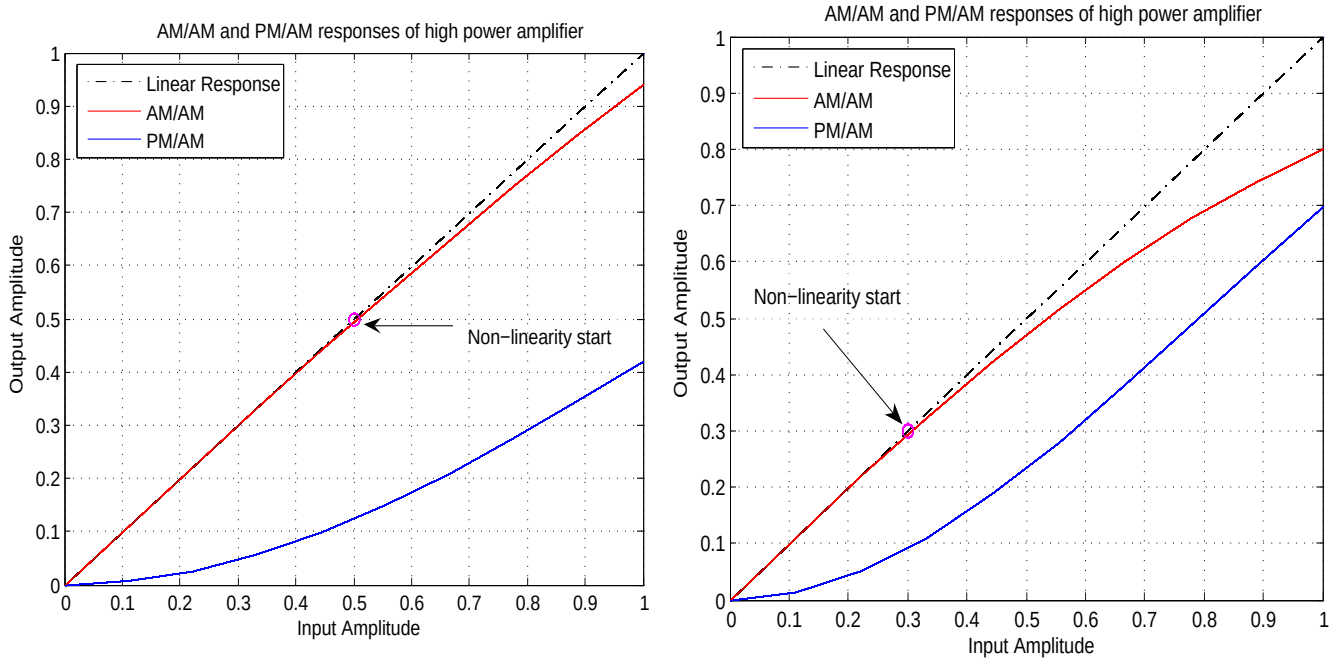

(a) OFDM Symbol without frequency shift

(b) OFDM Symbol with frequency shift

Figure 3.3: High power Amplifier Response

Therefore, the received signal $Y_R[k]$ can be expressed as

$$Y_R[k] = \widehat{X}[k] H_{r-1}[k] + W_R[k] \tag{3.3}$$

where $W_R[k]$ is the AWGN term at the RS with power $\sigma^2_R = E[|W_R[k]|^2]$. Considering the

frequency-domain signal at the HPA output $\widehat{X}[k]$ and Doppler Shift effect $\Phi_{Dop}[k]$, Eq.(3.3) can be rewritten as

$$Y_R[k] = X[k]H_{r-1}[k] + \Phi_{Amp,S}[k]\Phi_{Dop,SR}[k]H_{r-1}[k] + W_R[k] \quad (3.4)$$

where $\Phi_{Amp,S}[k]$ is the HPA effect at the source (MS), and $\Phi_{Dop,SR}[k]$ is the Doppler Shift effect at the first-hop. Figure 3.4 demonstrates the ICI effect in an OFDM symbol with 7 subcarriers.

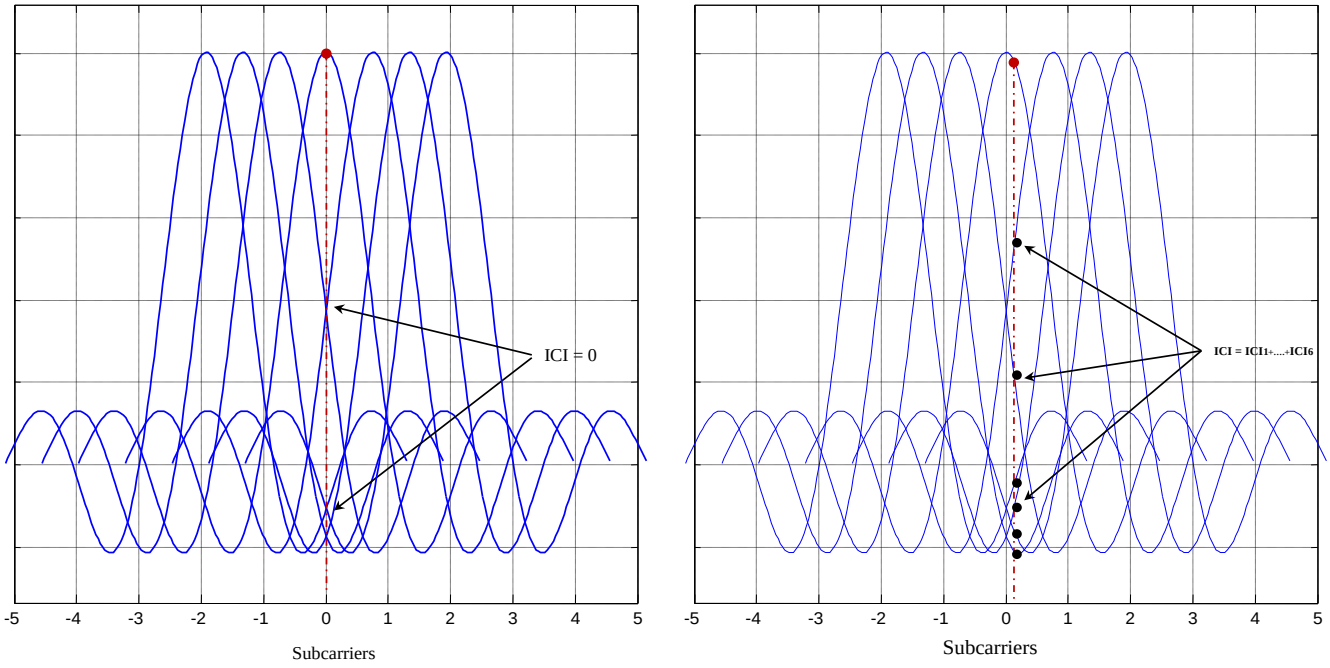

(a) OFDM Symbol without frequency shift

(b) OFDM Symbol with frequency shift

Figure 3.4: Inter-Carrier Interference effects in OFDM symbol

Therefore at the receiver side, after the cyclic prefix is removed, the time-domain received signal is fed to Fast Fourier Transform (FFT) function whose output is frequency-domain signal. Then the demodulation is performed to recover the QAM signals on each of the N_c subcarriers. The RS amplifies each subcarrier with amplification factor $\alpha[k]$, where $X_R[k] = \alpha[k]Y_R[k]$. The well known nonlinear memoryless amplifier [37], is adopted in this chapter, the expression for $\alpha[k]$ is given by

$$\alpha[k] = \sqrt{\frac{P_R}{(\sigma^2_{\Phi_{Amp,S}})P_S|H_{r-1}[k]|^2 + \sigma^2_R}} \tag{3.5}$$

Therefore, the signal at the RS's HPA output can be simplified as

$$X_R[k] = \alpha[k]X[k]H_{r-1}[k] + \alpha[k]\Phi_{Amp,S}[k]\Phi_{Dop,SR}[k]H_{r-1}[k] + \alpha[k]W_R[k] \tag{3.6}$$

After the amplified signal $X_R[k]$ transmitted over the channel of the second-hop $H_r[k]$, the received signal $Y_D[k]$ can be expressed as

$$Y_D[k] = X_R[k]H_r[k] + \Phi_{Amp,R}[k]\Phi_{Dop,RD}[k] + W_D[k] \tag{3.7}$$

where $W_D[k]$ is the AWGN term at the destination with power $\sigma^2_D = E[|W_D[k]|^2]$, $\Phi_{Amp,R}[k]$

is the HPA effect at the relay (RS), and $\Phi_{Dop,RD}[k]$ is the Doppler Shift effect at the second-hop. Substituting the amplified signal, $X_R[k]$ from Eq.(3.6) into Eq.(3.7) gives

$$\begin{aligned} Y_D[k] &= \alpha[k]X[k]H_{r-1}[k]H_r[k] + \alpha[k]X[k]\Phi_{Amp,S}[k]\Phi_{Dop,SR}[k]H_{r-1}[k]H_r[k] \\ &+ \alpha[k]W_R[k]H_r[k] + X[k]\Phi_{Amp,R}[k]\Phi_{Dop,RD}[k]H_r[k] + W_D[k] \end{aligned} \tag{3.8}$$

We consider that the HPA distortions and Doppler Shift effects are introduced at each hop the OFDM symbol traverse through [1],[4]. The received signal power $E[|Y_D[k]|^2]$ at the destination can be expressed as

$$\begin{aligned} E[|Y_D|^2][k] &= \underbrace{|\alpha[k]|^2 P_S |H_{r-1}[k]|^2 |H_r[k]|^2}_{desired \quad signal} \\ &+ \underbrace{|\alpha[k]|^2 P_S |H_{r-1}[k]|^2 |H_r[k]|^2 \sigma^2_{\Phi_{Amp,S}} \sigma^2_{\Phi_{Dop,SR}} + \sigma^2_{\Phi_{Amp,R}} \sigma^2_{\Phi_{Dop,RD}} P_R |H_r[k]|^2}_{ICI} \\ &+ \underbrace{|\alpha[k]|^2 \sigma^2_R |H_r[k]|^2 + \sigma^2_D}_{noise} \end{aligned} \tag{3.9}$$

3.3 BER Performance Analysis

In this section, we analyze the BER performance of two-hops relaying OFDM system, in the presence of HPA distortions and Doppler Shift effects. A closed-form expression for the probability of error $P_e(k)$ is derived, then used to calculate the symbol error rate as well as to measure the bit error rate performance. In the following section, the end-to-end SINR expression is derived.

3.3.1 End-to-End SINR Expression

We concentrate on the uplink communication, where the source is considered to be a mobile entity with non line-of-sight (NLOS) communication link with the RS, therefore the MS-RS channel, $H_{r-1}[k]$ is modeled as a Rayleigh fading. Thus, the first-hop SINR for the k^{th} subcarrier is considered to be an exponential RV, which has the probability density function expressed as

$$f_{\gamma_{r-1}}[k](z) = \Big(\frac{1}{\overline{\gamma}_{r-1}[k]}\Big) e^{\left(\frac{-z}{\overline{\gamma}_{r-1}[k]}\right)} \tag{3.10}$$

where the average SINR, $\overline{\gamma}_{r-1}[k] = E[\gamma_{r-1}[k]]$. The communication in the second-hop is between two fixed entities (i.e., base station and relay station), therefore the RS-BS channel, $H_r[k]$ can be considered as a slow fading. Thus, $\gamma_r[k] = \overline{\gamma}_r[k]$ for all k. On the other hand, the frequency selectivity can be achieved by allowing different $\overline{\gamma}_r[k]$ for different k. Therefore, the SINR expression of the two-hops can be defined as follow

$$\gamma_{r-1}[k] = \frac{P_S|H_{r-1}[k]|^2}{\sigma^2_{\Phi_{Amp,S}}\sigma^2_{\Phi_{Dop,SR}} + \sigma^2_R}, \qquad \gamma_r[k] = \frac{P_R|H_r[k]|^2}{\sigma^2_{\Phi_{Amp,R}}\sigma^2_{\Phi_{Dop,RD}} + \sigma^2_D} \tag{3.11}$$

Therefore, the end-to-end SINR, after defining the received signal power $E[|Y_D[k]|^2]$ terms, the desired signal P_{des}, the distortion signal P_{ICI} and noise term P_{noi}, can be expressed as

$$\gamma[k] \;=\; \frac{P_{des}}{P_{ICI} + P_{noi}} \tag{3.12}$$

After substituting the received signal terms P_{des}, P_{ICI} and P_{noi}, and considering the SINR in Eq. (3.11) with some manipulations, the end-to-end SINR can be simplified as

$$\gamma[k] = \frac{\frac{\gamma_{r-1}[k]\gamma_r[k]}{\left(\sigma^2_{\Phi_{Amp,S}}\sigma^2_{\Phi_{Dop,SR}}\gamma_{r-1}[k]+1\right)\left(\sigma^2_{\Phi_{Amp,R}}\sigma^2_{\Phi_{Dop,RD}}\gamma_r[k]+1\right)}}{\left(\frac{\gamma_{r-1}[k]}{\sigma^2_{\Phi_{Amp,S}}\sigma^2_{\Phi_{Dop,SR}}\gamma_{r-1}[k]+1}\right)+\left(\frac{\gamma_r[k]}{\sigma^2_{\Phi_{Amp,R}}\sigma^2_{\Phi_{Dop,RD}}\gamma_r[k]+1}\right)+1} \quad (3.13)$$

The end-to-end SINR formula shows the HPA nonlinearity distortion and Doppler Shift effects on the performance of the relay channels. Those effects are based on the Φ_{Amp} of the transmitters, MS or RS, and Φ_{Dop} of the relay channel.

3.3.2 Probability of error Expression Analysis

The probability of error $P_e(k)$ expression of the system over Rayleigh fading channels for M-ary QAM modulation scheme [36] is given by

$$P_e(k) = \frac{1}{\sqrt{M}log_2\sqrt{M}}\sum_{j=1}^{log_2\sqrt{M}}\sum_{n=0}^{v_j}p_n^j \times erfc(\sqrt{g_n\gamma[k]}) \quad (3.14)$$

where $v_j = (1-2^{-j})\sqrt{M}-1$, $p_n^j = (-1)^{\lfloor\frac{n2^{j-1}}{\sqrt{M}}\rfloor}(2^{j-1}-\lfloor\frac{n2^{j-1}}{\sqrt{M}}+\frac{1}{2}\rfloor)$, $g_n = \frac{(2n+1)^2 3log_2 M}{2M-2}$, M is the constellation order, erfc is the complementary error function ([61], Eq.(4A.6)), and $\lfloor.\rfloor$ is the floor. The average probability of error $P_e(k)$ can be calculated as follow

$$\overline{P}_e(k) = \int_0^\infty P_e(k)\big|_{\gamma_{r-1}[k]=z} f_{\gamma_{r-1}[k](z)}dz \quad (3.15)$$

Substituting Eqs.(3.13) and (3.14) into Eq.(3.15), gives

$$\overline{P}_e(k) = \int_0^{\infty} \frac{1}{\sqrt{M}log_2\sqrt{M}} \sum_{j=1}^{log_2\sqrt{M}} \sum_{n=0}^{v_j} p_n^j \times erfc(\sqrt{g_n\gamma[k]}) f_{\gamma_{r-1}[k](z)} dz \quad (3.16)$$

Substituting the pdf for the SINR of the first-hop, $f_{\gamma_{r-1}}[k](z)$, Eq.(3.16) can be rewritten as

$$\overline{P}_e(k) = \int_0^{\infty} \frac{1}{\sqrt{M}log_2\sqrt{M}} \sum_{j=1}^{log_2\sqrt{M}} \sum_{n=0}^{v_j} p_n^j \times erfc\big(\sqrt{g_n\gamma[k]}\big) \Big(\frac{1}{\overline{\gamma}_{r-1}[k]}\Big) e^{\left(\frac{-z}{\overline{\gamma}_{r-1}[k]}\right)} dz \quad (3.17)$$

which can be rearranged as

$$\overline{P}_e(k) = \frac{1}{\sqrt{M}log_2\sqrt{M}} \sum_{j=1}^{log_2\sqrt{M}} \sum_{n=0}^{v_j} p_n^j \times \int_0^{\infty} erfc\big(\sqrt{g_n\gamma[k]}\big) \Big(\frac{1}{\overline{\gamma}_{r-1}[k]}\Big) e^{\left(\frac{-z}{\overline{\gamma}_{r-1}[k]}\right)} dz \quad (3.18)$$

The closed-form formula for $\overline{P}_e(k)$ can be expressed as follow

$$\overline{P}_e(k) = \frac{1}{\sqrt{M}log_2\sqrt{M}} \sum_{j=1}^{log_2\sqrt{M}} \sum_{n=0}^{v_j} p_n^j \left(1 - \sqrt{\frac{g_n\overline{\gamma}_{r-1}[k]^{-1}}{1+g_n\overline{\gamma}_{r-1}[k]^{-1}}}\right) \quad (3.19)$$

Using the obtained probability of error, $\overline{P}_e(k)$ the SER of the OFDM symbol can be expressed as [46].

$$SER_{(OFDM)} = \frac{1}{N_c} \sum_{k=0}^{N_c-1} \overline{P}_e(k) \tag{3.20}$$

Substituting Eq.(3.19) into Eq.(3.20) gives

$$SER_{(OFDM)} = \frac{1}{N_c\sqrt{M}log_2\sqrt{M}} \sum_{k=0}^{N_c-1} \sum_{j=1}^{log_2\sqrt{M}} \sum_{n=0}^{v_j} p_n^j \left(1 - \sqrt{\frac{g_n\overline{\gamma}_{r-1}[k]^{-1}}{1+g_n\overline{\gamma}_{r-1}[k]^{-1}}}\right) \tag{3.21}$$

Finally, the BER in a two-hops relaying network can be measured using the obtained $SER_{(OFDM)}$ as

$$BER = \frac{SER_{(OFDM)}}{log_2(M)} \tag{3.22}$$

Section 3.4, presents numerical and simulation results for BER performance, in the presence of HPA distortions and Doppler Shift effects. The derivation of the BER performance is obtained for a WiMAX network model which has two-hops maximum. The derivation can be extended to a general number of hops for any broadband network for instance, long term evolution (LTE).

3.4 Performance Evaluation

In this section, we evaluate the performance of our system by means of analytical analysis and simulation experiments. Simulation experiments were carried out using MATLAB. The obtained simulation results are used to validate the analytical analysis. The effects of HPA nonlinearity and Doppler Shift are considered in this evaluation. We first begin by describing the simulation model, then we discuss the channel model. Next, we present simulation results to verify the BER performance analysis of the MMR systems.

3.4.1 Simulation Model

We consider a single-cell scenario in our simulation. The base station is located at the center of the cell, and six fixed relay stations, each equidistant from the base station and located at the center of each side of the hexagon as shown in Figure 3.1. We consider the uplink scenario, where the transmitted OFDM symbol passes through a relay station to the base station. Also, we assume that the mobile stations are uniformly distributed in the coverage area of the base station, and each OFDM symbol is occupied by one user. A special case is considered where the power amplifier is linear and the MS is stationary, $\Phi_{Amp} = \pi/24$, and $\Phi_{Dop} = 0$, respectively. In the simulation model, three signal constellations are used 4-QAM, 16-QAM, and 64-QAM. The CP is added to each OFDM symbol ($N_c = 256$ subcarriers), to overcome ISI effects, the CP can take the values 25%, 12.5%, 6.25%, and 3.125% of the OFDM symbol length, however in this work only *CP* = 25% is used. The Doppler Shift values used in the simulation are 0Hz, and 100Hz, while the HPA distortion values are $\pi/24$, and $\pi/6$, respectively. The transmission of sufficient OFDM symbols through $R = 2$ hops is simulated, then the BER performance is measured. The obtained simulation results are used to validate those obtained by analytical analysis.

3.4.2 Channel Model

The channel model describes the attenuation of the radio signal when transmitted from source to destination, and therefore, it describes how the channel condition of the MS changes with time depending on the $MS's$ location and speed. In our simulation, the mobile channel for the first-hop transmission (MS-RS) is modelled as a Rayleigh fading channel, therefore the SINR of the first-hop can be considered as an exponential random variable (RV). In the second-hop, the source and destination are fixed infrastructure (relay station and base station), therefore the (RS-BS) channel can be considered as slow fading. The Amplify-and-Forward (AF) relay option is employed at the relay stations, where RSs simply amplify and froward the OFDM symbol at the radio frequency (RF) stage. The RS demodulates the OFDM symbol, then amplifies all subcarriers separately.

3.4.3 Performance Results

In this section, we show and discuss the simulation and analytical results of the BER performance in the MMR system for different QAM signal constellations, mobile speeds and HPA distortions.

Figure 3.5 and Figure 3.6 present the BER performance of single-hop ($R = 1$) and two-hop ($R = 2$) OFDM systems, respectively. The performance is measured using different QAM constellations (4, 16, and 64-QAM). For the illustration in these figures, the frequency shift is set to $f_d = 0$, and the amplifier distortion is set $\alpha = \pi/24$, which means the *MS* is stationary, and the HPA is applying the ideal linear characteristics. A perfect agreement is observed between the simulation and the analytical results in both systems. This means that neither Doppler Shift nor HPA distortion have any affect on the BER performance.

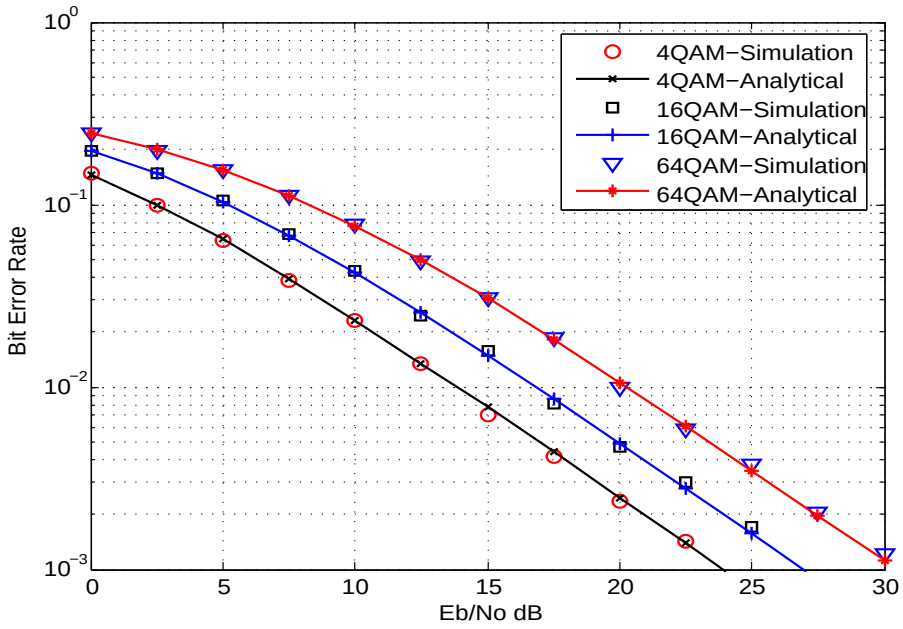

Figure 3.5: BER Performance versus E_b/N_0 of OFDM system over Rayleigh Fading channel, Single-Hop, R = 1, $f_d = 0Hz$, $\alpha = \pi/24$, $M = 4, 16, 64QAM$

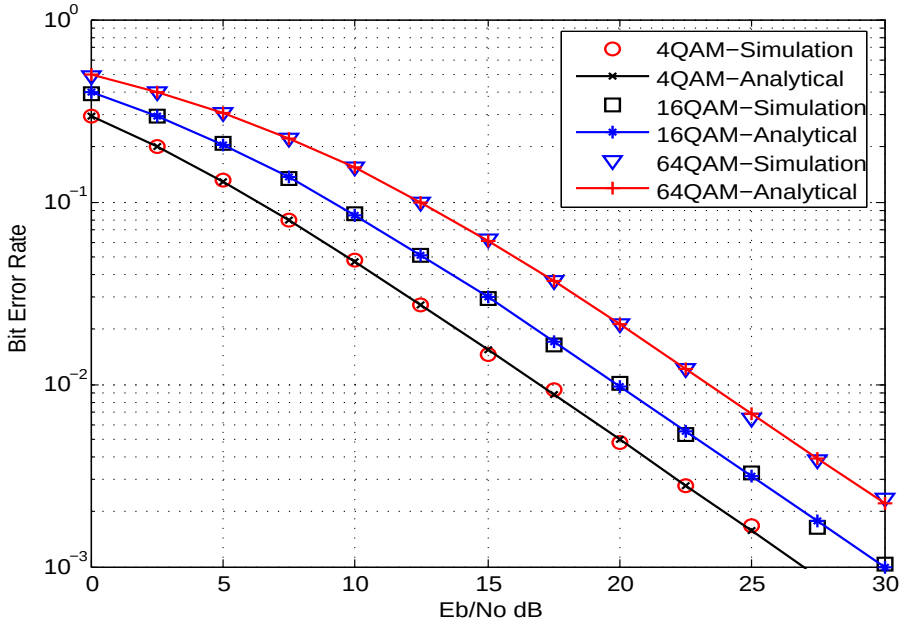

Figure 3.6: BER Performance versus E_b/N_0 of OFDM system over Rayleigh Fading channel, Two-Hop, R = 2, $f_d = 0Hz$, $\alpha = \pi/24$, $M = 4, 16, 64QAM$

Figure 3.7 and Figure 3.8 show the BER performance of single-hop and two-hop OFDM systems, respectively. For the demonstration in Figure 3.7 and Figure 3.8, we used the following values $f_d = 100Hz$, and $\alpha = \pi/6$. It can be observed from Figure 3.7 for single-hop system that the error floor is presented because of the HPA distortion and Doppler Shift impairments. In the case of 16QAM constellation, the error floor is higher than that in the case of 4QAM constellation order, while the highest error floor is measured for 64QAM constellation order. This is because more bits are transmitted which increase the probability of loss for the transmitted bits. Therefore, as the constellation order M increases, the ICI effect increases resulting in a higher error floor.

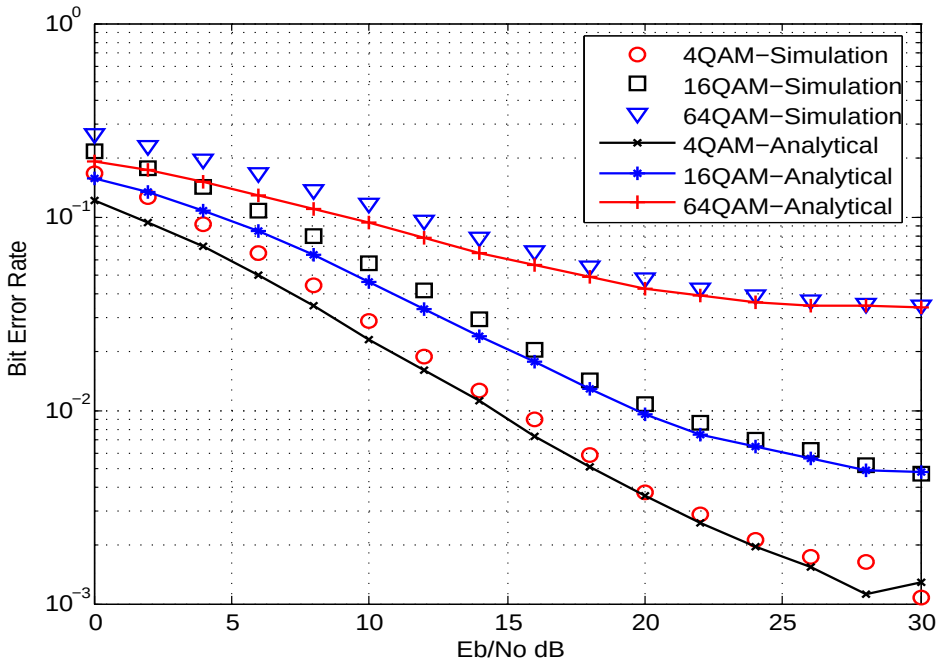

Figure 3.7: BER Performance versus E_b/N_0 of OFDM system over Rayleigh Fading channel, Single-Hop, R = 1, $f_d = 100Hz$, $\alpha = \pi/6$, $M = 4, 16, 64QAM$

Figure 3.8 illustrates the BER performance of two-hops OFDM system. It can be observed that the error floor in the case of 16QAM constellation order and two-hop relaying

system is higher than that in the case of single-hop system for the same constellation order. The highest measured error floor is in the case of two-hop relaying system and 64QAM constellation order due to ICI component as a result of Doppler Shift and HPA distortion as well as their cumulative effects over two-hop relaying channels. Hence, the number of hops and the constellation order control the performance of the BER in the relaying system, when channel impairments are present.

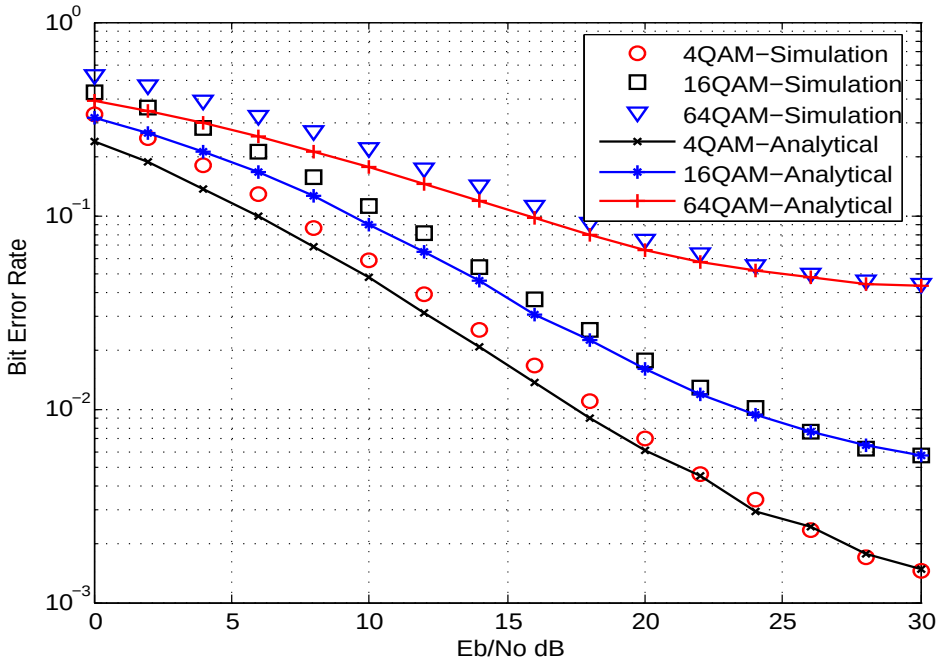

Figure 3.8: BER Performance versus E_b/N_0 of OFDM system over Rayleigh Fading channel, Two-Hop, R = 2, $f_d = 100Hz$, $\alpha = \pi/6$, $M = 4, 16, 64QAM$

3.5 Summary

In this chapter, BER performance analysis on the OFDM relaying system has been presented. Unlike most existing BER analysis, the work presented in this thesis considers the effects of amplifier nonlinearity and Doppler Shift over relaying channels. The HPA shifts

the transmitted signal before transmission over the channel, resulting in ICI. In addition, the relative speed between the transmitter and receiver shifts the transmitted frequency at the receiver side also causing ICI. The resulting ICI due to the cumulative effects of the amplifier nonlinearity and Doppler Shift per hop becomes very significant in the MMR systems. In this analysis the end-to-end SINR is obtained considering the aforementioned effects, that used to derive the closed-form formula for bit error probability. The derived closed-formula is used to obtained BER expression. Analytical BER performance of the system is provided and simulation results are presented to verify the analysis. A good match is observed between the analytical and simulation results. Based on the observations from the BER curves, the BER performance is influenced by the HPA's characteristics and MS's speed as well as their cumulative effects per hop.

Chapter 4

Directional Antennas for Bit Error Rate Improvement

4.1 Introduction

One of the main issues causing phase noise in OFDM systems is the Doppler effect. Relative speed between the transmitter and receiver in a mobile wireless channel, introduces Doppler Shift in the received frequencies, causing ICI. This effect poses a significant problem in the MMR systems as the end-to-end Doppler Shift increases with the number of hops traversed by the transmitted signal. Thus the cascade effect of the multiple relaying channel dramatically amplifies the phase noise problem for the underlying OFDM system [1]. Doppler Shift effect should therefore be given due consideration in the design of broadband MMR systems, where the OFDM symbols typically traverse several hops from source to the destination nodes.

Directional antennas have been employed for spatial filtering in the literature [79], [9], [74] and [47], traditionally in the context of single-hop transmissions. In [79], directional

antennas were employed for spatial filtering in a single-hop transmission in WiMAX networks. In [9], the deployment of a directional antenna at the mobile station (MS) or receiver side was investigated, where it was shown that the multipath components can be significantly mitigated. The effect of directional antennas on the ICI power in an OFDM system was analyzed in [74]. It was shown that the ICI power can be reduced substantially when directional antenna is employed at the MS. In [47], the probability density function (pdf) of the angle-of-arrival (AOA) of the multipath components is derived and the effects of directional antennas at the BS on the Doppler Shift was studied. All these works were conducted in the context of single-hop communications. For the multi-hop case, the work in [13] examines the throughput gain achievable using directional antennas in multi-hop wireless networks, where it was inferred that low power consumption due to lower interference when using directional antennas can lead to throughput gain. In [60] and [40] respectively, scheduling and routing schemes that rely on directional antenna in multi-hop systems were developed, using simulation studies. To the best of our knowledge however, no work has thus far presented error rate performance results to illustrate the behavior of directional antenna solution in mobile OFDM relaying system.

A major requirement in BWANs (LTE and WiMAX) is the provisioning of services of certain data rate and certain QoS. Thus for every scheme deployed in BWANs such as multi-hop relaying, service providers must have documented works not only on the potential impacts of the scheme on data rate (or throughput) for various SNR, but also on the corresponding error rate performance at different SNR since the latter significantly impact wireless QoS. In this chapter, we present the first documented work in the literature, on the effect of directional antenna on the error rate performance of the MMR systems. We

derive the BER performance of the MMR system employing directional antennas and evaluate analytically and by simulation, the effectiveness of this solution in the MMR channels.

The remainder of this chapter is organized as follows. Section 4.2, presents the system model. Section 4.3, shows the analysis of the Doppler effects [1], as well as the benefits of deploying directional antenna at the MS and RS. Section 4.4, presents the BER improvement using directional antenna at both the MS and RS. Section 4.5, describes the simulation parameters and the obtained results. Finally, Section 4.6, summarizes the chapter.

4.2 System Model

We adapt a similar system model to that presented in Chapter 3, by considering an OFDM symbols transmission over multi-hop relaying channels, with each OFDM symbol consisting of N_c subcarriers. The transmitted signal from a MS originating the data, passes through a number of relay station(s) (RS) enroute to the base station (BS). We consider that there are *U* users, each user occupy one OFDM symbol and equipped with directional antennas, uniformly distributed in the coverage area of the BS. Furthermore, each user can be associated with the BS or a RS whichever provides stronger signal-to-noise ratio (SNR). An example of this model for the case $R = 2$ (two-hops relay network) is illustrated in Figure 4.1 for a cellular deployment, in which each cell is serviced by a BS, located at the center of the cell, and six RSs ($N = 6$) equipped with directional antennas, each equidistant from the BS and located at the center of each side of the hexagon as shown.

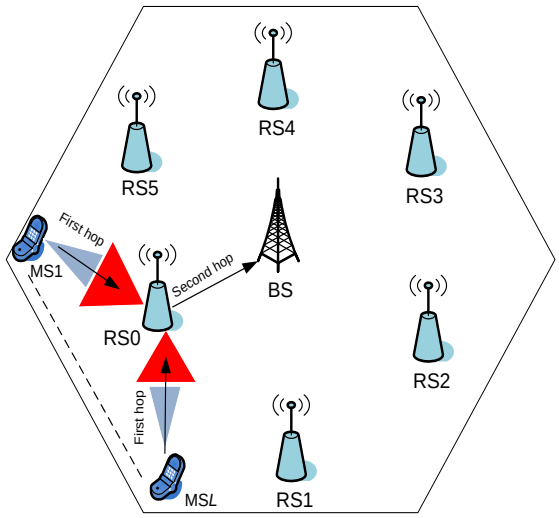

Figure 4.1: Mobile Multi-hop Relaying System deploying directional antennas

BWAN terminals that experience high Doppler Shift effects are most likely to be highly mobile, therefore the scenario studied in this chapter considers a BWAN terminal placed in a moving vehicle. In this situation, the orientation of the directional antenna is aligned toward the motion of the vehicle. If we assume a uniform distribution of scatterers in the azimuth plane, then for a given directional antenna orientation, relative to the direction of motion, the resulting Doppler Shift can be computed as illustrated in Figure 4.2. This figure demonstrates the situation when a directional antenna with a beamwidth $2\psi_a$ is deployed at the RS. If the scatterers are assumed to be placed in a circle around the MS, then the AOA of the signal is limited to a region of $2\theta_{max}$, therefore two cases can be considered: First, when $\psi_a \geq \theta_{max}$, then the directional antenna at the RS will eliminate all the scatterers, and the pdf of the AOA will be uniform. Second, when $\psi_a < \theta_{max}$, then the directional antenna at the RS will eliminate some of the scatterers, and the pdf of the AOA will not be uniform [47]. Through out this chapter, the symbol ϖ is used to denote the case when antenna orientation is parallel to the direction of the motion, while $-\varpi$ is used to denote

the case when antenna orientation is perpendicular to the direction of the motion.

4.3 Doppler Shift Effect Analysis

Since the BWANs terminals are usually highly mobile, the transmitted signal is shifted by Doppler effect $\Phi_{Dop,r}(n)$ as a result of the movement of the MS, which is given by $2\pi f_d T_s$, where T_s is the OFDM symbol duration and f_d denotes the frequency offset between the transmitter and the receiver which can be expressed as

$$f_d = f_m \cos(\theta_2 - \theta_1) \tag{4.1}$$

where θ_2 is the angle-of-arrival of the received signal and θ_1 is the angle of the motion as illustrated in Figure 4.2. θ_1 and θ_2 are measured with respect to the direct line-of-sight (LOS) component. f_m denotes the Doppler Shift, which can be observed when the signal arrives directly in front or behind the direction of motion.

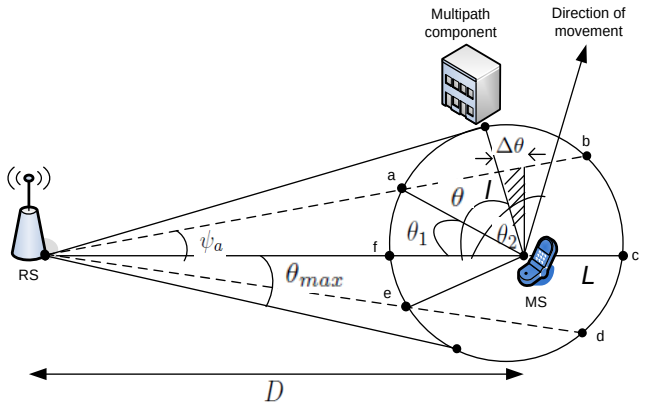

Figure 4.2: AOA of Signals at Mobile Station with Respect to the Direct Line-of-Sight Component

The maximum Doppler Shift is given by

$$f_m = \frac{f_c * V_{S,D}}{c} = \frac{V_{S,D}}{\lambda} \tag{4.2}$$

where f_c is the transmitted frequency, $V_{S,D}$ is the velocity of the transmitter relative to the receiver (m/s), c is the speed of light $(3 \times 10^8 (m/s))$, and $\lambda = \frac{c}{f_c}$ is the wavelength. Therefore, substituting Eq.(4.2) into Eq.(4.1) gives

$$f_d = \frac{V_{S,D}}{\lambda} \cos(\theta_2 - \theta_1) \tag{4.3}$$

Using the second term in Eq.(4.2), Eq.(4.3) can be rewritten as

$$f_d = \frac{f_c * V_{S,D}}{c} \cos(\theta_2 - \theta_1) \tag{4.4}$$

Typically, the Doppler effect can be reduced from $2f_d$ to $(1 - cos(\psi_a/2)) \times f_d$ using a directional antenna with a beam-width ψ_a if the bore-sight is aligned in either direction, straight ahead or behind the MS [79]. If the bore-sight is aligned straight ahead, this case corresponds to the ϖ condition. On the other hand, if the antenna is rotated such that its bore-sight is pointing to either side, right or left of the MS, then the Doppler Shift is reduced to $2 \times f_d \times sin(\psi_a/2)$, and this case corresponds to the $-\varpi$ condition [79].

4.3.1 Using Directional Antennas at Relay Station

Deploying directional antennas at the RS mitigates the effect of Doppler Shift introduced as a result of MS's movement. From Figure 4.2, the region of scatterers that can be successfully mitigated by the deployed directional antenna at the RS is a,b,c,d,e,f. Because of the symmetry, considering the region a, b, c, MS, f, where $0 < \theta \leq \pi$, the pdf of AOA of the received signal, $p_{(\theta)}$ at the MS, when $\psi_a < \theta_{max}$ can be derived by measuring the area of the small shaded portion in Figure 4.2. The area defined by θ and $\theta + \Delta\theta$ can be calculated as [47].

$$C = \frac{1}{2}\int_{\theta}^{\theta+\Delta\theta} l^2 d\theta \tag{4.5}$$

Therefore, the value of *l* is given by

$$l = \begin{cases} L, & if \quad 0 < \theta \leq \theta_1 \\ \frac{Dtan(\psi_a)}{sin(\theta)+cos(\theta)tan(\psi_a)}, & if \quad \theta_1 < |\theta| \leq \theta_2 \\ L, & if \quad \theta_2 < |\theta| \leq \pi \end{cases} \tag{4.6}$$

Using the geometry in Figure 4.2, gives

$$\theta = cos^{-1}\left[\frac{D}{l}sin^2(\psi_a) \pm \frac{cos(\psi_a)}{l}\sqrt{l^2 - D^2sin^2(\psi_a)}\right] \tag{4.7}$$

Recall that, assuming the scatterers are uniformly distributed in the region a, b, c, d, e, f, the density area can be given by

$$f_{dens.} = \frac{1}{L^2(\pi + \theta_1 - \theta_2) + 2Dsin(\psi_a)\sqrt{L^2 - D^2sin^2(\psi_a)}} \tag{4.8}$$

Using Eqs.(4.5) and (4.8), the cumulative distribution function (cdf) of the AOA, $F(\theta)$ can be calculated as

$$F_{(\theta)} = \int_0^{\theta} \frac{f_{dens.} \times l^2}{2} d\alpha \tag{4.9}$$

Considering the derivative of Eq.(4.9) and α as a dummy variable, the pdf of AOA, $p_{(\theta)}$ can be expressed as

$$p_{(\theta)} = \begin{cases} \frac{L^2}{A}, & if \quad -\theta_1 < \theta \leq \theta_1 \\ \frac{[Dtan(\psi_a)]^2}{A[sin(\theta)+cos(\theta)tan(\psi_a)]^2}, & if \quad \theta_1 < |\theta| \leq \theta_2 \\ \frac{L^2}{A} & if \quad \theta_2 < \theta \leq -\theta_2 \end{cases} \tag{4.10}$$

where,

$$A = 2L^2(\pi + \theta_1 - \theta_2) + 4Dsin(\psi_a \sqrt{L^2 - D^2 sin^2(\psi_a)}) \tag{4.11}$$

4.3.2 Using Directional Antenna at Both Relay and Mobile Station

Considering the deployment of directional antennas at the RS and MS helps to reduce the Doppler effect, consequently improves the BER performance. The pdf of AOA of the received signal, $p_{(\theta)}$, when a directional antenna is deployed at the MS [2],[75] is given by

$$p_{(\theta)} = \begin{cases} \frac{1}{2\psi_m}, & if \quad |\theta| < \psi_m \\ \\ 0, & otherwise \end{cases} \tag{4.12}$$

where ψ_m is the beamwidth of the directional antenna at the MS. When using directional antennas at both the RS and MS sides, the pdf of AOA of the received signal, $p_{(\theta)}$, is derived

by multiplying Eq.(4.10) and Eq.(4.12) and it can be written as

$$p_{(\theta)} = \begin{cases} \frac{Q}{2\psi_m}\frac{L^2}{A}, & if \quad |\theta| < \theta_2 \\ \frac{Q}{2\psi_m}\frac{[Dtan(\psi_a)]^2}{A[sin(\theta)+cos(\theta)tan(\psi_a)]^2}, & if \quad \theta_2 < |\theta| < \psi_m \\ 0, & otherwise \end{cases} \tag{4.13}$$

where Q is a constant and $p_{(\theta)}$ is the pdf of AoA of the received signal.

4.4 BER Performance Analysis

In this section, we derive the BER performance of OFDM systems in two-hop relaying systems employing quadrature amplitude modulation (QAM) signals over time-varying channel in the presence of Doppler Shift, $\Phi_{Dop,r}$ impairment. The improvement of BER performance when directional antennas are employed at both the RS and the MS sides is evaluated. The received signal at the end of the r^{th} hop transmission, $r = 1, \ldots, R$, can be expressed, after accounting for the Doppler effect, as [4], [1]

$$\begin{aligned} Y_r[k] &= H_{r-1}[k]H_r[k]X[k]\Phi_{Dop,r-1}[0]\Phi_{Dop,r}[0] + H_r[k] \\ &\quad \beta_{r-1}[k]\Phi_{Dop,r}[0] + H_r[k]W_{r-1}[k]\Phi_{Dop,r}[0] + \\ &\quad \beta_r[k] + W_r[k] \end{aligned} \tag{4.14}$$

where $H_r[k]$ and $H_{r-1}[k]$ are the frequency-domain channels coefficients on the k^{th} sub-carrier, $k = 0, 1, \ldots, N_c - 1$ for the first and second- hop, respectively. $W_r[k]$ and $W_{r-1}[k]$ are the complex Gaussian noise with variances $\sigma^2_{W_r[k]}$ and $\sigma^2_{W_{r-1}[k]}$, respectively. $\beta_r[k]$ and

$\beta_{r-1}[k]$ are the ICI terms caused by the loss of orthogonality between subcarriers as a result of Doppler Shift in the first and the second-hop.

$$\begin{aligned} \beta_r[k] &= \left(\sum_{m=0, m\neq k}^{N_c-1} H_r[m]X[m]\Phi_{Dop,r}[m-k] \right) \\ & m = 0, 1, \ldots, N_c - 1 \end{aligned} \tag{4.15}$$

and the ICI power $P_{\beta_r[k]}$ is given by

$$P_{\beta_r[k]} = \left| \left(\sum_{m=0, m\neq k}^{N_c-1} H_r[m]X[m]\Phi_{Dop,r}[m-k] \right) \right|^2 \tag{4.16}$$

We assume that the data symbol $X[.]$ has an average power E_s normalized to one, and the phase rotation imposed by the channel $\Phi_{Dop,r}[0]$ can be accurately estimated at the r^{th} hop receiver, therefore Eq.(4.14) can be simplified as

$$Y_r[k] = H_{r-1}[k]H_r[k]X[k] + H_r[k]\beta_{r-1}[k] + H_r[k]W_{r-1}[k] + \beta_r[k] + W_r[k] \tag{4.17}$$

The signal-to-interference-plus-noise ratio $\gamma_{r[k]}$ at the receiver side can be obtained using Eq. (4.17) as

$$\gamma_{r[k]} = \frac{E[|H_r[k]|^2]E[|H_{r-1}[k]|^2]}{E[|H_r[k]|^2]P_{\beta_{r-1}[k]} + E[|H_r[k]|^2]\sigma^2_{W_{r-1}[k]} + P_{\beta_r[k]} + \sigma^2_{W_r[k]}} \tag{4.18}$$

1) Probability Density Function of SINR

Considering the received signal at the end of the r^{th} hop transmission, $Y_r[k]$ above, the SINR expression for the case when $r = 1$ (*first-hop*) in Eq.(4.18), can be rewritten as

$$\gamma_{r[k]} = \frac{E[z^2]}{\sigma^2_{\beta r[k]} + \sigma^2_{W_r[k]}} \tag{4.19}$$

$\gamma_{r[k]}$ is considered to be an exponential random variable, which have the pdf and the cdf defined, respectively as

$$f_{\gamma_{r[k]}}(\gamma) = \frac{1}{\overline{\gamma}_{r[k]}} e^{-\frac{\gamma}{\overline{\gamma}_{r[k]}}} \tag{4.20}$$

$$F_{\gamma_{r[k]}}(\gamma) = 1 - e^{-\frac{\gamma}{\overline{\gamma}_{r[k]}}} \tag{4.21}$$

where $\overline{\gamma}_{r[k]} = E[\gamma_{r[k]}]$, and may be different for all k. The SINR is considered to be static when $\overline{\gamma}_{r[k]}$ is same for all k. On the other hand, frequency selectivity can be achieved by allowing different $\overline{\gamma}_{r[k]}$ for different k. The two-hop channel case can be modeled as an equivalent single-hop channel case whose SINR equivalent $\gamma_{eq[k]}$ is approximated as [64].

$$\gamma_{eq[k]} \approx \min_{r=1,...R} \gamma_{r[k]} \tag{4.22}$$

Using the assumption that the hops are independent but not necessarily identically distributed gives the cdf and pdf of $\gamma_{eq[k]}$ as

$$\begin{aligned} F_{\gamma_{eq[k]}}(\gamma) &= 1 - P[\gamma_r > \gamma, \ldots, \gamma_R > \gamma] \\ &= 1 - \prod_{r=1}^{R}[1 - F_{\gamma_{r[k]}}(\gamma)] \end{aligned} \tag{4.23}$$

Therefore, the joint pdf of $\gamma_{eq[k]}(\gamma)$ for R = 2 hops is given by differentiating Eq.(4.23) as

$$f_{\gamma_{eq[k]}}(\gamma) = \sum_{r=1}^{R} f_{\gamma_{r[k]}}(\gamma) \prod_{j=1, j\neq r}^{R} [1 - F_{\gamma_{j[k]}}(\gamma)] \tag{4.24}$$

Substituting Eqs.(4.20) and (4.21) into Eq.(4.24), the joint pdf of $\gamma_{eq[k]}$ can be expressed as

$$f_{\gamma_{eq[k]}}(\gamma) = \sum_{r=1}^{R} \left(\frac{1}{\overline{\gamma}_{r[k]}} e^{-\frac{\gamma}{\overline{\gamma}_{r[k]}}} \right) \prod_{j=1, j\neq r}^{R} [1 - (1 - e^{-\frac{\gamma}{\overline{\gamma}_{j[k]}}})] \tag{4.25}$$

which can be simplified as

$$f_{\gamma_{eq[k]}}(\gamma) = \sum_{r=1}^{R} \left(\frac{1}{\overline{\gamma}_{r[k]}} e^{-\frac{\gamma}{\overline{\gamma}_{r[k]}}} \right) \prod_{j=1, j\neq r}^{R} e^{-\frac{\gamma}{\overline{\gamma}_{j[k]}}} \tag{4.26}$$

After some manipulations, Eq.(4.26) can be rewritten as

$$f_{\gamma_{eq[k]}}(\gamma) = \sum_{r=1}^{R} \left(\frac{1}{\overline{\gamma}_{r[k]}} e^{-\gamma \sum_{j=1}^{R} \overline{\gamma}_{j[k]}^{-1}} \right) \quad (4.27)$$

This can be simplified as

$$f_{\gamma_{eq[k]}}(\gamma) = Ge^{-\gamma G} \quad (4.28)$$

where $G = \sum_{r=1}^{R} \overline{\gamma}_{r[k]}^{-1}$

2) Probability of error Expression Analysis

The probability of error $P_e(k)_r$ expression of the system for M-ary QAM modulation scheme [36] can be written as

$$P_e(k)_r = \int_0^{\infty} \frac{1}{\sqrt{M} log_2 \sqrt{M}} \sum_{j=1}^{log_2 \sqrt{M}} \sum_{n=0}^{v_j} p_n^j \times erfc(\sqrt{g_n \gamma}) f_{\gamma_{eq[k]}} C(T_s) d\gamma \quad (4.29)$$

where $v_j = (1 - 2^{-j})\sqrt{M} - 1$, $p_n^j = (-1)^{\lfloor \frac{n 2^{j-1}}{\sqrt{M}} \rfloor} (2^{j-1} - \lfloor \frac{n 2^{j-1}}{\sqrt{M}} + \frac{1}{2} \rfloor)$, $g_n = \frac{(2n+1)^2 3 log_2 M}{2M-2}$, M is the constellation order, erfc is the complementary error function ([61], Eq.(4A.6)), and $\lfloor . \rfloor$ is the floor. The correlation function $C(T_s)$ of the Rayleigh fading channel with the pdf

of AOA, $p_{(\theta)}$ [73], [66] can be expressed as

$$C(T_s) = \int_{-\pi}^{+\pi} p_{(\theta)} e^{j2\pi f_d T_s \cos\theta} d\theta \tag{4.30}$$

Eq.(4.30), can be rewritten as

$$C(T_s) = \int_{-\pi}^{+\pi} p_{(\theta)} sinc^2(f_d T_s \cos\theta) d\theta \tag{4.31}$$

Substituting Eqs.(4.27) and (4.31) into Eq.(4.29) gives

$$P_e(k)_r = \int_0^{\infty} \int_{-\pi}^{+\pi} \frac{1}{\sqrt{M} log_2 \sqrt{M}} \sum_{j=1}^{log_2\sqrt{M}} \sum_{n=0}^{v_j} p_n^j \times erfc(\sqrt{g_n \gamma}) \sum_{r=1}^{R} \overline{\gamma}_{r[k]}^{-1} e^{-\gamma \sum_{r=1}^{R} \overline{\gamma}_{r[k]}^{-1}} p_{(\theta)} sinc^2(f_d T_s \cos\theta) d\gamma d\theta \tag{4.32}$$

which can be rearranged as

$$P_e(k)_r = \frac{1}{\sqrt{M} log_2 \sqrt{M}} \sum_{j=1}^{log_2\sqrt{M}} \sum_{n=0}^{v_j} p_n^j \times \int_0^{\infty} \int_{-\pi}^{+\pi} erfc(\sqrt{g_n \gamma}) \sum_{r=1}^{R} \overline{\gamma}_{r[k]}^{-1} e^{-\gamma \sum_{r=1}^{R} \overline{\gamma}_{r[k]}^{-1}} p_{(\theta)} sinc^2(f_d T_s \cos\theta) d\gamma d\theta \tag{4.33}$$

Performing the first integral with respect to γ and using $G = \sum_{r=1}^{R} \overline{\gamma}_{r[k]}^{-1}$, the $P_e(k)_r$ formula can be expressed as

$$P_e(k)_r = \frac{1}{\sqrt{M} log_2 \sqrt{M}} \sum_{j=1}^{log_2 \sqrt{M}} \sum_{n=0}^{v_j} p_n^j \left(1 - \sqrt{\frac{g_n G^{-1}}{1 + g_n G^{-1}}}\right) \int_{-\pi}^{+\pi} p_{(\theta)} sinc^2(f_d T_s \cos\theta) d\theta \tag{4.34}$$

Consequently, the average SER can be expressed as [46].

$$SER_r = \frac{1}{N_c} \sum_{k=0}^{N_c - 1} P_e(k)_r \tag{4.35}$$

Finally, the BER in a two-hop relaying system can be estimated using the derived SER_r expression as

$$BER_r = \frac{SER_r}{log_2(M)} \tag{4.36}$$

4.5 Performance Evaluation

In this section, we evaluate the proposed method using directional antennas for alleviating the effect of Doppler Shift to improve the BER performance of the MMR systems. We evaluate analytically and by simulation, the effectiveness of this solution in the MMR channels.

4.5.1 Simulation Model

We consider a two-hop relaying system and adopt the network model presented in Figure 4.1. The channel between each transmitter and receiver is modeled as a Rayleigh fading channel. The parameters of the BWAN used in the simulation are listed in table 4.1, [25]. The simulated mobile speeds are 50 and 100km/h which results in Doppler Shift values, $f_d = 320$ and $f_d = 650Hz$. The antenna configurations used in the simulations are $60°$, $90°$ and $120°$, parallel and perpendicular orientations to the direction of the motion. An OFDM symbols with $N_c = 256$ subcarriers each are generated, than each symbol is occupied by one user. Those generated OFDM symbols are transmitted through the channel after the CP extension to overcome ISI effect. The received bits with errors are calculated and compared with those were transmitted to calculated the BER performance. The BER performance of the MMR system with directional antennas are then obtained for different MS speeds.

Table 4.1: Parameters of the BWAN simulated

Parameter	**Value**
N_c	256
Bandwidth	20 MHz
Operating Frequency	3.5 GHz
Data subcarriers	192
Guard subcarriers	64
Total Symbol Duration	55.5 μs
Modulation Scheme	QAM

We obtain representative BER performance curves for both the perpendicular and parallel antenna orientation, for each and every one of the antenna configurations $60°$, $90°$ and

120° used, thus depicting the most possible scenarios for Directional antenna deployments in the broadband MMR systems.

4.5.2 Performance Results

In this section, we show and discuss the simulation and analytical results of the BER performance in the MMR system when the directional antennas are deployed at the MS and RS side.

Figures 4.3 and 4.4 illustrate the BER performance of the MMR system (two-hop case) employing directional antennas with two different antenna orientations, perpendicular and parallel orientations respectively. The MS speed used for these simulations is 50 km/h, representing city traffic. This speed translates to a maximum Doppler Shift of $f_d = 320$ Hz. For the perpendicular elements (Figure 4.3), it is interesting to note that when a directional antenna is used, the BER is significantly enhanced as the beamwidth of the directional antenna is reduced from 120° to 60°. For example at $E_b/N_0 = 30dB$, while the BER of the MMR system with 120° beamwidth has reached an error floor around 10^{-1} due to the MMR channel impairments, the BER performance of the system for the case of 60° directional antenna has improved to 10^{-3} at same E_b/N_0, which means a two-hop transmission at practically acceptable error rate is achievable with directional antenna with beamwidth of 60° for the perpendicular antenna orientation.

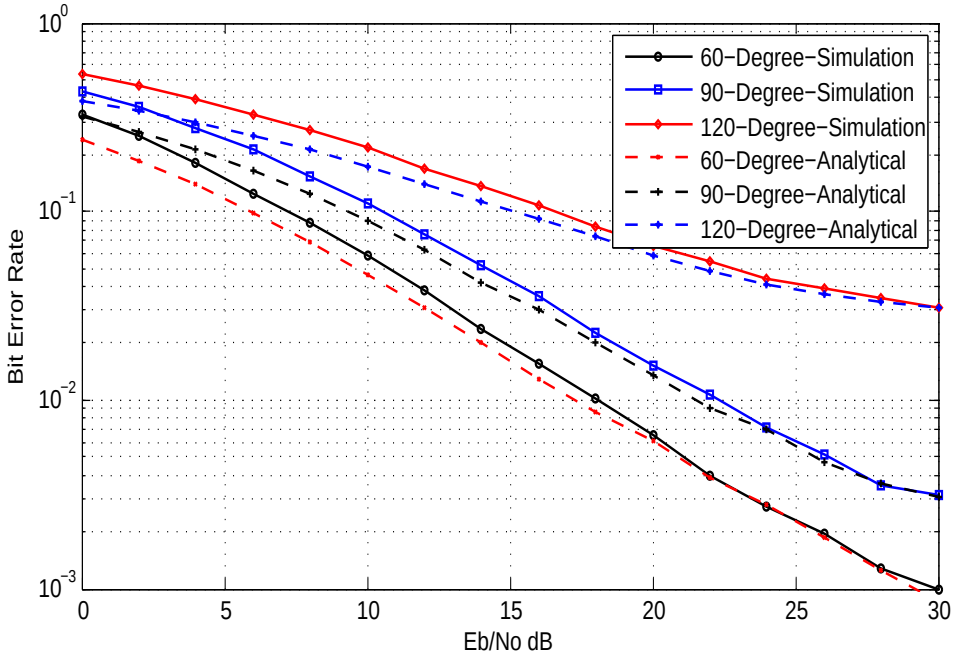

Figure 4.3: BER Performance with perpendicular directional antenna configuration, $-\varpi$, R = 2, Speed = 50 km/h (city traffic)

For parallel elements (Figure 4.4), the BER performance of the MMR system is similarly enhanced for smaller antenna beamwidth compared to the larger ones. Comparing the respective results for the perpendicular and vertical antenna orientation cases in Figure 4.3 and 4.4, we observe that the parallel antenna orientation case has better BER enhancements for the MMR system than the perpendicular orientation case. However in general, directional antennas can effectively enhance the performance of the MMR system to practically acceptable error rate level in both cases, for a moderate vehicular speed such as 50 km/h (representing in intra-city traffic).

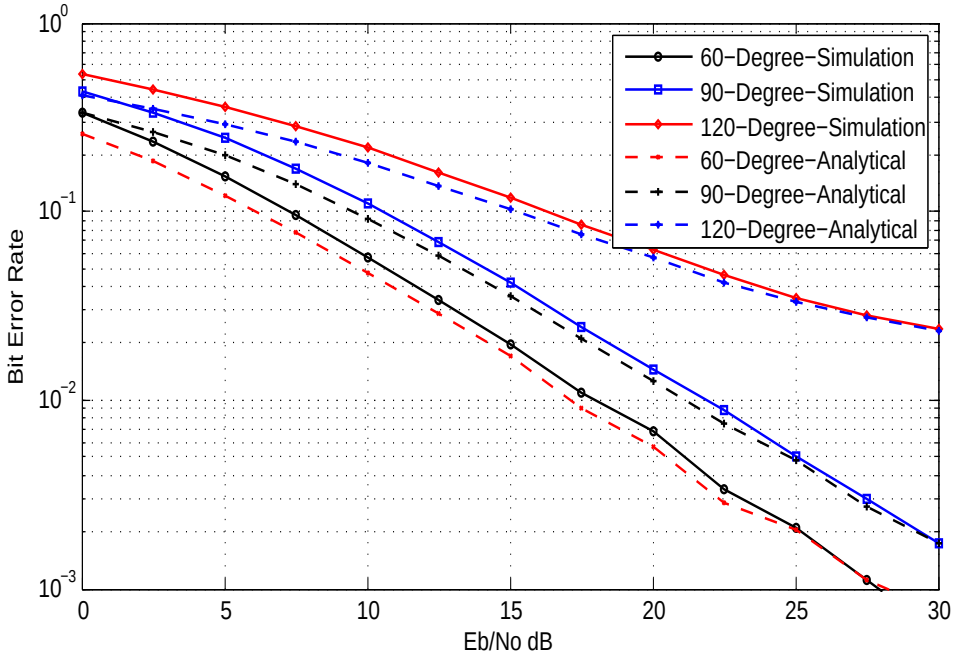

Figure 4.4: BER Performance with parallel directional antenna configuration, ϖ, R = 2, Speed = 50 km/h (city traffic)

Figures 4.5 and 4.6 present respectively the BER performance of the MMR system employing directional antennas for the cases of perpendicular and parallel antenna orientations, after the simulated MS speed is increased to 100 km/h, representing highway traffic. Since the Doppler Shift becomes larger as the MS's speed increases, the BER performance of the system in Figure 4.5 and 4.6 are more degraded compared to their counterpart results for lower MS speed in Figure 4.3 and 4.4. The general observation from Figure 4.5 and 4.6 is that for both the parallel and perpendicular antenna orientations in high vehicular speed, the directional antenna is still able to provide some BER performance enhancement for the MMR system as the antenna beamwidth is reduced from 120° to 60°. However, since the BER performance exhibit error floors somewhere above 10^{-3} for this case, additional BER performance enhancement techniques such as encoding schemes would need to be

combined with the directional antenna deployment in order to obtain practically acceptable BER performance ($> 10^{-6}$) in high vehicular speeds. Finally comparing the analytical and simulation results in Figure 4.3 - 4.6, it is generally observed that the effects of approximating the equivalent multi-hop SINR as in Eq. (4.22) on the analytical results becomes less appreciable at high SINR.

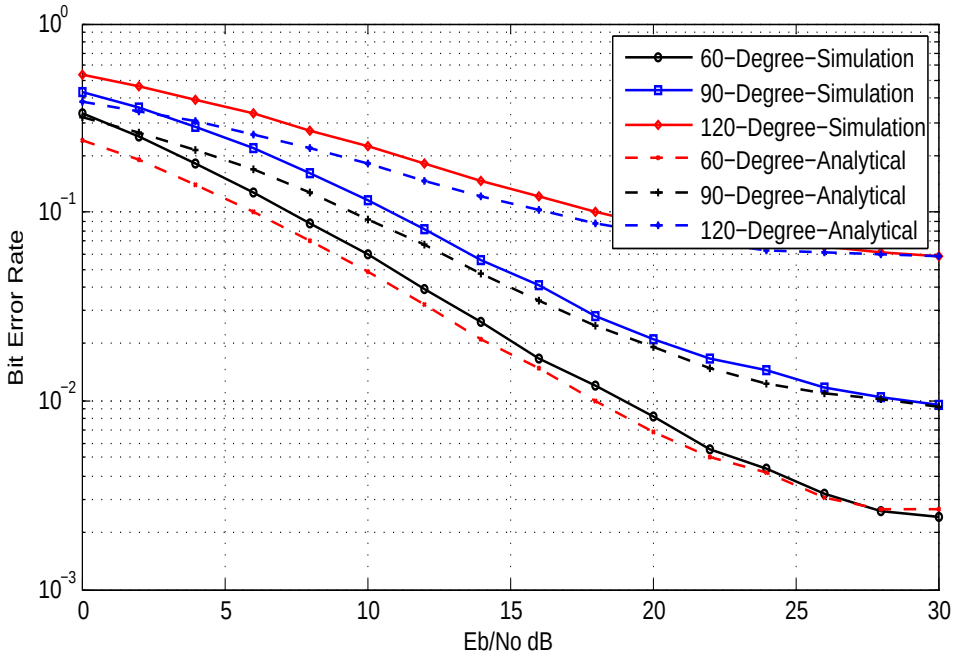

Figure 4.5: BER Performance with perpendicular directional antenna configuration, $-\varpi$, R = 2, Speed = 100 km/h (highway traffic)

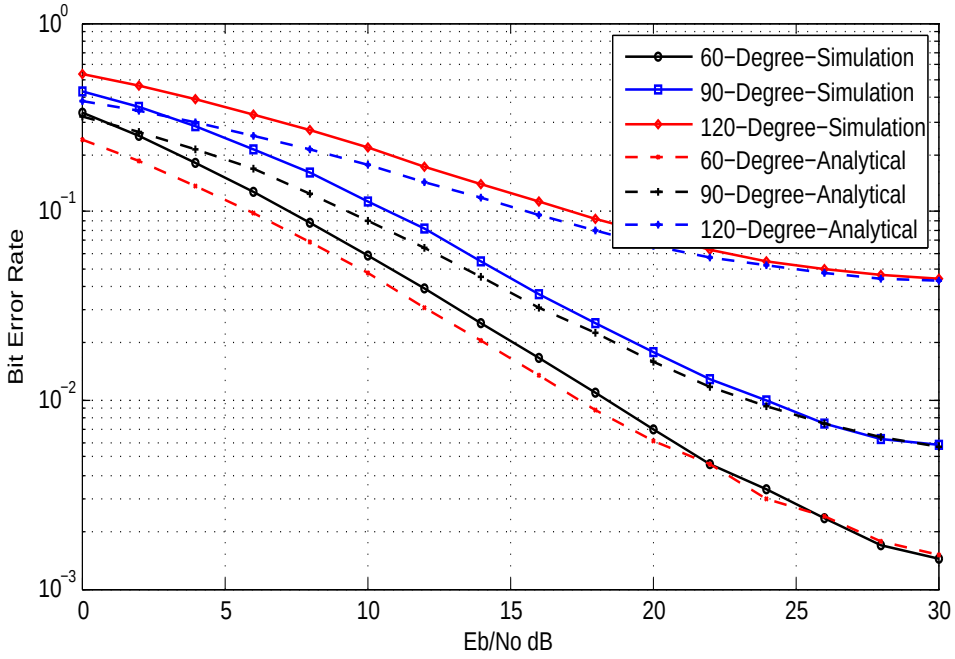

Figure 4.6: BER Performance with parallel directional antenna configuration, ϖ, R = 2, Speed = 100 km/h (highway traffic)

4.6 Summary

This chapter investigated the possibility of deploying directional antennas at both the MS and RS sides in the MMR systems, for mitigating the BER performance degradation caused by the Doppler Shifts experienced over mobile multi-hop relaying channels. A directional antenna at either side of the communication link eliminates some multipath components, therefore the narrower the beamwidth of the directional antenna, the more the multipath components that would be canceled.

Different MS speeds and antenna orientations were used to evaluate the effectiveness of the proposed solution. We showed that the proposed scheme generally enhances the BER performance of the MMR system as the beamwidth of the directional antenna is reduced

from 120° down to 60°, and that significant enhancements are possible for both the perpendicular and parallel antenna orientations, even though the latter is observed to provide better BER enhancement than the former.

Also, we observed that significant BER enhancements are observed at low and high MS speeds using this solution. However for high vehicular speeds, the system exhibits significant error floor above 10^{-3} for all antenna beamwidth studied, which suggests that extra BER enhancements techniques will be required in addition to directional antenna technique to achieve practically acceptable BER for this case.

Chapter 5

Subcarriers Collision Analysis

5.1 Introduction

One of the limitations of OFDM-based systems like WiMAX, is frequency reuse, as a channel can only be reused if the interference in the network is minimized. Frequency reuse allows one or more MSs to share same OFDM symbol, therefore interference level in the network increases as the number of MSs sharing OFDM subchannels increases. This also makes the OFDMA system more sensitive to subcarrier collisions, which further increases the level of interference.

An analytical model to capture and quantify the effect of collisions in multi-hop relaying (MMR) systems resulting from the simultaneous use of subcarriers is thus needed. To the best of our knowledge there is no study to date quantifying collisions between subcarriers of OFDMA access technique in a MMR system.

In this chapter, we derive the expected number of collisions between two or more NTRSs. Using the derived expression, we calculate the probability of symbol loss for OFDMA techniques in the MMR system. It is note worthy to clarify that not all symbols

involved in a collision are lost, but collisions can increase the level of interference, making the symbol loss probability high. The IEEE 802.16 standard [26] defines a threshold for the SNR, below which the bit-error-rate (BER) is unacceptable ($> 10^{-6}$). Using this threshold, we also estimate the proportion of symbols with degraded SNR as well as the collision rate in the MMR system with two or more NTRSs.

The remainder of this chapter is organized as follows. Section 5.2 presents the system model. Section 5.3, analyzes the probability of subcarriers collisions. Section 5.4 presents the performance analysis of the system. Section 5.5 demonstrates the numerical results. Section 5.6 summarizes the chapter.

5.2 System Model

Similar to the previous two chapters, we consider a broadband wireless network employing OFDMA access mechanism over mobile multi-hop relaying channels, with each OFDM symbol consisting of N_c subcarriers. There are U mobile stations (MSs) in the system uniformly distributed in the coverage area of the BS, and that each MS can be associated with the BS or a RS whichever provides the stronger SNR. An example of this model for the case $R = 2$ (two-hops relay network) is illustrated in Figure 5.1 for a cellular deployment, in which each cell is serviced by a BS, located at the center of the cell, and six RSs ($N = 6$), each equidistant from the BS and located at the center of each side of the hexagon as shown.

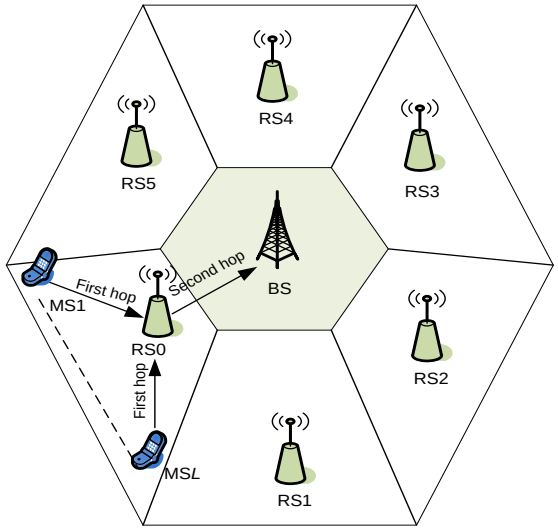

Figure 5.1: Mobile Multi-hop Relaying System deploying frequency reuse

We model a wireless relaying system as presented in Figure 5.1, where the OFDM symbol consisting of N_c subcarriers is divided into G groups (subchannels), each consisting of N_c/G subcarriers as illustrated in Figure 5.2. Frequency assignment is realized in two stages, first the BS allocates the same frequencies (channels) to each RS in its vicinity (centralized), second, each RS assigns the frequencies to MSs on the basis of subchannels, by randomly picking a subcarrier from each subchannel. This frequency allocation is made in each RS in a distributed manner, therefore no collisions are possible between MSs belonging to the same RS. However, collisions are possible if nearby RSs use the same subcarriers. In this work, we calculate the expected number of collisions between subcarriers of the target relay station, RS_0 and the subcarriers of the n^{th} relay station, $n \in \{0, \ldots, N-1\}$. In RS_n, there are S_n subcarriers for possible allocation and the vector $\mathbf{S} = (S_0, \ldots, S_{n-1})$ denotes the number of allocated subcarriers in the n^{th} relay stations.

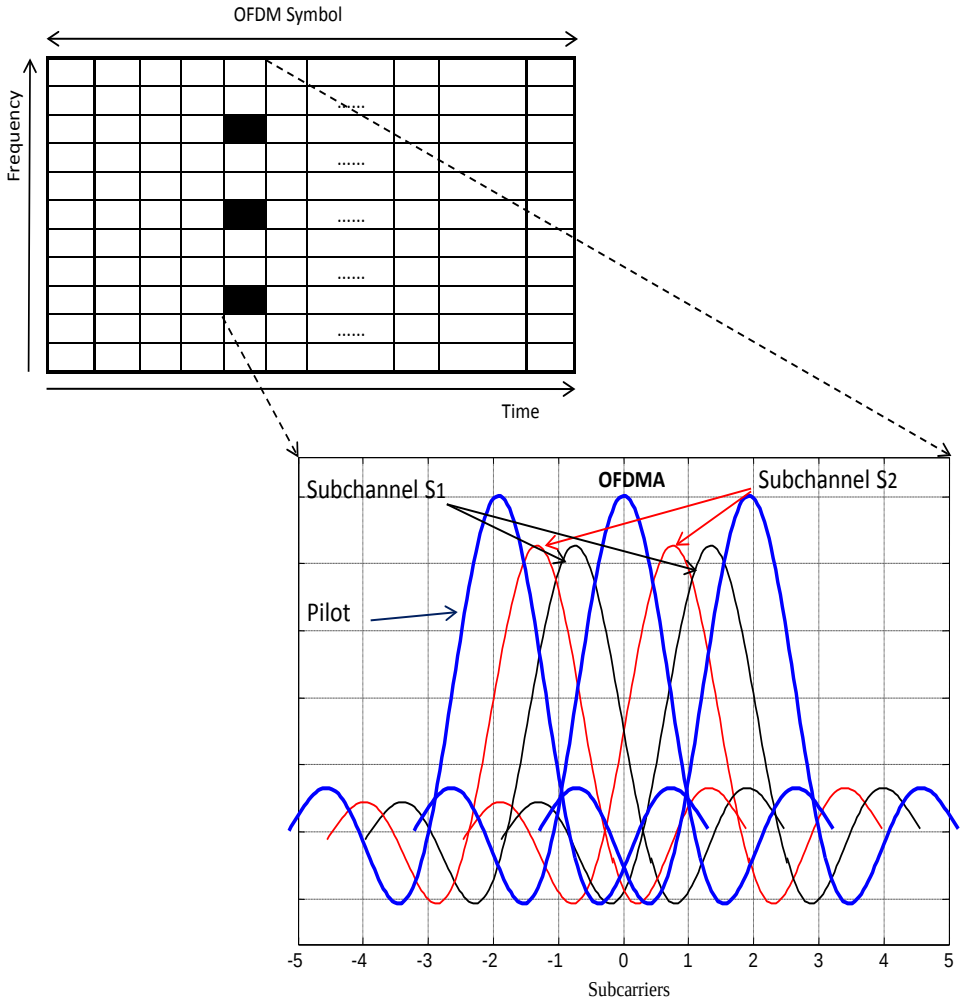

Figure 5.2: Subchanneling of OFDMA subcarriers

5.3 Analysis of Subcarriers Collision Probability

To illustrate the analysis we started with two interfering relay stations, than a general case, where *N* relay stations are present is considered. In both cases, the probability of collision is obtained for N_c subcarriers.

A) Special Case: Two interfering Non-Transparent Relay Stations

The expected number of collisions resulting from the simultaneous use of subcarriers in two NTRSs is obtained in this section. The expected number of collisions for all the G subchannels in the system for the case of $N = 2$ relay stations, given the vector **S** of occupied subcarriers in the subchannels is given by

$$E_{\mathbf{S}}[g] = G.\widehat{E}_{\mathbf{S}}[g] \tag{5.1}$$

where g is a random variable denoting the subchannel where a collision could occur, and $\widehat{E}_{\mathbf{S}}[.]$ is the expected value of the number of collisions in a subchannel given the number of occupied subcarriers **S**, and can be written as

$$\widehat{E}_{\mathbf{S}}[g] = \sum_{i \epsilon I} i \widehat{P}_{\mathbf{S}}(i) \tag{5.2}$$

where $\widehat{P}_{\mathbf{S}}(i)$ is the probability of having i collisions in each subchannel and is given by Eq.(5.4). In each subchannel, there are S_n occupied subcarriers in relay n. We calculate the probability of having i collisions in each subchannel. This is similar to the probability that the two relays choose independently subcarriers S_0 and S_1 from the available N_c/G subcarriers. There are $\binom{N_c/G}{S_0}$ possible combinations for RS_0, therefore the probability of choosing one of these combinations is equal to $1/\binom{N_c/G}{S_0}$. If the RS_0 chooses a given set of

S_0 subcarriers, the probability of i collisions can be expressed as [35].

$$\widehat{P}_{\mathbf{S}}(i) = \frac{\binom{S_0}{i}\binom{N_c/G-S_0}{S_1-i}}{\binom{N_c/G}{S_1}} \tag{5.3}$$

B) General Case: N interfering Non-Transparent Relay Stations

A general case $(N > 2)$ is considered in the following, and the expected number of collisions resulting from the simultaneous use of subcarriers in *N* NTRs is obtained.

Lemma 1: The probability of having i collisions in the case of *N* NTRs, in a given subchannel can be expressed as [34],[35] and [33].

$$\widehat{P}_{\mathbf{S}}(i) = \binom{S_0}{i}\left[1-\prod_{n=1}^{N-1}\frac{N_c/G-S_0-S_n+i}{N_c/G-S_0+i}\right]^i\prod_{n=1}^{N-1}\left[\prod_{m=0}^{S_n-1}\frac{N_c/G-(S_0-i)-m}{N_c/G-m}\right] \tag{5.4}$$

Proof of Lemma 1:

We calculate the probability that $S_0 - i$ subcarriers in a given subchannel belonging to RS_0 do not experience collision. The probability that the m^{th} subcarrier of RS_n does not collide with the $S_0 - i$ subcarriers of RS_0 can be expressed as

$$\left[\frac{N_c/G-(S_0-i)-m}{N_c/G-m}\right] \tag{5.5}$$

Since the assigned subcarrier is randomly picked up from the remaining subcarriers in the group $(\frac{N_c}{G}-(S_0-i)-m)$, and there are only $(\frac{N_c}{G}-m)$ available subcarriers in each RS,

the probability that $(S_0 - i)$ subcarriers do not experience collision can be expressed as

$$\widehat{q}_{\mathbf{S}}(S_0 - i) = \prod_{n=1}^{N-1} \prod_{m=0}^{S_n - 1} \left[\frac{N_c/G - (S_0 - i) - m}{N_c/G - m} \right] \tag{5.6}$$

The probability that i subcarriers of RS_0 collide, with the knowledge that the remaining $S_0 - i$ subcarriers do not collide based on the probability that at least one of these i subcarriers do not collide with the m^{th} RS_n subcarriers is given by

$$\left[\frac{N_c/G - (S_0 - i) - m - 1}{N_c/G - (S_0 - i) - m} \right] \tag{5.7}$$

The collision probability, when the collisions are independent of each other can be expressed as

$$\widehat{P}_{\mathbf{S}}(i|S_0 - i) = \left[1 - \prod_{n=1}^{N-1} \prod_{m=0}^{S_n - 1} \frac{N_c/G - (S_0 - i) - m - 1}{N_c/G - (S_0 - i) - m} \right]^i \tag{5.8}$$

Moreover, Eq.(5.8) can be simplified as

$$\widehat{P}_{\mathbf{S}}(i|S_0 - i) = \left[1 - \prod_{n=1}^{N-1} \frac{N_c/G - S_0 - S_n) + i}{N_c/G - S_0 + i} \right]^i \tag{5.9}$$

Hence, considering the number of possible combinations of subcarriers, the probability of i collisions in the same subchannel in the case of *N* relay stations can be calculated by

Eq.(5.4). ∎

5.4 Performance Analysis

We evaluate the symbol loss probability when a collision occur between subcarriers in different NTRSs. We also evaluate the system performance when different types of traffic (i.e., voice and data) are present.

5.4.1 Probability of Symbol Loss

It is well known that for a given power and carrier frequency, the available data rate is inversely proportional to the MS's distance from the BS, as a result of SNR degradation. Consider RS_n interferes with RS_0, $(n \neq 0)$, the SNR at a given subcarrier can be obtained from the received signal on that subcarrier as [1].

$$Y_1[k] = H_0[k]H_1[k]X[k] + H_1[k]W_0[k] + W_1[k] \tag{5.10}$$

where $X[k]$ represents the transmitted symbol on subcarrier k, $k = 0, 1, \ldots, N_c - 1$ and $H_0[k]$ and $H_1[k]$ represent the flat Rayleigh fading channel for the first and second hop, respectively. Assume that there is no inter-carrier-interference (ICI) between subcarriers in the same subchannel, therefore the SNR expression for a two-hop network can be expressed

as

$$SNR = \frac{E_s E[z^2]}{\sigma^2_{W_0[k]} + \sigma^2_{W_1[k]}} \tag{5.11}$$

where E_s denotes the power of the transmitted signal per subcarrier k, and $E[z^2] = E[H_0^2]E[H_1^2]$. $\sigma^2_{W_0}$, and $\sigma^2_{W_1}$ are the variances of the AWGN in the first and second hop, respectively. The path loss p_n between relay station *n* and a given receiver can be expressed as [50].

$$p_n = d_n^{\mu} 10^{\frac{\xi_n}{10}} \tag{5.12}$$

where d_n denotes the distance from relay station n to a receiver, ξ_n is the shadowing effect, and μ varies between $2.7 \sim 5$, with a typical value of 4 [16]. When a collision occurs at a given subcarrier, the BER performance degrades below a specific target if the SNR goes below a given threshold ρ, which depends on the modulation order (see table 5.1). Using Eq.(5.11) and Eq.(5.12), the probability for a symbol to be lost when a collision occurs between RS_0 and RS_n can be expressed as

$$p_{0n} = P\left(E_s \left(\frac{d_0}{d_n}\right)^{\mu} 10^{\frac{\xi_0 - \xi_n}{10}} + W_0 d_0^{\mu} 10^{\frac{\xi_0}{10}} + W_1 d_0^{\mu} 10^{\frac{\xi_0}{10}} > \frac{E_s}{\rho} \right) \tag{5.13}$$

At any MS's position, we model the shadowing by a component ϵ common to all RSs and another component ϵ_n for RS_n, and $\xi_n = x\epsilon + y\epsilon_n$, where $x^2 = y^2 = \frac{1}{2}$, Eq.(5.13) can be

written as

$$p_{0n}=P\left(E_s(\frac{d_0}{d_n})^{\mu}10^{\frac{y(\epsilon_0-\epsilon_n)}{10}}+W_0d_0^{\mu}10^{\frac{\xi_0}{10}}+W_1d_0^{\mu}10^{\frac{\xi_0}{10}}>\frac{E_s}{\rho}\right) \tag{5.14}$$

The effect of the interference generated by collision is stronger than the effect of the AWGN, therefore we assume that $\frac{E_s}{d_1^{\mu}} \gg W_0+W_1$. Hence, assuming $E_s=1$, Eq.(5.14) can be simplified as

$$p_{0n}=P\left((\frac{d_0}{d_n})^{\mu}10^{\frac{y\epsilon}{10}}>\frac{1}{\rho}\right) \tag{5.15}$$

When a collision takes place between subcarriers of two NTRs, RS_0 and RS_n, the probability of symbol loss can be derived as follows. Let $A=\frac{d_0}{d_n}$ and $B=10^{\frac{y\epsilon}{10\mu}}$ be independent random variables [50], Eq.(5.15) can be expressed as

$$p_{0n}=P(AB>\frac{1}{\rho^{\frac{1}{\mu}}}) \tag{5.16}$$

Therefore, Eq.(5.16) can be written as

$$p_{0n}=\int_0^A\int_{\frac{1}{\rho^{\frac{1}{\mu a}}}}^{\infty}f_B(b)f_A(a)dbda \tag{5.17}$$

The inner integral can be expressed as

$$\int_{\frac{1}{\rho^{\frac{1}{\mu a}}}}^{\infty} f_B(b)db = P\left(\epsilon > \frac{-10ln(\rho a^{\mu})}{yln(10)}\right) \tag{5.18}$$

where $\epsilon = \epsilon_0 - \epsilon_n$ is the summation of two Gaussian random variables with zero mean and variance ς^2. Then Eq.(5.18) can be expressed using the complimentary error function (erfc) as

$$\int_{\frac{1}{\rho^{\frac{1}{\mu a}}}}^{\infty} f_B(b)db = \frac{1}{2}erfc\left(\frac{-5ln(\rho a^{\mu})}{\varsigma yln(10)}\right) \tag{5.19}$$

Substituting Eq.(5.19) into Eq.(5.18) gives

$$p_{0n} = \frac{1}{2}\int_0^A erfc\left(\frac{-5ln(\rho a^{\mu})}{\varsigma yln(10)}\right) f_A(a)da \tag{5.20}$$

Hence, the probability of symbol loss can be expressed in a closed-form as

$$p_{0n} = E_A\left[\frac{1}{2}erfc\left(\frac{-5ln(\rho A^{\mu})}{\varsigma yln(10)}\right)\right] \tag{5.21}$$

where $erfc(.)$ is the complementary error function and A is the random variable representing the ratio, in each position of RS_0, of the distances to the RS_0 and RS_n ($A = \frac{d_0}{d_n}$) [50]. The expectation $E[.]$ is taken over the RS.

Recall that not all symbols involved in a collision are lost, but collision can increase the level of interference making a symbol loss probability high. Therefore, the proportion of symbol, $P(S)$ with degraded SNR as a function of the number of occupied subcarriers, S_n and using the obtained probability p_{0n} can be expressed as

$$P(S) = \left[\frac{M \sum_{n=1}^{N-1} p_{0n} S_n}{\sum_{n=1}^{N-1} S_n} \right] \tag{5.22}$$

where $M = \frac{E_S[g]}{S_0 G}$.

5.4.2 System Performance under a given Load

Consider that we have U MSs uniformly distributed in the coverage area of the BS. These MSs can be connected either to the BS or any RS which ever provides better SNR. There are C classes of calls that can be supported. The arrival of class-s calls to relay *n* follow a Poisson process with arrival rate $\lambda_{s,n}$ and requires c_s subchannels. The service time has a mean $\frac{1}{\mu_{s,n}}$. When a class-s call arrives, it will be accepted only if there are more than $N_c/G - c_s$ subcarriers available, otherwise it will be rejected. Let Vector $V_n = (V_{0,n}, \ldots, V_{C-1,n})$ represents the number of calls belonging to class C in relay n. Vector **S** represents the number of occupied subcarriers in relay *n* given by [31],[30].

$$\mathbf{S} = \left[\sum_{s=0}^{C-1} c_s V_{s,n-1} \right] \tag{5.23}$$

The expected number of collisions is equal to

$$E[i] = \sum_{S} \left[\prod_{n=1}^{N-1} P_n(S_n) \right] E_{\mathbf{S}}[i] \tag{5.24}$$

where $E_{\mathbf{S}}[i]$ is the expected number of collisions given the number of occupied subcarriers S_n obtained in Eq.(5.1), and $P_n(S_n)$ is the probability of having a collision with S_n occupied subcarriers in relay *n* and is given by

$$P_n(S_n) = \sum_{V_n} p_n(V_n) = \sum_{s=0}^{U-1} u_s V_{s,n} \tag{5.25}$$

where $p_n(V_n)$ is the probability of having $V_{s,n}$ class-s calls in relay *n* given by

$$p_n(V_n) = \frac{1}{Q} \prod_{s=0}^{U-1} \frac{(\frac{\lambda_{s,n}}{\mu_{s,n}})^{V_{s,n}}}{V_{s,n}!} \tag{5.26}$$

and Q is a normalizing constant. Substituting Eq.(5.26) into Eq.(5.25) gives

$$P_n(S_n) = \sum_{V_n} \frac{1}{Q} \prod_{s=0}^{U-1} \frac{(\frac{\lambda_{s,n}}{\mu_{s,n}})^{V_{s,n}}}{V_{s,n}!} \tag{5.27}$$

Inserting Eq.(5.27) into Eq.(5.24) gives the expected number of collisions as

$$E[i] = \frac{1}{Q} \sum_{S} \sum_{V_n} \prod_{n=1}^{N-1} \prod_{s=0}^{U-1} \frac{(\frac{\lambda_{s,n}}{\mu_{s,n}})^{V_{s,n}}}{V_{s,n}!} E_{\mathbf{S}}[i] \tag{5.28}$$

5.5 Performance Evaluation

In this section, we evaluate our system performance considering the expected number of subcarriers collision. The symbol loss probability, collision rate and proportion of symbol with degraded SNR are evaluated. The evaluation experiments were carried out using MATLAB. The obtained simulation results are compared with those obtained analytically.

5.5.1 Simulation Model

We consider a single-cell of MMR system, where each cell is serviced by a BS and six RSs deployed in the coverage area of the BS as presented in Figure 5.1. NTRSs mode is used in this scenario, in which the RS operates in different frequency bands than the BS.

The OFDM symbol consisting of N_c subcarriers is divided into G groups (subchannels), each consisting of N_c/G subcarriers. Frequency assignment is realized in two stages, first the BS allocates the same frequencies (channels) to each RS in its vicinity (centralized), second, each RS assigns the frequencies to MSs on the basis of subchannels randomly. This frequency allocation is made in each RS in a distributed manner, therefore no collisions are possible between MSs belonging to the same RS. However, collisions are possible if nearby RSs use the same subcarriers. Table 5.1 lists the parameters used in obtaining the simulation results presented in this chapter.

Table 5.1: Simulation Parameters

Parameter	**Value**
Number of Base Stations	1
Base Stations Radius (meter)	1000
Number of Relay Stations	6
Relay Station Radius (meter)	350
Log-normal Shadowing (dB)	8

We consider an OFDMA system with $N_c = 1024$ subcarriers, in which there are 120 pilot subcarriers and 184 guard subcarriers. The remaining 720 subcarriers are used as data subcarriers [25],[26]. In each RS the data subcarriers are grouped into $G = 40$ subchannels of 18 subcarriers each. A subchannel, which is the smallest unit of resource allocation is realized by randomly picking a subcarrier from each subchannel.

A) Probability of symbol loss under collision

When a collision occurs between subcarriers in RS_0 and RS_n, $n \neq 0$, the interference will cause some SNR degradation at the receiver side. For BER less than 10^{-6}, the SNR requirement depends on the modulation scheme as listed in table 5.2. In our calculations, we set $y = 1/\sqrt{(2)}$ and $\mu = 4$. We calculate the probability of loss in Eq.(5.21) by dividing the RS surface into a grid and calculate for each point the value $\frac{1}{2}erfc\left(\frac{-5ln(\rho A^{\mu})}{\varsigma yln(10)}\right)$. This probability of loss is demonstrated in Figure 5.3, for different interfering RSs as a function of the required SNR.

Table 5.2: SNR requirements based on the modulation scheme

Modulation Scheme	**Required SNR**
4QAM	9dB
16QAM	15dB
64QAM	21dB

B) Performance under different traffic types

We consider two classes of traffic: class-A (real-time), where the service time does not depend on the transmission rate (e.g., voice) and class-B (non real-time), where the service time becomes longer when the transmission rate is decreased (i.e., data) [49]. These classes have a number of calls with the same arrival rate, following a Poisson Process.

1) Real-time service

The calls belonging to class-A are assigned one subchannel each, the service time is independent of the modulation scheme, and it is considered to have a mean $1/\mu_n$ = 2 minutes, then we calculate the probability of symbol loss in the system. Figure 5.4, represents the proportion of symbols with degraded SNR as a function of the offered load. We can observe that, when the load increases, the SNR degradation becomes more rapid because more collisions occur in the system. As shown in Figure 5.5, the collision rate increases, when more calls arrive to the system.

2) Non Real-time service

The calls belonging to class-B are assigned two subchannels and for comparison, we consider a file that needs mean service time, $1/\mu_n$ = 2 minutes. This corresponds to a file

with mean size of 4.6 Mbyte [25]. For the non real-time services, a higher order efficiency modulation scheme minimizes the service time because the amount of data to be sent is fixed. For instance, a modulation scheme where 2 data bits are carried in a symbol (16 QAM), decreases the mean service time for non real-time services by factor 2 compared with a modulation scheme with one data bit per symbol (4QAM). Using a high order efficient modulation scheme results in a lower effective load, decreases the number of simultaneously active calls as well as lowers the collision rate. When using a higher-efficiency modulation, the required SNR increases and the probability of loss when collision occurs increases. Therefore, a high-order efficient modulation scheme decreases the number of collisions but makes a collision more disturbing.

5.5.2 Performance Results

To study the analysis of the system when a collision takes place between subcarriers in different NTRSs, we first consider one service class (voice) for which the results are presented in Figure 5.3, Figure 5.4, and Figure 5.5. Then we consider a case when two service classes exist in the system (voice and data), for which the results are shown in Figure 5.6.

Figure 5.3 depicts the probability of symbol loss as a function of the required SNR for different interfering NTRSs. We can observe that at different target SNR values, as the number of interfering RSs increases, the symbol loss probability also increases. For example, in the case of six relay stations, when the target SNR is 30dB, the probability of symbol loss is ≈ 0.19, while in the case of two interfering RSs, the probability of symbol loss is ≈ 0.062. Hence, we conclude from these results that the symbol loss probability due to collisions between subcarriers increases as the number of calls arrive to interfering RSs increases.

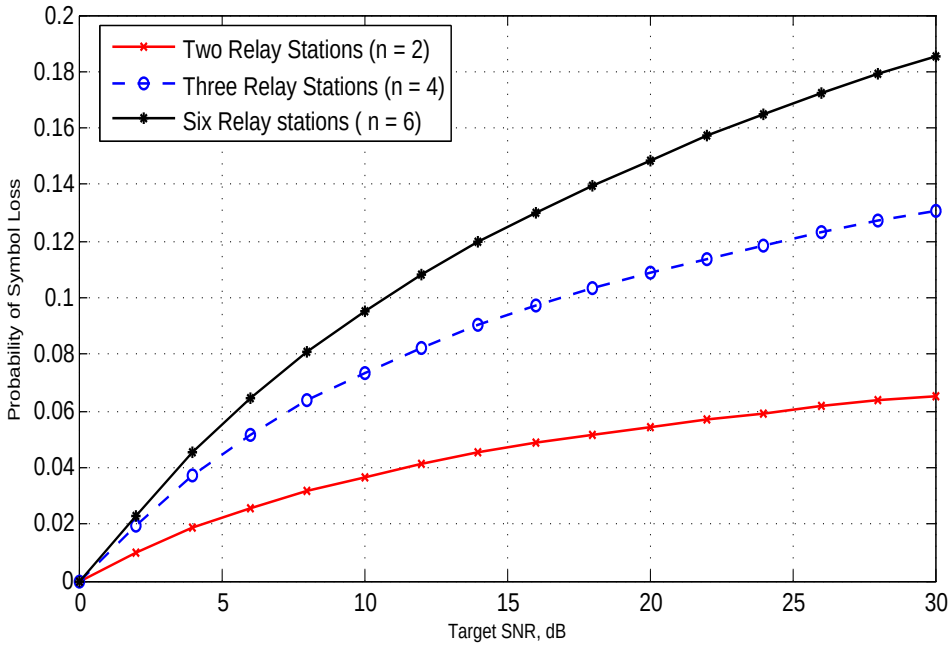

Figure 5.3: Probability of symbol loss when collision occurs for different SNR values

Figure 5.4 demonstrates the proportion of symbols with degraded SNR when different NTRs interfere with each other as a function of call arrival rate. It is observed from this figure that when the system becomes more loaded, and the number of interfering RSs increases, the SNR degradation becomes more rapid. This is because more collisions occur in the system in such a case. For example, in the case of six interfering RSs, when the load reaches 22 calls per minute, the proportion of symbol with degraded SNR is ≈ 0.08, while in the case of two interfering RSs, the proportion of symbol with degraded SNR is ≈ 0.045. Thus, as the load increases in the system, more collisions will occur, and more symbols will be lost.

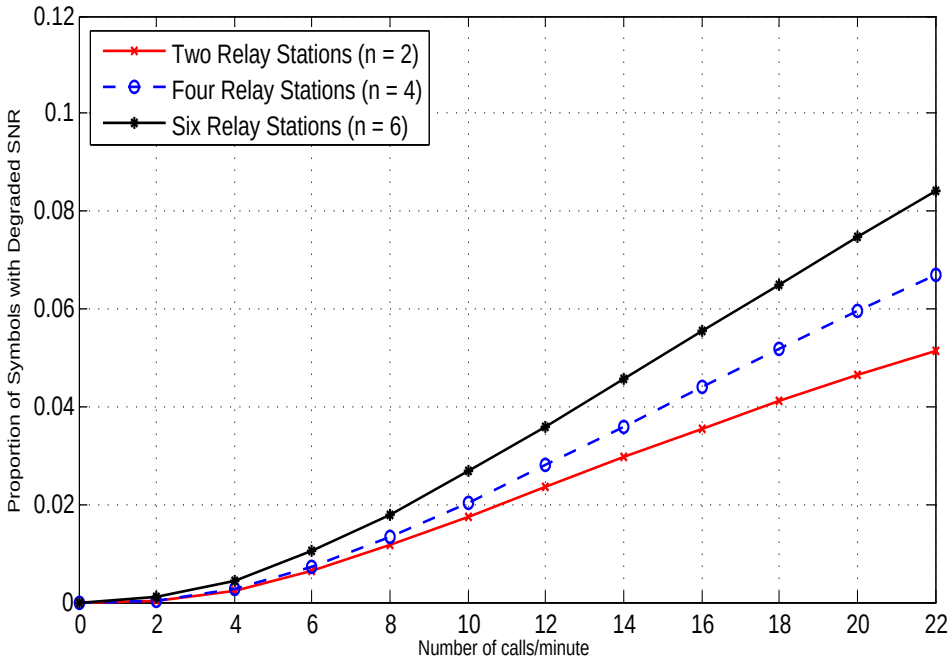

Figure 5.4: Proportion of symbols with degraded SNR values

Figure 5.5 presents the collision rate in the system. When the system becomes more loaded, the chance for MSs in different RSs to use the same subcarriers increases, therefore the SNR degraded frequently, as a result of subcarriers collision. From Figure 5.5, one can observe that in the case of six interfering RSs, when the load is 22 calls per minute, the collision rate is ≈ 0.25, while in the case of two interfering RSs, and the same number of calls, the collision rate is ≈ 0.11. Hence, as the system becomes more loaded and the number of interfering RSs increases, the collision rate increases.

Figure 5.6 presents the average proportion of symbols with degraded SNR when different types of traffic exist in the system. We can observe that when the network becomes more loaded, the SNR degradation becomes more frequent.

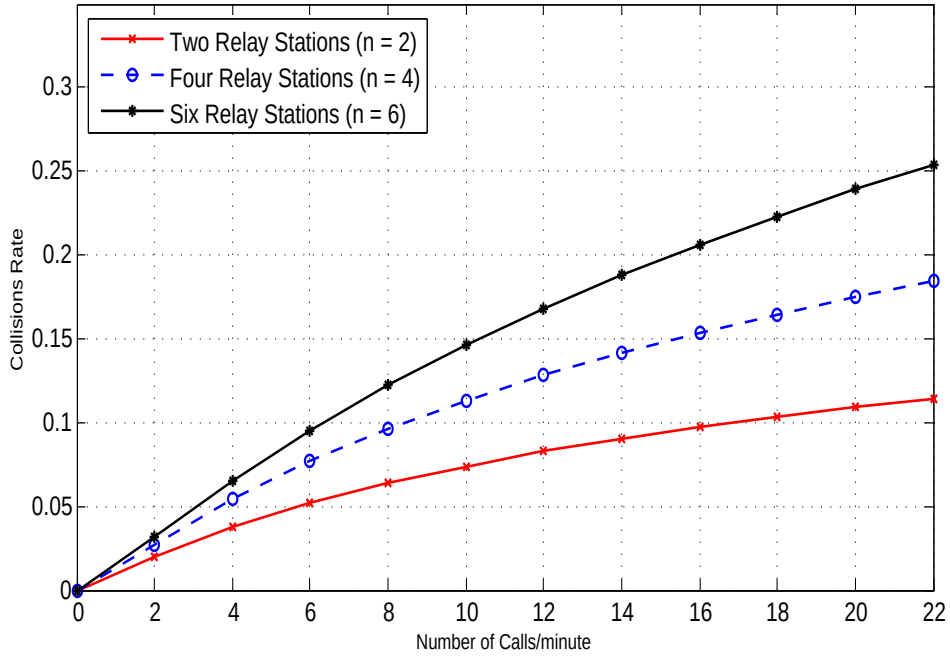

Figure 5.5: Collision Rate

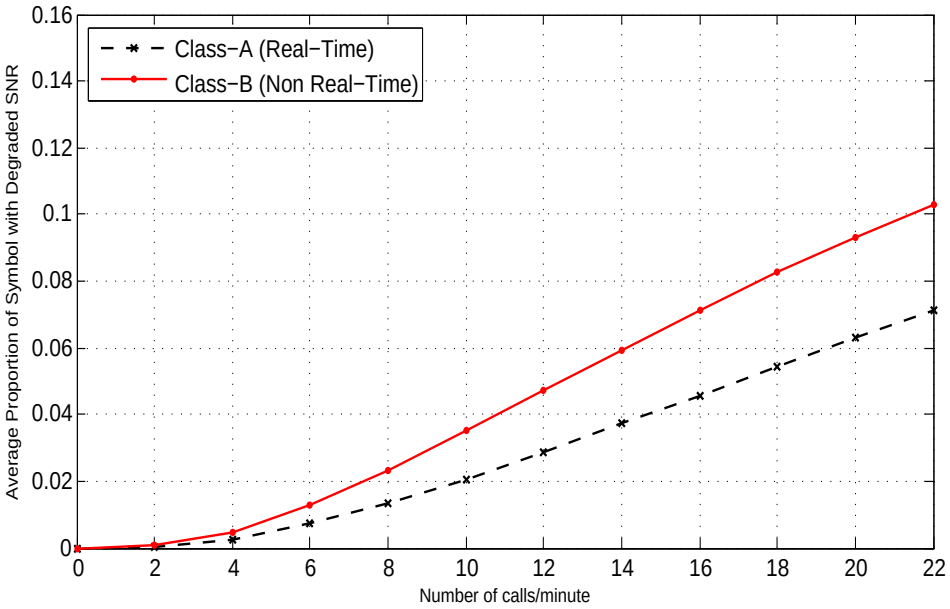

Figure 5.6: Average Proportion of symbols with degraded SNR values for class-A and class-B

As expected, the average proportion of symbols with degraded SNR is less in the case of class-A compared to the case of class-B. This lower SNR degradation is due to the fact that class-A is assigned fewer subchannels, therefore the chance for a collision to occur is less compared to the case of class-B. For example, when there are 22 calls per minute present in the system for class-A, the average proportion of symbol with degraded SNR is ≈ 0.07, while it is ≈ 0.1 in the case of class-B with the same load (22 calls/min.). Hence, we conclude that as more subchannels are occupied, as the collision rate increases, consequently the proportion of symbol with degraded SNR increases resulting in more symbol loss.

5.6 Summary

In this chapter, we developed an analytical model for estimating the expected number for collisions of OFDMA technique in a MMR system. In our analytical model, we calculated the expected number of collisions resulting from the simultaneous use of subcarriers in different NTRSs. Then for different numbers of interfering RSs, we obtained the symbol loss probability as a function of the desired SNR. In addition, we obtained the average proportion of symbol with degraded SNR when two service classes (voice and data) do exist in the system. We showed that subcarrier collision rates increase with the number of calls as well as the number of interfering RSs in the system, and that the resulting SNR degradation becomes more severe as more calls arrive in the system, degrading the QoS support.

Chapter 6

Capacity Analysis

6.1 Introduction

In OFDM systems, for high data rates, it is desirable to increase the number of subcarriers per OFDM symbol but as the number of subcarriers increases for a fixed channel size, the frequency spacing between the subcarriers in the OFDM symbol reduces. This makes the OFDM system more sensitive to phase noise which destroys the orthogonality between the subcarriers, causing inter-carrier interference (ICI). The resulting ICI has unacceptable impact on the data rates, consequently the system capacity is degraded. Some researches on capacity analysis of OFDM that do not consider the effects of ICI are presented in [14], [20], [72], [38], [52], [32], [27], [6], [76], and [80]. The capacity of OFDM system with frequency offset in Rician Fading was derived in [18], it was shown that the capacity drops as the frequency offset increases. Moreover, the cascade effect of the multiple relaying channel dramatically amplifies the ICI for the underlying OFDM system [63]. However, neither the available analysis is accomplished for OFDM systems with the consideration of ICI effect nor takes into consideration the accumulative ICI effect over multi-hop relaying

channels. This motivates us to evaluate the OFDM systems capacity over relaying channels in the presence of the ICI.

In this chapter, we evaluate the capacity of OFDM systems over multi-hop relaying channels employing AF relaying scheme and consider the effect of the ICI on the system capacity. We derive a closed-form expression for the MMR system capacity and compare the results for different number of hops. Simulation results provided to validate the analysis.

The remainder of this chapter is organized as follows. Section 6.2 presents the system model. Section 6.3 demonstrates the analysis of the system's capacity taking into consideration the effect of the ICI. Section 6.4 provides the system performance evaluation. Section 6.5 summarizes this chapter.

6.2 System Model

We adapt a similar system model to that presented in Chapter 3, by considering a R hop broadband wireless relaying network, in which the communication between a mobile station (MS) or (source, S) and a base station (BS) or (destination, *D*) passes through *R-1* relay stations (RSs), $RS_1, RS_2, \ldots, RS_{R-1}$. The channel in each hop is modeled as a frequency Rayleigh fading channel. Orthogonal frequency division multiplexing (OFDM) is employed as a transmission mechanism, with each OFDM symbol consisting of N_c subcarriers. There are *U* mobile stations in the system, uniformly distributed in the coverage area of the BS, and that each MS occupy one OFDM symbol and can be associated with the BS or a RS whichever provides stronger signal-to-noise ratio (SNR). Figure 6.1 represents a network model with *R=2* hops for a cellular deployment, in which each cell is serviced by a *BS*, located at the center of the cell, and six RSs $(N = 6)$, each equidistant from the BS

and located at the center of each side of the hexagon as shown.

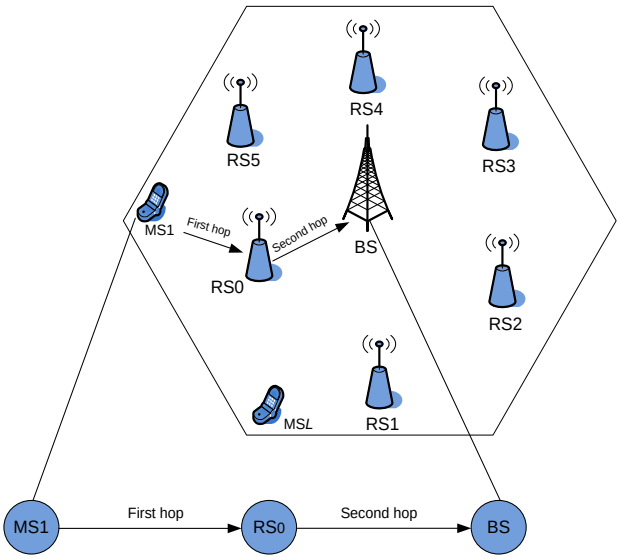

Figure 6.1: Mobile Multi-hop Relaying System

The AF relaying option is employed at each RS, therefore the R^{th} relay receives the transmitted signal from MS or the preceding RS, after the amplification, the received signal is forwarded to the next hop.

1) Multi-Hop Relaying Channel Model

Consider a wireless relaying network where the transmitted signal from a MS (source node) passes through R multi-hop relaying channels ($H_1, \ldots, H_{R-1}$) to reach the BS (destination node). These channels modeled as independent and identically distributed (i.i.d) Rayleigh fading random variables. Recall that, the AF relaying option is employed at each RS and these RSs amplify and forward the OFDM symbols at the frequency stage without decoding its contents. Amplifier with amplification factor α_R is deployed at each RS. The received

signal at the R^{th} hop, $Y_R[k]$ at the subcarrier k is given by

$$Y_R[k] = H_R[k]Y_{R-1}[k]\Phi_{Dop,R}[0] + \beta_R[k] + W_R[k] \tag{6.1}$$

This can be rewritten as

$$\begin{aligned} Y_R[k] = {} & H_1[k] \dots H_R[k]X[k]\Phi_{Dop,1}[0] \dots \Phi_{Dop,R}[0] \\ & + \sum_{r=1}^{R-1} \Bigg(H_{r+1}[k] \dots H_R[k]\beta_r[k]\Phi_{Dop,r+1}[0] \dots \Phi_{Dop,R}[0] \\ & + H_{r+1}[k] \dots H_R[k]W_r[k]\Phi_{Dop,r+1}[0] \dots \Phi_{Dop,R}[0] \Bigg) \\ & + \beta_R[k] + W_R[k] \end{aligned} \tag{6.2}$$

where H_r denotes the channel for the r^{th} hop, with variance σ_r^2, k is the subcarrier index, $k = 0, \dots, N_c - 1$, where $N_c - 1$ denotes the number of subcarriers per OFDM symbol and X denotes the transmitted signal. W_r is the noise at the r^{th} hop modeled as complex Gaussian random variable with variances $\sigma_{W_r}^2$. In the MMR system employing AF relaying option, the R^{th} relay amplifies the received signal by a gain α_R given by [37].

$$\alpha_R = \sqrt{\frac{P_R}{P_{R-1}H_R^2 + \sigma_{W_R}}}, \qquad r = 1, \dots, R-1 \tag{6.3}$$

where P_R denotes the transmitter power from the R^{th} relay. The R^{th} relay transmits the signal $X = \alpha_R Y_R[k]$ to the next hop. The received signal at the R-hop with AF relaying

option is given by

$$\begin{aligned} Y_R[k] = & \alpha_R H_1[k] \dots H_R[k] X[k] \Phi_{Dop,1}[0] \dots \Phi_{Dop,R}[0] \\ & + \sum_{r=1}^{R-1} \Bigg(H_{r+1}[k] \dots H_R[k] \beta_r[k] \Phi_{Dop,r+1}[0] \dots \Phi_{Dop,R}[0] \\ & + H_{r+1}[k] \dots H_R[k] W_r[k] \Phi_{Dop,r+1}[0] \dots \Phi_{Dop,R}[0] \Bigg) \\ & + \beta_R[k] + W_R[k] \end{aligned} \tag{6.4}$$

The signal-to-interference-plus-noise ratio (SINR) expression $\gamma_R[k]$ for R hops, after we assume that the rotation experienced by the whole symbol $\Phi_{Dop,r}[0]$ is corrected can be expressed as

$$\gamma_R[k] = \frac{|\alpha_R H_1[k] \dots H_R[k] X[k]|^2}{|\sum_{r=1}^{R-1} (H_{r+1}[k] \dots H_R[k] \beta_r[k] + H_{r+1}[k] \dots H_R[k] W_r[k]) + \beta_R[k] + W_R[k]|^2} \tag{6.5}$$

6.3 Multi-Hop Relaying System Capacity Analysis

The Multi-hop capacity is the maximum information that traverses from a source node through a number of hops and can be received at the destination node [26], [17]. We derive the capacity of the MMR system and consider the effect of ICI in the over all system

capacity. The capacity of the MMR system employing AF option is obtained as [67][7].

$$C_{AF-R-Relay} = \frac{1}{R} E\Big(log(1+\gamma_R[k])\Big) \tag{6.6}$$

where $\gamma_R[k]$ denotes the instantaneous SINR expressed in Eq.(6.5). Using the assumption that the channel is modelled as a Rayleigh fading, $\gamma_R[k]$ is an exponential random variable with expected value give as $\overline{\gamma}_R[k]$. The closed-formula expression for the probability density function (pdf) of $\gamma_R[k]$ for R hops is difficult to obtain, therefore deriving the MMR system capacity using $\gamma_R[k]$ is a challenging task. The received end-to-end SINR, $\gamma_R[k]$ can be upper bounded as follow

$$\gamma_R[k] \leq \gamma_{Upp}[k] \tag{6.7}$$

Considering a single-hop network $r = 1$, therefore the pdf and the cdf of SINR γ_r can be defined, respectively as follow

$$f_{\gamma_{r[k]}}(\gamma) = \frac{1}{\overline{\gamma}_{r[k]}} e^{-\frac{\gamma}{\overline{\gamma}_{r[k]}}} \tag{6.8}$$

$$F_{\gamma_{r[k]}}(\gamma) = 1 - e^{-\frac{\gamma}{\overline{\gamma}_{r[k]}}} \tag{6.9}$$

[7]The capacity of multi-hop relaying system is obtained in [67] without consideration of the ICI effect. In this thesis we take into consideration the effect of ICI on the overall system capacity.

where $\overline{\gamma}_{r[k]} = E[\gamma_{r[k]}]$. The multi-hop relaying channel can be modelled as an equivalent single-hop whose SINR equivalent $\gamma_{Upp[k]}$ can be approximated as follow [6].

$$\gamma_{Upp[k]} \approx \max_{r=1,\ldots R} \gamma_{r[k]} \tag{6.10}$$

Using the assumption that the hops are independent identically distributed Rayleigh fading leads to give the cdf and pdf of $\gamma_{Upp[k]}$ as

$$\begin{aligned} F_{\gamma_{Upp[k]}}(\gamma) &= 1 - P[\gamma_r > \gamma, \ldots, \gamma_R > \gamma] \\ &= 1 - \prod_{r=1}^{R} [1 - F_{\gamma_{r[k]}}(\gamma)] \end{aligned} \tag{6.11}$$

Therefore, the joint pdf of $\gamma_{Upp[k]}$ for R hops is given by differentiating Eq.(6.11) as

$$f_{\gamma_{Upp[k]}}(\gamma) = \sum_{r=1}^{R} f_{\gamma_{r[k]}}(\gamma) \prod_{j=1, j\neq r}^{R} [1 - F_{\gamma_{j[k]}}(\gamma)] \tag{6.12}$$

Substituting Eqs.(6.8) and (6.9) into Eq.(6.12), the joint pdf of $\gamma_{Upp[k]}$ can be expressed as

$$f_{\gamma_{Upp[k]}}(\gamma) = \sum_{r=1}^{R} \left(\frac{1}{\overline{\gamma}_{r[k]}} e^{-\frac{\gamma}{\overline{\gamma}_{r[k]}}} \right) \prod_{j=1, j\neq r}^{R} [1 - (1 - e^{-\frac{\gamma}{\overline{\gamma}_{j[k]}}})] \tag{6.13}$$

which can be simplified as

$$f_{\gamma_{Upp[k]}}(\gamma)=\sum_{r=1}^{R}\left(\frac{1}{\overline{\gamma}_{r[k]}}e^{-\frac{\gamma}{\overline{\gamma}_{r[k]}}}\right)\prod_{j=1,j\neq r}^{R}e^{-\frac{\gamma}{\overline{\gamma}_{j[k]}}} \tag{6.14}$$

After some manipulations, Eq.(6.14) can be rewritten as

$$f_{\gamma_{Upp[k]}}(\gamma)=\sum_{r=1}^{R}\left(\frac{1}{\overline{\gamma}_{r[k]}}e^{-\gamma\sum_{j=1}^{R}\overline{\gamma}_{r[k]}^{-1}}\right) \tag{6.15}$$

This can be simplified as

$$f_{\gamma_{Upp[k]}}(\gamma)=Ge^{-\gamma G} \tag{6.16}$$

where $G=\sum_{r=1}^{R}\overline{\gamma}_{r[k]}^{-1}$. Since $\gamma_R[k]\leq\gamma_{Upp[k]}$, therefore the term $log(1+\gamma_R[k])\leq log(1+\gamma_{Upp}[k])$, consequently the upper bound for the capacity of OFDM system over multi-hop relaying channels employing AF option is expressed as

$$C_{AF-R-Relay}=\frac{1}{R}E\Big(log(1+\gamma_{Upp}[k])\Big) \tag{6.17}$$

Substituting Eq.(6.16) into Eq.(6.17) gives

$$C_{AF-R-Relay} = \frac{1}{R} E\left(log(1 + Ge^{-\gamma G}) \right) \tag{6.18}$$

Substituting $G = \sum_{r=1}^{R} \overline{\gamma}_{r[k]}^{-1}$ into Eq.(6.18) and after some manipulations gives

$$C_{AF-R-Relay} = \frac{\left(\sum_{r=1}^{R} \overline{\gamma}_{r[k]}^{-1} e^{-\gamma \sum_{r=1}^{R} \overline{\gamma}_{r[k]}^{-1}} \right)}{R * ln2} \tag{6.19}$$

This closed-form expression can be evaluated using a technical tool such as MATLAB or MAPLE.

6.4 Performance Evaluation

In this section, we evaluate the obtained formula for the capacity of the MMR system. Simulation experiments were carried out using MATLAB. The obtained simulation results are used to validate the analytical analysis. The effect of Doppler Shift is considered in this evaluation. We first begin by describing the simulation model, then we present simulation results to verify the capacity analysis of multi-hop relaying channels.

6.4.1 Simulation Model

We consider a multi-hop relaying system and adopt the network model presented in Figure 6.1. The channel between each transmitter and receiver is modelled as a Rayleigh fading

channel, and amplify-and-forward option is considered at each RS. The simulated mobile speeds are 50 and 100km/h which results in Doppler Shift values, $f_d = 320$ and $f_d = 650Hz$. Those Doppler Shift values result in different ICI effects. A number of OFDM symbol each with $N_c = 256$ subcarriers are generated, than transmitted through the channel after adding the CP to overcome the ISI effect. At the receiver side, the effected signal is received than the bits with errors are calculated and compared with the total number of transmitted bits to calculated the total capacity. The capacity of multi-hop relaying channels is evaluated for different MS speeds.

6.4.2 Performance Results

In this section, we present simulation results to validate the analysis. The ICI effect as a result of the MS's speed and the accumulation over multi-hop relaying channels are considered. The capacity results are presented to reported the unacceptable effect of Doppler Shift on the MMR system's performance.

Figure 6.2 compares our simulation results for the capacity of the MMR system for a MS's speed of 50km/h, which translates into a Doppler Shift value of $f_d = 320Hz$, with the analytical results. It can be seen the perfect agreement between the analytical and the simulation results. It is observed from the results that the capacity of the MMR system is degraded with the number of hops. For instance, for the cases R = 1, R = 2, and R = 3 hops and 50km/h MS speed in this figure, the achieved capacity is: $\approx 5.1, \approx 4.1, and \approx 3.4$ bits/sec/Hz, respectively. The capacity loss is due to the R hops and the accumulative ICI effect over the number of hops.

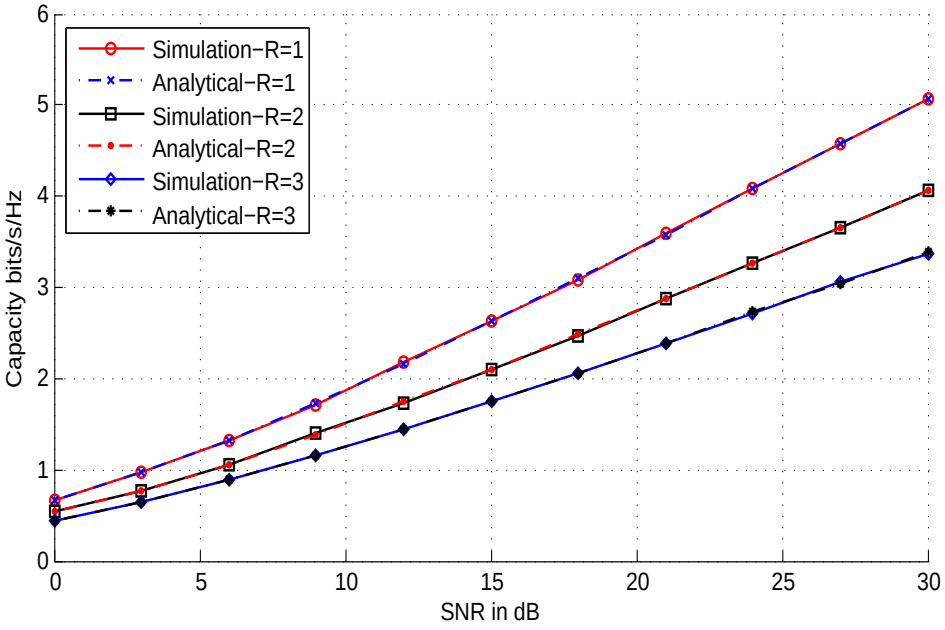

Figure 6.2: Capacity of multi-hop relaying employing amplify-and-forward relaying, speed = 50km

Figure 6.3 presents the capacity of the MMR system employing AF relaying option at each RS, after the simulated MS speed is increased to 100km/h, which translates into a Doppler Shift value of $f_d = 650Hz$. Since the Doppler Shift becomes larger as the MSs speed increases, the capacity results of the system in Figure 6.3 are more degraded compared to their counterpart results for lower MS speed in Figure 6.2. For example, for the cases R = 1, R = 2, and R = 3 hops and 100km/h MS speed in this figure, the achieved capacity is: $\approx 4.1, \approx 3.4, and \approx 2.8$ bits/sec/Hz, respectively. The capacity loss due to the R hops and the accumulative ICI effect over the number of hops. Comparing these results with the counterpart results in Fig.6.2, we conclude that larger number of hops with the consideration of ICI effect incur higher capacity loss.

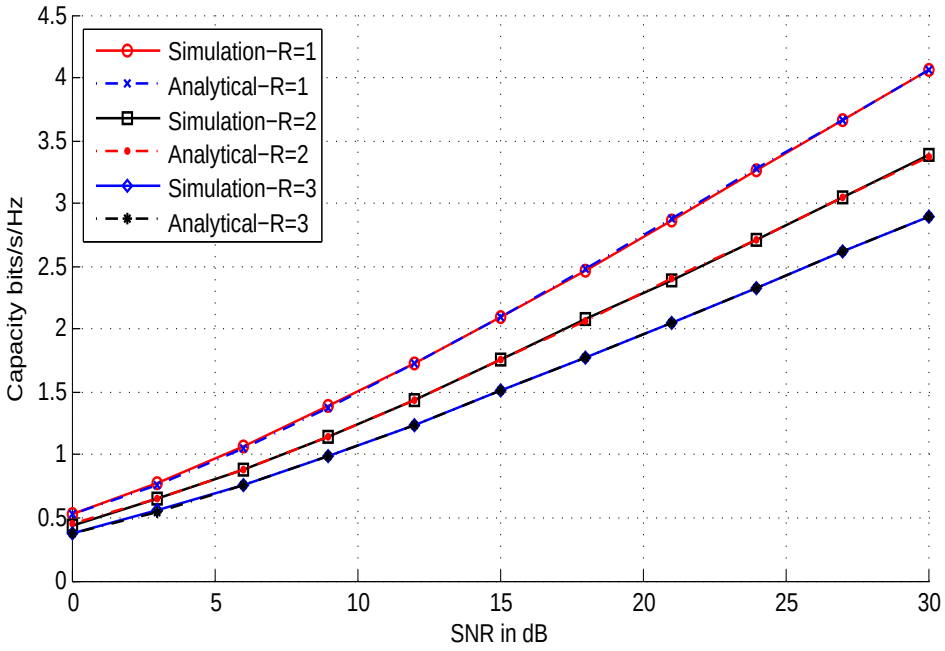

Figure 6.3: Capacity of multi-hop relaying employing amplify-and-forward relaying, speed = 100km

6.5 Summary

In this chapter, we evaluated the capacity of an OFDM systems over multi-hop relaying channels employing AF relaying scheme and taking into consideration the effect of the ICI on the system capacity. We derived a closed-form expression for the MMR system capacity and compared the results for various number of hops. Simulation results provided to validate the analysis. Different MSs speeds which result in different Doppler Shift values are considered. We observed that the ICI as a result of Doppler Shift have unacceptable effect on the MMR system's capacity, therefore it should be give due consideration to improve the MMR system's performance.

Chapter 7

Conclusions and Future Work

Broadband wireless access networks (BWANs) promise to improve the mobile users experience by offering higher data rates and increase the coverage area to accommodate larger numbers of mobile users and offer them better services than what 3G wireless systems are providing. The Mobile multi-hop relaying concept is proposed for both LTE-advanced and WiMAX to increase the coverage area and improve the system capacity. In order to support larger number of users, these systems utilize the use of a shared channel for data delivery instead of dedicated ones. Despite these advantages, the use of a shared channel introduces some issues. Since these systems are based on orthogonal frequency division multiplexing (OFDM) technology, inter-carrier interference, and subcarriers collisions are more annoying problems for the performance of these systems. Also, the cascade effect of the multi-hop relaying channel dramatically amplifies the effect of the introduced issues for the underlying OFDM system.

This thesis studied the interference effects in a multi-hop relaying system based on OFDM technology, and proposed an efficient solution to mitigate the interference effect in BWANs. Also, we analyzed the system capacity with the consideration of ICI effect. In this

chapter, we summarize and discuss the conclusions from this thesis and provide directions for future research work.

7.1 Summary of Contributions

In this thesis, we quantified issues that degrade the performance of mobile multi-hop relaying (MMR) systems, namely inter-carrier interference (ICI), and subcarriers collision as well as study the system capacity in the presence of ICI. We then proposed a solution using directional antennas to mitigate the ICI effect on the system performance. The aim of this thesis was to achieve the following objectives:

- Quantify issues that destroy the orthogonality between subcarriers in OFDM symbol and introduce ICI as well as study the accumulative effect over *multi-hop relaying* channels.
- Mitigate the ICI effect resulting from Doppler Shift by deploying directional antennas at both RS and MS side.
- Quantify the subcarriers collision effect in MMR system, and study the accumulative effect over *multi-hop relaying* channel.
- Analyze the system capacity of *multi-hop relaying* channels taking into consideration the effect of ICI.

In chapter 3, we presented analysis of the effects of HPA nonlinearity and Doppler Shift on the OFDM relaying system. The HPA shifts the transmitted signal before transmission over the channel, resulting in ICI. Also, the relative speed between the transmitter and the receiver shifts the transmitted frequency at the receiver side also causing ICI. The resulting

ICI due to the cumulative effects of the amplifier nonlinearity and Doppler shift per hop becomes very significant in the MMR system. Analytical BER performance of the system is evaluated and simulation results are presented to verify the analysis.

Simulation results are shown to conform those obtained by analytical. Based on observations from the BER curves, the following conclusions can be drawn, (1) OFDM system is sensitive to ICI and this sensitivity is increased with the constellation order M, (2) Amplifier distortion is one cause of the ICI, which depends on the amplifier characteristics, (3) The Doppler Shift is another cause of the ICI, which increases with the speed of the MS, (4) The resulting ICI due to the cumulative effects of these impairments per hop becomes very significant in the MMR systems, and severely degrades the BER performance of the system. The aforementioned issues should therefore be given due consideration to ensure acceptable BER performance in the upcoming MMR system such as IEEE 802.16j and LTE-advanced.

In chapter 4, investigation of the possibility of deploying directional antennas at both the MS and RS sides in the MMR systems was presented, for mitigating the BER performance degradation caused by the Doppler Shift experienced over multi-hop relaying channels. A directional antenna at either side of the communication link eliminates some multipath components, therefore the narrower the beamwidth of the directional antenna, the more chance that the multipath components would be canceled. Different MS speeds and antenna orientations were used to evaluate the effectiveness of the proposed solution. We show that the proposed scheme effectively enhances the BER performance of the MMR system as the beamwidth of the directional antenna is reduced, and that significant enhancements are possible for both the perpendicular and parallel antenna orientations, even though the latter is observed to provide better BER enhancement than the former. Also,

we observed that significant BER enhancements are observed at low and high MS speeds using this solution. However for high vehicular speeds, the system exhibits significant error floor above 10^{-3} for all antennas beamwidth studied, which suggests that extra BER enhancements techniques will be required in addition to directional antenna technique to achieve practically acceptable BER for this case.

In chapter 5, we developed an analytical model for estimating the expected number for collisions of OFDMA technique in the MMR system. In our analytical model, we calculated the expected number of collisions resulting from the simultaneous use of subcarriers in different NTRSs. Then for different numbers of interfering RSs, we obtained the symbol loss probability as a function of the desired SNR. In addition, we obtained the average proportion of symbol with degraded SNR when two service classes (voice and data) exist in the system. We showed that subcarriers collision rate increases with the number of calls as well as the number of interfering RSs in the system, and that the resulting SNR degradation becomes more severe as more calls arrive in the system, degrading the QoS support.

In chapter 6, we evaluated the capacity of an OFDM systems over multi-hop relaying channels employing an AF relaying scheme and considered the effect of the ICI on the system capacity. We derived a closed-form expression for the MMR system capacity and compared the results for various numbers of hops. Simulation results provided to validate the analysis.

7.2 Future Research Directions

There are several possible directions by which the work presented in this thesis could be extended. In this section, we point out a few of these directions. We have shown the

HPA nonlinearity and Doppler Shift effects on the transmitted OFDM signal over multi-hop relaying channels. The channels are modelled as a Rayleigh fading channels. The effect of ICI on the transmitted signal in multi-hop relaying system was studied in chapter 3 only over Rayleigh fading channels, this work can be extended to consider other channel models such as Nakagami and Rician fading channels. Therefore, studying the effect of ICI on the transmitted OFDM signal over these alternate channel models will be a significant contribution to study the BER performance in a multi-hop relaying system.

Also, we proposed a solution in chapter 4 to mitigate the effect of Doppler Shift by deploying directional antennas at both the mobile station and relay station. Similarly, a solution for reducing the effect of HPA nonlinearity is still needed in order to improve the BER performance.

In chapter 5, we quantified the possible number of collisions in OFDMA system when the same subcarrier is used simultaneously at different relay stations, therefore a mechanism to assign different subcarriers to different mobile stations will be a possible extension in order to further improve the system performance.

In addition, we considered a two-hop network in our study, a general case when the transmitted OFDM signal traverse over R number of hops will be another possible extension. The further analysis of BER performance when the ICI effect is present will be a significant achievement in the area of multi-hop relaying system.

In chapter 6, we analyzed the multi-hop relaying system capacity considering the ICI effect and AF relaying option at the RSs. Considering DF option at the RSs when the ICI effect is taking into count would be a significant contribution in the area of broadband multi-hop relaying systems. Also, comparing the capacity improvement in the cases of fixed and variable amplifying gain at the RSs will help to decide which option can be better

for different deployments scenarios.

Bibliography

[1] Ahmed, H., Sulyman, Ahmed, Iyanda, and Hassanein, H. "BER Performance of OFDM Systems in Mobile Multi-Hop Relaying Channels". *In Proceeding of the International Wireless Communications and Mobile Computing Conference*, pages 905 – 910, June 2010.

[2] Rappaport, T. "Wireless Communications: Principles and Practice". *Second Edition*, 2001.

[3] 3GPP Technical Report 36.913. "Requirements for further advancements for E-UTRA (LTE-advanced)". 2008.

[4] Ahmed, H., Sulyman, Ahmed, Iyanda, and Hassanein, H. "BER Performance of OFDM Systems with Channel Impairments". *In Proceedings of the IEEE 34th Conference on Local Computer Networks*, pages 1027 – 1032, October 2009.

[5] Armada, A., and Calvo, M. "Phase Noise and Sub-Carrier Spacing Effects on the Performance of an OFDM Communication System". *IEEE Communications Letters*, vol. 2, no. 1, pages: 11 - 13, January 1998.

[6] Beaulieu, N., and Farhadi, G. "On the Ergodic Capacity of Multi-Hop Wireless Relaying Systems". *IEEE Transactions on Wireless Communications*, vol. 8, no. 5, pages: 2286 - 2291, May 2009.

[7] Bingham, J. "Multicarrier Modulation for data transmission: an idea for whose time has come". *IEEE Communication Magazine*, vol. 28, pages: 5 - 14, May 1990.

[8] Bosisio, R., and Spagnolini, U. "Collision Model for the Bit Error Rate Analysis of Multicell Multiantenna OFDMA Systems". *In Proceedings of the IEEE International Conference on Communications*, pages 5732 – 5737, June 2007.

[9] Chang Q., Choi L., and Yoshida S. "On the Doppler Power Spectrum at the Mobile Unit Employing a Directional Antenna". *IEEE Communications Letters*, vol. 5, no. 1, pages: 13 - 15, January 2001.

[10] Chiavaccini, E., and Vitetta, G. "Error performance of OFDM signaling over doubly-selective Rayleigh fading channels". *IEEE Communications Lettetrs*, pages: 328 - 330, November 2000.

[11] Costa, E., and Pupolin, S. "M-QAM-OFDM System Performance in the Presence of a Nonlinear Amplifier and Phase Noise". *IEEE Transactions on Communications*, vol. 50, no. 3, pages: 462 - 472, March 2002.

[12] Dardari, D., Tralli, V., and Vaccari, A. "A theoretical characterization of nonliner distortion effects in OFDM systems". *IEEE Transactions on Wireless Communications*, vol. 48, no. 10, pages: 1755 - 1764, October 2000.

[13] Dritsoula, L., and Papadias, C. "On The Throughput of Linear Wireless Multi-Hop Networks Using Directional Antennas". *In Proceeding of the IEEE 10th Workshop on Signal Processing Advances in Wireless Communications*, pages 384 – 388, 2009.

[14] El Gamal, A., and Zahedi, S. "Capacity of a class of relay channels with orthogonal components". *IEEE Transactions on Information Theory*, vol. 51, no. 5, pages: 1815 - 1817, May 2005.

[15] El Gamal, A., Mohseni, M., and Zahedi, S. "Bounds on capacity and minimum energy-per-bit for AWGN relay channels". *IEEE Transactions on Information Theory*, vol. 52, no. 4, pages: 1545 - 1561, April 2006.

[16] Gilhousen, K. S., Jacobs, I. M., Padovani, R., Viterbi, A. J., Weaver, L. A., and Wheatley, C. E. III. "On the capacity of a cellular CDMA system". *IEEE Transactions on Vehicular Technology*, vol. 40, no. 2, pages: 303-312, May 1991.

[17] Goldman, H., and Sommer, R. "An Analysis of Cascaded Binary Communication Links". *IRE Transactions on Communications Systems*, vol. 10, no. 3, pages: 291 - 299, 1962.

[18] Hamdi, K. "Average Capacity Analysis of OFDM with Frequency Offset in Rician Fading". *In Proceedings of the Global Telecommunications Conference*, pages 1678 – 1682, 2007.

[19] Hasna, M., and Alouini, M. "A performance study of dual-hop transmissions with fixed gain relays". *IEEE Transactions on Communications*, vol. 3, no. 6, pages: 1963 - 1968, November 2004.

[20] Host-Madsen A., and Zhang, J. "Capacity bounds and power allocation for wireless relay channels". *IEEE Transactio on Information Theory*, vol. 51, no. 6, pages: 2020 - 2040, June 2005.

[21] Hyunsoo, C., and Daesik, H. "Effect of channel estimation error in OFDM-based WLAN". *IEEE Communications Letters*, vol. 6, no. 5, pages: 190 - 192, May 2002.

[22] IEEE C802.16e-04/453r2. "Add sub-segment to the PUSC mode". *Huawei*, November 2004.

[23] IEEE C802.16maint-05/083. "Hit ratio problems with the PUSC permutation". *Alvarion Ltd-13/03/2005*.

[24] IEEE Std 802.11a. "Wireless LAN medium access cotrol (MAC) and physical layer (PHY) specifications: high speed physical layer in the 5GH band". December 1999.

[25] IEEE, Std, 802.16e-2005. "IEEE Standard for Local and metropolitan area networks, Part 16: Air Interface for Fixed and Mobile Broadband Wireless Access Systems, Amendment for Physical and Medium Access Layers for Combined Fixed and Mobile Operation in Licensed Bands". February 2006.

[26] IEEE, Std, 802.16j-2009. "IEEE Standard for Multihop Relay networks, Part 16: Air Interface for Fixed and Mobile Broadband Wireless Access Systems, Amendment for Physical and Medium Access Layers for Mobile multihop Relay". June 2009.

[27] Karagiannidis, G., Tsiftsis, T., and Mallik, R. "Bounds for Multihop relaying communications in Nakagami-m fading". *IEEE Transactions on Communications*, vol. 54, no. 1, January 2006.

[28] Keller, T., and Hanzo, L. "Adaptive multicarrier modulation: A convenient framework for time-frequency processing in wireless communication". *IEEE Proceeding of the IEEE*, vol. 88, no. 5, 2000.

[29] Ketseoglou, T. "Cooperative diversity for clipped OFDM with iterative reception". *In Proceedings of the 42nd Asilomar Conference on Signals, Systems and Computers*, pages 1025 – 1029, October 2008.

[30] Kobayashi, H., and Mark, B. "Generalized Loss Models and Queueing-Loss Networks". *International Transaction in Operational Research*, vol. 9, no. 1, pages: 97 - 112, January 2002.

[31] Kobayashi, H., and Mark, B. L. "Generalized Loss Models, Loss Networks and Their Applications". *In Proceeding of the Annual Conference on Information Sciences and Systems*, March 1997.

[32] Kramer, G., Gastpar, M., and Gupta, P. "Cooperative strategies and Capacity theorms for relay networks". *IEEE Transactions on Information Theory*, vol. 51, no. 12, pages: 3037 - 3063, September 2005.

[33] Kurt, T., and Delic, H. "Collision avoidance in space-frequency coded FH-OFDMA". *In Proceedings of the IEEE International Conference on Communications*, pages 269 – 273, June 2004.

[34] Kurt, T., and Delic, H. "On symbol collisions in FH-OFDMA". *In Proceedings of the 59th IEEE Vehicular Technology Conference*, pages 1859– 1863, May 2004.

[35] Kurt, T., and Delic, H. "Space-frequency coding reduces the collision rate in FH-OFDMA". *IEEE Transactions on Wireless Communications*, vol. 4, no. 5, pages: 2045 - 2050, Septembr 2005.

[36] Kyongkuk, C., and Dongweon, Y. "On the general BER expression of one-and two-dimensional amplitude modulations". *IEEE Transactions on Communications*, vol. 50, no. 7, pages: 1074 - 1080, July 2002.

[37] Laneman, J., Tse D., and Wornell, G. "Cooperative diversity in wireless networks: efficient protocols and outage behavior". *IEEE Transactions on Information Theory*, vol. 50, no. 12, pages: 3062 - 3080, December 2004.

[38] Liang-Liang X., and Kumar, P. "An achievable rate for the multiple level relay channel". *In Proceedings of the International Symposium on Information Theory*, June/July 2004.

[39] Liao, Y., Yu, C., Lin, I., and Chen, K. "Phase noise estimation in OFDMA uplink communications, Book chapter in K. -C. Chen and J. R. de Marca Eds., Mobile WiMAX". *John Wiley and Sons, Ltd*, 2008.

[40] Lu, X., Towsley, D., Lio, P., Wicker, F., and Xiong, Z. "Minimizing Detection Probability Routing in Ad Hoc Networks Using Directional Antennas". *EURASIP Journal on Wireless Communications Networks*, pages: 1 - 8, 2009.

[41] Mogensen, P., Koivisto, T, Pedersen, K. and Kovacs, I. "LTE-Advanced: The Path towards Gigabit/s in Wireless Mobile Communications". *1st International Conference on Wireless Communication, Vehicular Technology, Information Theory and Aerospace and Electronic Systems Technology,*, 2009.

[42] Moose, P. "A technique for orthogonal frequency division multiplexing frequency offset correction". *IEEE Transactions on Communications*, vol. 42, no. 10, pages: 2908 - 2914, October 1994.

[43] Morelli, M., and Mengali, U. "An improved frequency offset estimator for OFDM applications". *IEEE Communications Letters*, vol. 3, no. 3, pages: 75 - 77, March 1999.

[44] Pan, L., and Bar-Ness, Y. "Closed Expressions for BER performance in OFDM Syestems with Phase Noise". *In Proceedings of the IEEE International Conference on Communications*, pages 5366 – 5370, June 2006.

[45] Parkvall, S., Dahlman, E., and Furuskar, A. "LTE-advanced evolving LTE towards IMT-advanced". *IEEE Vehicular Technology Conference*, pages 1–5, September 2008.

[46] Pascual-Iserte, A., Perez-Neira, A., and Lagunas, M. "On power allocation strategies for maximum signal to noise and interference ratio in an OFDM-MIMO system". *IEEE Transactions on Wireless Communications*, vol. 3, no. 3, pages: 808 - 820, May 2004.

[47] Petrus, P., Reed, J., and Rappaport, T. "Effects of directional antennas at the base station on the Doppler spectrum". *IEEE Communications Letters*, vol. 1, no. 2, pages: 40 - 42, March 1997.

[48] Pollet, T., Van Bladel, M., and Moeneclaey, M. "BER Sensitivity of OFDM Systems to Carrier Frequency Offset and Wiener Phase Noise". *IEEE Transactions on Communications*, vol. 43, no. 234, pages: 191 - 193, April 1995.

[49] Racz, S., Gero, B., and Fodor, G. "Flow Level Performance Analysis of a Multi-service System Supporting Elastic and adaptive Services". *Elsevier Journal, Performance Evaluation*, vol. 49, no. 1-4, pages: 451-469, September 2002.

[50] Radwan, A., and Hassanein, H. "Capacity Enhancement in CDMA Cellular Networks using Multi-hop Communication". *IEEE Symposium Computers and Communications*, pages 832– 837, June 2006.

[51] Razo, V., Riihonen, T., Gregorio, F., Werner, S., and Wichman, R. "Nonlinear amplifier distortion in cooperative amplify-and-forward OFDM systems". *In Proceddings of the IEEE conference Wireless Communications and Networking*, pages 1 – 5, April 2009.

[52] Reznik, A., Kulkarni, S., and Verdu, S. "Degraded Gaussian multirelay channel: capacity and optimal power allocation". *IEEE Transactions on Information Theory*, vol. 50, no. 12, pages: 3037 - 3046, December 2004.

[53] Riihonen, T., Werner, S., Gregorio F., Wichman R., and Hamalainen J. "BEP Analysis of OFDM Relay Links with Nonlinear Power Amplifiers". *In Proceeding of the IEEE Wireless Communications and Networking Conference*, pages 1 – 6, April 2010.

[54] Russell, M., and Stuber, G. "Interchannel Interference analysis of OFDM in Mobile environment". *In Proceddings of the IEEE 45th Vehicular Technology Conference*, pages 820 – 824, July 1995.

[55] Saleh, A. "Frequency independent and frequency dependent nonlinear models of TWT amplifiers". *IEEE Transactions on Communications*, vol. 29, no. 11, pages: 1715 - 1720, November 1981.

[56] Sankaran, C., Fan W., and Ghosh, A. "Performance of Frequency Selective Scheduling and Fractional Frequency Reuse Schemes for WIMAX". *In Proceeding of the IEEE 69th Vehicular Technology Conference*, pages 1 – 5, April 2009.

[57] Sathananthan, K., and Tellambura, C. "Probability of error calculation of OFDM systems with frequency offset". *IEEE Transactions on Communications*, vol. 49, no. 11, pages: 1884 - 1888, November 2001.

[58] Schmidl, T., and Cox, D. "Robust frequency and timing synchronization for OFDM". *IEEE Transactions on Communications*, vol. 45, no. 12, pages: 1613 - 1621, December 1997.

[59] Schober, H., and Jondral, F. "Velocity Estimation for based Wireless Communication Systems". *In Proceddings of the IEEE 56th Vehicular Technology Conference*, pages 715 – 718, September 2002.

[60] Shiang-Jiun L., Wern Ho S., I-Kang F., and Chia-chi H. "Resource scheduling with directional antennas for multi-hop relay networks in Manhattan-like environment". *IEEE Mobile WiMAX Symposium*, pages 108 – 113, March 2007.

[61] Simon, M., and Alouini, M. "Digital communication over fading channels". *2nd ed. Hoboken, N.J.: John Wiley and Sons*, 2005.

[62] Stuber, G. "Principles of Mobile Communications". *Boston: Kluwer Academic Publishers*, 1996.

[63] Sulyman, Ahmed, Iyanda; Takahara, G.; Hassanein, H.; Kousa, M. "Multi-hop capacity of MIMO-multiplexing relaying systems". *IEEE Transactions on Wireless Communications*, vol. 8, no. 6, pages: 3095 - 3103, June 2009.

[64] Tairan, W., Cano, A., Giannakis, G., and Laneman, J. "High-Performance Cooperative Demodulation With Decode-and-Forward Relays". *IEEE Transactions on Communications*, vol. 55, no. 7, pages: 1427-1438, July 2007.

[65] Tarhini, C., and Chahed, T. "On capacity of OFDMA-based IEEE802.16 WiMAX including Adaptive Modulation and Coding (AMC) and inter-cell interference". *In Proceedings of the 15th IEEE Local and Metropolitan Area Networks*, pages 139 – 144, June 2007.

[66] Tasi, J., Buehrer, M., Woerner, B. "BER Performance of a Uniform Circular Array Versus a Uniform Linear Array in a Mobile Radio Environment". *IEEE Transactions on Wireless Communications*, vol. 3, no. 3, pages: 695 - 700, May 2004.

[67] Telatar, I. "Capacity of multi-antenna gaussian Channels". *European Transactions on Telecommunications*, vol. 10, no., pages: 585 - 595, November/December 1999.

[68] Tiejun, W., Proakis, J., Masry, E., and Zeidler, J. "Performance degradation of OFDM systems Due to Doppler Spreading". *IEEE Transactions on Wireless Communications*, vol. 5, no. 6, pags: 1422 - 1276, June 2006.

[69] Van D., Meulen, E. "Transmission of information in a T-terminal discrete memoryless channel". *Department Statistics, University of California, Berkeley, CA, USA*, September 1968.

[70] Van D., Meulen, E. "Three-terminal communication channels". *Advances in Applied Probability, Book*, no. 3, 1971.

[71] Wan, L., and Dubey, V. "Bit error probability of OFDM system over frequency nonselective fast Rayleigh fading channels". *IEEE Electronics Letter*, pages 1306 – 1307, July 2000.

[72] Wang, B., Zhang, J., and Host-Madsen, A. "On the capacity of MIMO relay channels". *IEEE Transactions on Information Theory*, vol. 51, no. 1, pages: 29 - 43, January 2005.

[73] Wee, N. and Dubey, V. "Effect of Employing Directional Antennas on Mobile OFDM System With Time-Varyiing Channel". *IEEE Communications Letters*, vol. 7, no. 4, pages: 165 - 167, April 2003.

[74] Wee T., and Dubey V. "Effect of Employing Directional Antennas on Mobile OFDM System With Time-Varying Channel". *IEEE Communications Letters*, vol. 7, no. 14, pages: 165 - 167, April 2003.

[75] Wee, T., and Dubey, V. "Comments on the Doppler spectrum at the mobile unit employing directional antenna". *IEEE Communications Letters*, vol. 6, no. 11, pages: 472 - 474, November 2002.

[76] Xue, F., Xie L. , and Kumar, P. "The Transport Capacity of Wireless Networks Over Fading Channels". *IEEE Transactions on Information Theory*, vol. 51, no. 3, pages: 834 - 847, March 2005.

[77] Yucek, T., Tannious, R., and Arslan, H. "Doppler Spread Estimation for Wireless OFDM Systems". *In Proceddings of the IEEE Symposium on Advances in Wired and Wireless Communication*, pages 233 – 236, April 2005.

[78] Yuping, Z., and Haggman, S. "BER analysis of OFDM communication systems with intercarrier interference". *In Proceeding of the International Conference on Communication Technology*, pages 1 – 5, October 1998.

[79] Zaggoulos, G., Nix, A., and Doufexi, A. "WiMAX System Performance in High Scenarios With Directional Antennas". *In Proceedings of the IEEE International Symposium on Personal, Indoor and Mobile Radio Communications*, pages 80 – 89, 2007.

[80] Zahedi, S., Mohseni, M., and El Gamal, A. "On the capacity of AWGN relay channels with linear relaying functions". *In Proccedings of the IEEE International Symposum Information Theory*, page 399, June/July 2004.

[81] Zhang, Z., Jiang, W., Zhou, H., Liu, Y., and Gao, J. "UMTS Networks, Architecture, Mobility, and Services". *2nd edition, John Wiley and Sons*, 2005.

[82] Zhongshan Z., Weiyu J., Haiyan Z., Yuanan L., and Jinchun G. "High accuracy frequency offset correction with adjustable acquisition range in OFDM system". *IEEE Transactions on Communications*, vol. 4, no. 1, pages: 228 - 237, January 2005.